

THEORY AND APPLICATIONS OF HIGH CODIMENSION BIFURCATIONS

CHUNHUA SHAN

**A DISSERTATION SUBMITTED TO THE FACULTY OF GRADUATE STUDIES
IN PARTIAL FULFILMENT OF THE REQUIREMENTS
FOR THE DEGREE OF**

DOCTOR OF PHILOSOPHY

**GRADUATE PROGRAM IN MATHEMATICS AND STATISTICS
YORK UNIVERSITY
TORONTO, ONTARIO
AUGUST 2013**

**THEORY AND APPLICATIONS OF HIGH
CODIMENSION BIFURCATIONS**

by **Chunhua Shan**

a dissertation submitted to the Faculty of Graduate Studies
of York University in partial fulfilment of the requirements
for the degree of

DOCTOR OF PHILOSOPHY

© 2013

Permission has been granted to: a) YORK UNIVERSITY LIBRARIES to lend or sell copies of this dissertation in paper, microform or electronic formats, and b) LIBRARY AND ARCHIVES CANADA to reproduce, lend, distribute, or sell copies of this dissertation anywhere in the world in microform, paper or electronic formats *and* to authorise or procure the reproduction, loan, distribution or sale of copies of this dissertation anywhere in the world in microform, paper or electronic formats.

The author reserves other publication rights, and neither the dissertation nor extensive extracts for it may be printed or otherwise reproduced without the author's written permission.

THEORY AND APPLICATIONS OF HIGH CODIMENSION BIFURCATIONS

by **Chunhua Shan**

By virtue of submitting this document electronically, the author certifies that this is a true electronic equivalent of the copy of the dissertation approved by York University for the award of the degree. No alteration of the content has occurred and if there are any minor variations in formatting, they are as a result of the conversion to Adobe Acrobat format (or similar software application).

Examination Committee Members:

1. Huaiping Zhu (Supervisor)
2. Zijiang Yang (Chair/Dean's Representative)
3. Asia Ivic Weiss (Supervisory Committee Member)
4. Jianhong Wu (Supervisory Committee Member)
5. Richard Bello (Internal Examiner)
6. Xinfu Zou (External Examiner)

Abstract

The study of bifurcation of high codimension singularities and cyclicity of related limit periodic sets has a long history and is essential in the theory and applications of differential equations and dynamical systems. It is also closely related to the second part of Hilbert's 16th problem.

In 1994, Dumortier, Roussarie and Rousseau launched a program aiming at proving the finiteness part of Hilbert's 16th problem for the quadratic vector fields. For the program, 125 graphics need to be proved to have finite cyclicity. Since the launch of the program, most graphics have been proved to have finite cyclicity, and there are 40 challenging cases left. Among the rest of the graphics, there are 4 families of HH-graphics with a triple nilpotent singularity of saddle or elliptic type.

Based on the work of Zhu and Rousseau, by using techniques including the normal form theory, global blow-up techniques, calculations and analytical properties of Dulac maps near the singular point of the blown-up sphere, properties of quadratic systems and the generalized derivation-division methods, we prove that these 4 families of HH-

graphics (I_{12}^1) , (I_{13}^1) , (I_{9b}^1) and (I_{11b}^1) have finite cyclicity. Finishing the proof of the cyclicity of these 4 families of HH-graphics represents one important step towards the proof of the finiteness part of Hilbert's 16th problem for quadratic vector fields.

Acknowledgements

First of all, I would like to express my sincere gratitude to my supervisor Professor Huaiping Zhu for his patient guidance, constructive advices, consecutive encouragement and generous support throughout my PhD study. He brings me into the field of nonlinear dynamics and bifurcation theory. From him I have learned not only the mathematics but also how to do researches as a mathematician.

I would like to thank Professor Christiane Rousseau for her valuable suggestions and comments. I want to thank the committee members, Professor Asia Ivic Weiss and Professor Jianhong Wu for their suggestions, advices and the time of reviewing my thesis.

I am very grateful for the help and support from Laboratory of Mathematical Parallel System, Centre for Disease Modelling and Department of Mathematics and Statistics.

I would like to thank my wife and my parents for their love, understanding and support.

Lastly, I would like to acknowledge York University for the financial support from Sept. 2009 to Aug. 2013.

Table of Contents

Abstract	iv
Acknowledgements	vi
Table of Contents	vii
List of Tables	xi
List of Figures	xii
1 Introduction	1
2 Preliminaries	11
2.1 General finite cyclicity theorems	11
2.2 Transition maps	12
2.2.1 Derivative of a regular transition map	12
2.2.2 Dulac map near a hyperbolic saddle in the plane	12

2.2.3	Transition map near a semi-hyperbolic singularity	15
2.3	Normal forms near nilpotent singularities of multiplicity 3	18
2.4	Blow-up of the family	20
2.5	Dulac maps near P_i ($i = 1, 2, 3, 4$)	24
3	Finite cyclicity of (I_{12}^1)	31
3.1	Main theorem	32
3.2	Preliminaries	32
3.3	Proof of the main theorem	37
3.3.1	The lower boundary graphic S_{xhh1c}	37
3.3.2	The intermediate graphics S_{xhh1b}	44
3.4	Finite cyclicity of (I_{12}^1)	48
4	Finite cyclicity of (I_{13}^1)	50
4.1	Main theorem	51
4.2	The upper boundary graphic	51
4.3	The intermediate and lower boundary graphics	55
4.3.1	Family S_{xhh1}	59
4.3.2	Families S_{xhh4} and S_{xhh6}	68
4.3.3	Family S_{xhh5}	72
4.3.4	Family S_{xhh7}	76

4.3.5	Family Sxhh8	83
5	Finite cyclicity of (I_{9b}^1)	89
5.1	Lemmas	90
5.2	Main theorem	93
5.3	Proof of the main theorem	93
6	Finite cyclicity of (I_{11b}^1)	110
6.1	Main Theorem	111
6.2	The upper boundary graphic	111
6.3	The lower boundary graphic	112
6.3.1	Ehh1c, Ehh2e and Ehh3e	112
6.3.2	Ehh4c	121
6.3.3	Ehh5c	121
6.3.4	Ehh6c	125
6.3.5	Ehh7c	127
6.3.6	Ehh8c	133
6.4	The intermediate boundary graphic	137
6.4.1	Family Ehh1	138
6.4.2	Families Ehh2 and Ehh3	138
6.4.3	Family Ehh4	141

6.4.4 Families Ehh5–Ehh8	141
------------------------------------	-----

Bibliography	144
---------------------	------------

List of Tables

1.1	The progress of the DRR program	4
2.1	Convex limit periodic sets of HH-type for the saddle case [53]	23
2.2	Limit periodic sets of HH-type for the elliptic case [53]	24

List of Figures

1.1	Graphics through a nilpotent saddle	6
1.2	Nilpotent graphics with an elliptic point	7
1.3	Graphics for which we prove finite cyclicity	8
2.1	Dulac map near a hyperbolic saddle in the plane	14
2.2	Two types of transitions near a semi-hyperbolic point	16
2.3	The different topological types	19
2.4	The stratified set $\{r\rho = 0\}$ in the blown-up	21
2.5	Common blow-up of the nilpotent singularity	22
2.6	Two types of Dulac maps	28
3.1	The graphic (I_{12}^1)	31
3.2	Transition maps for the HH-graphics of saddle type	33
3.3	Transition maps for the lower boundary graphic S_{xhh1c}	35
3.4	Transition maps for S_{xhh1c} in the chart F.R. on $r = 0$	40

3.5	Transition maps for the family $Sxhh1b$ in the chart F.R. on $r = 0$	46
4.1	The graphic (I_{13}^1)	50
4.2	Upper boundary graphics of saddle type	52
4.3	Transition maps for the HH-graphics of saddle type	56
4.4	Transition maps for the family $Sxhh1$	59
4.5	Transition maps for the family $Sxhh4$	69
4.6	Transition maps for the family $Sxhh5$	73
4.7	Transition maps for the family $Sxhh7$	77
4.8	Transition maps for the family $Sxhh8$	83
5.1	The graphic (I_{9b}^1)	89
5.2	Transition maps for the graphic $Ehh1c$ of (I_{9b}^1)	94
6.1	The graphic (I_{11b}^1)	110
6.2	Transition maps for the graphics $Ehh1c$, $Ehh2e$ and $Ehh3e$ of (I_{11b}^1) . . .	113
6.3	Transition maps for the graphic $Ehh5c$	122
6.4	Transition maps for the graphic $Ehh6c$	126
6.5	Transition maps for the graphic $Ehh7c$	128
6.6	Transition maps for the graphic $Ehh8c$	133
6.7	Transition maps for the intermediate graphics of $Ehh1$	139
6.8	Transition maps for the intermediate graphics of $Ehh2$ and $Ehh3$	140

6.9 Transition maps for the intermediate graphics of Ehh5 and Ehh6 142

1 Introduction

The study of the bifurcation of singularities and cyclicity of limit periodic sets is essential in the theory and applications of differential equations and dynamical systems, and it is also closely related to the second part of Hilbert's 16th problem.

The second part of Hilbert's 16th problem. [25] *For any $n \in \mathbb{N}$, find a uniform upper bound $H(n) < \infty$ and relative positions of limit cycles for the planar polynomial vector fields*

$$P_n(x, y) \frac{\partial}{\partial x} + Q_n(x, y) \frac{\partial}{\partial y},$$

where $P_n(x, y)$ and $Q_n(x, y)$ are polynomials of degree n .

The second part of Hilbert's 16th problem is still open even for $n = 2$ and till now we only know that $H(2) \geq 4$ [3, 47]. However, this problem has inspired significant progress in the geometric theory of planar differential equations, bifurcation theory, normal forms, foliations and some topics in algebraic geometry. For the introduction and recent progress of Hilbert's 16th problem, one may look at the surveys and books [28, 30, 35, 43].

For the quadratic vector fields

$$P_2(x, y) \frac{\partial}{\partial x} + Q_2(x, y) \frac{\partial}{\partial y},$$

where $P_2(x, y)$ and $Q_2(x, y)$ are quadratic polynomials, in 1994, Dumortier, Roussarie and Rousseau launched a program [DRR program] aiming at proving the finiteness part of Hilbert's 16th problem for the quadratic vector fields. The DRR program aims to prove that $H(2)$ is finite.

In [15], Dumortier, Roussarie and Rousseau proved the following theorem using the compactness arguments based on the ideas of Roussarie [39].

Theorem 1.0.1. *There exists a uniform bound for the number of limit cycles of quadratic vector fields if and only if all limit periodic sets surrounding the origin inside the family*

$$\begin{cases} \dot{x} = \lambda x - \mu y + a_1 x^2 + a_2 xy + a_3 y^2, \\ \dot{y} = \mu x + \lambda y + b_1 x^2 + b_2 xy + b_3 y^2 \end{cases} \quad (1.0.1)$$

with $(\lambda, \mu) \in \mathbb{S}^1$ and $(a_1, a_2, a_3, b_1, b_2, b_3) \in \mathbb{S}^5$ have finite cyclicity.

The above theorem is important and significant. It transfers the global problem into a local problem of proving the finite cyclicity of all limit periodic sets in family (1.0.1).

Definition 1.0.2. [22] *Let \mathcal{X}_λ be any family of vector fields. A limit periodic set Γ is a nonempty compact set invariant by \mathcal{X}_{λ_0} , such that there exists a sequence $\{\lambda_n\}_{n \in \mathbb{N}}$ and for each λ_n , \mathcal{X}_{λ_n} has a limit cycle γ_{λ_n} with the property: $\lambda_n \rightarrow \lambda_0$ and $dist_H(\Gamma, \gamma_{\lambda_n}) \rightarrow 0$ for $n \rightarrow \infty$.*

Definition 1.0.3. [2] *A limit periodic set Γ of a vector field \mathcal{X}_{λ_0} inside a family \mathcal{X}_λ has finite cyclicity in \mathcal{X}_λ if there exist $N \in \mathbb{N}$ and $\varepsilon > 0$, $\delta > 0$ such that \mathcal{X}_λ with $|\lambda - \lambda_0| < \delta$ has at most N limit cycles γ_i with $\text{dist}_H(\Gamma, \gamma_i) < \varepsilon$. The minimum of such N when ε and δ tend to zero is called the cyclicity of Γ in \mathcal{X}_λ which we denote by $\text{Cycl}(\Gamma)$.*

A limit periodic set surrounding the origin inside the family (1.0.1) can be a periodic orbit, a graphic or the origin itself [15]. It was shown that the center-type singularity and the periodic orbit have finite cyclicity in [2] and [22], respectively. Therefore, in order to prove the finiteness part of Hilbert's 16th problem for the quadratic vector fields, according to Theorem 1.0.1, one needs to

- list all the graphics surrounding the origin inside the family (1.0.1);
- show that each graphic has finite cyclicity.

In [15], all the possible graphics inside the family (1.0.1) were listed and named, and there are a total of 125 graphics. For the DRR program, these 125 graphics are needed to be proved to have finite cyclicity. The program is progressing well since 1994 when the program was launched, and lots of works have been done towards the program [10–12, 14, 18, 19, 21, 26, 36–38, 40, 41, 44, 46, 53]. We summarize the DRR progress in Table 1.1.

A graphic of planar quadratic vector fields can be an elementary graphic, a nilpotent graphic or a degenerate graphic. A graphic is elementary if all singular points of the graphic are elementary, i.e., hyperbolic saddle or semi-hyperbolic point (one nonzero

eigenvalue). A graphic is nilpotent if there is a nilpotent singularity in the graphic. A graphic is degenerate if it contains a line or circle of singular points.

Table 1.1: The progress of the DRR program

Class of graphics	Done	Open	My work
Hyperbolic graphics	10		
Elementary non-hyperbolic graphics	47	1	
Nilpotent graphics of saddle type		2	1* +1
Nilpotent graphics of elliptic PP-type	20		
Nilpotent graphics of elliptic HP-type	6	4	
Nilpotent graphics of elliptic HH-type		10	1*+1
The four additional cases		4	
Nilpotent graphics of saddle-node type		4	
Degenerate graphics	2	11	
Total=125	85	36	4

For the elementary graphics, some essential progresses have been made towards the understanding of the bifurcation and cyclicity of elementary graphics through the works of Roussarie [40,41], Mourtada [37,38], Morsalani and Mourtada [36], Il'yashenko [26], Dumortier, Roussarie and Rousseau [14], Il'yashenko and Yakovenko [29], Kotova and

*Finite cyclicity was proved when the nilpotent singularity is of codimension 3 [53].

Stanzo [33], Dumortier, El Morsalani and Rousseau [12], El Morsalani [21] and Dumortier, Guzmán and Rousseau [10]. For the DRR program, nearly all elementary graphics have been proved to have finite by these works, and only the cyclicity of the graphic (I_{16a}^1) is still open.

For the graphics with nilpotent singularity, it presents analytic difficulties for the transition maps near the nilpotent singularity compared to the elementary graphics. In [18], Dumortier, Roussarie and Sotomayor studied the cuspidal loop by an analytic and geometric method based on the global blow-up techniques for the unfolding [4, 7, 42], which desingularizes the nilpotent graphic of families of vector fields into elementary graphics of foliated local vector fields. Their work was the first study of a graphic with a nilpotent point, and made the study of finite cyclicity of nilpotent graphics possible. Later, Zhu and Rousseau refined and developed the ideas in [18] to study the finite cyclicity of several graphics passing through a nilpotent point of saddle or elliptic type of codimension 3 [46, 52, 53]. They proved that more than 20 nilpotent graphics have finite cyclicity. Recently, Roussarie and Rousseau studied and proved finite cyclicity of 4 families of nilpotent graphics of elliptic PP-type surrounding a center by using the Bautin Ideal [44].

For the degenerate graphics, only the graphics (DF_{1a}) and (DF_{2a}) were proved to have finite cyclicity by Dumortier and Rousseau [19], and the cyclicity of the rest 11 degenerate graphics are still open.

The study of the finite cyclicity of graphics can not only give a deep understanding of the existence of limit cycles of planar polynomial vector fields, but also promote inventions of new mathematical tools and development of nonlocal bifurcations for dynamical systems.

For the graphics with a nilpotent singular point of multiplicity 3, they can be one of the following types:

- graphic through a nilpotent saddle: Fig. 1.1;
- graphic through a nilpotent elliptic point: Fig 1.2.

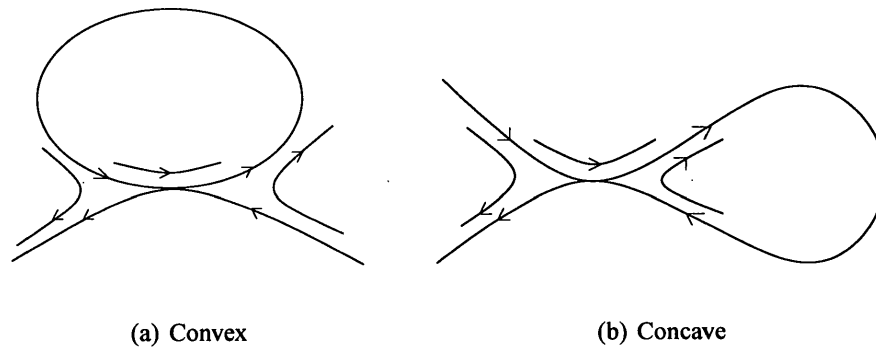


Figure 1.1: Graphics through a nilpotent saddle

A graphic through a nilpotent saddle can happen in two cases: convex HH-graphic and concave HH-graphic. For the quadratic vector fields, since any non-degenerate graphic is convex, so only the convex HH-graphic through a nilpotent saddle appears in the quadratic vector fields.

A graphic through a nilpotent elliptic point can happen in three cases: PP-graphic,

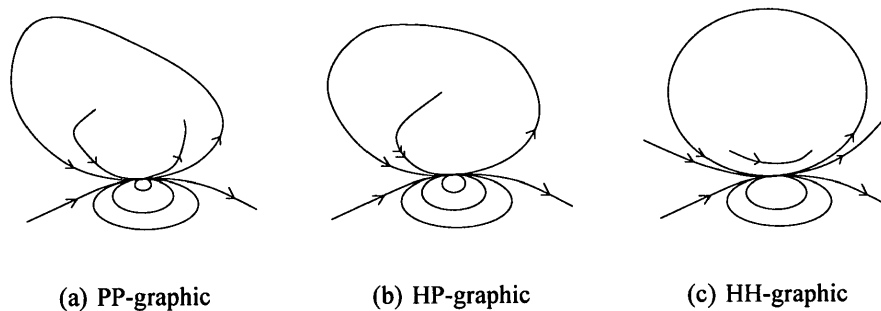


Figure 1.2: Nilpotent graphics with an elliptic point

HP-graphic and HH-graphic. Following the convention in [33, 53], we use PP to denote a graphic going out of a parabolic sector to a parabolic sector, HP to denote a graphic going out of a hyperbolic sector to a parabolic sector, and HH to denote the graphic going out of a hyperbolic sector to a hyperbolic sector.

Among these 125 graphics, there are 4 families of HH-graphic with a nilpotent saddle. They are (I_{12}^1) , (I_{13}^1) , (F_5^1) and (I_{14}^1) , where the graphics (I_{12}^1) and (I_{13}^1) surround a focus, and the graphics (F_5^1) and (I_{14}^1) surround a center.

There are 12 families of HH-graphics with a nilpotent elliptic point. Among these 12 families of HH-graphics, there are 4 families of graphics (H_4^1) , (H_8^3) , (H_{12}^3) and (H_{15}^3) which are hemicycles, there are 6 families of graphics (H_5^1) , (F_{7b}^1) , (H_{13}^1) , (I_{6b}^1) , (H_{13}^3) and (H_{14}^3) which surround a center, and the rest 2 graphics are (I_{9b}^1) and (I_{11b}^1) surrounding a focus.

In the thesis, we will prove that 2 families of convex HH-graphics of saddle type (I_{12}^1) ,

(I_{13}^1) and 2 families of HH-graphics of elliptic type (I_{9b}^1) , (I_{11b}^1) have finite cyclicity. For these 4 families of HH-graphics, each family of HH-graphics surrounding a focus has an invariant parabola and a triple nilpotent singularity at infinity which could be of codimension 3 or 4 as shown in Fig. 1.3. There is an additional attracting saddle-node on the invariant parabola for the graphic (I_{13}^1) and (I_{11b}^1) , respectively.

For the graphics (I_{12}^1) and (I_{9b}^1) , if the nilpotent singularity is of codimension 3, it has been done by Zhu and Rousseau [53]. Therefore, we only need to study these two graphics when the nilpotent singularity is of codimension 4.

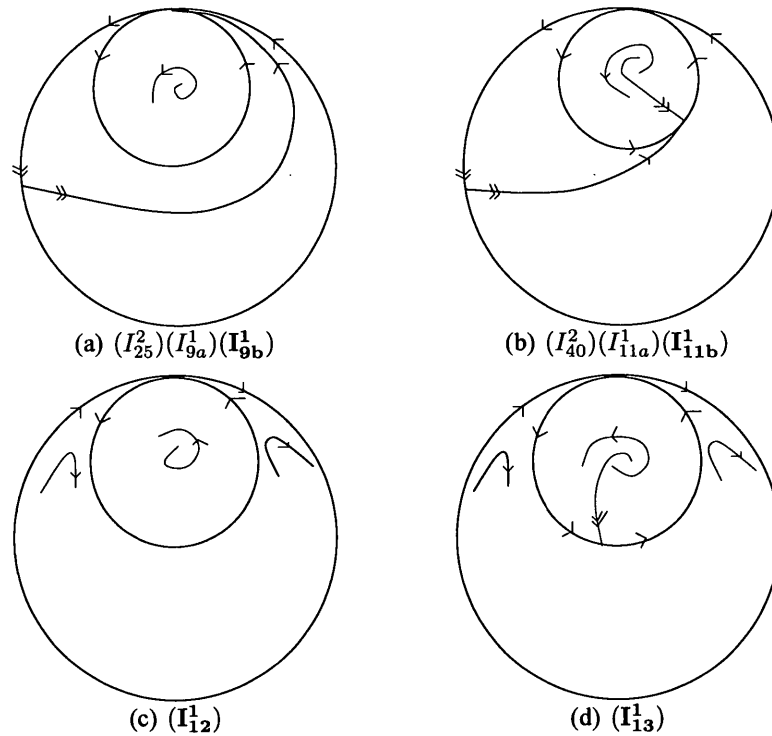


Figure 1.3: Graphics for which we prove finite cyclicity

To prove the finite cyclicity of graphics (I_{12}^1) , (I_{13}^1) , (I_{9b}^1) and (I_{11b}^1) , one basic ingredient is the blow-up of families developed in [18]. Some mathematical tools have been introduced and developed for the study of the cuspidal loop [18] and nilpotent singularity of saddle or elliptic type [52, 53]. These tools include:

1. a special normal form for a family with a nilpotent singularity;
2. blow-up of the family to allow the calculations of the transition maps near the nilpotent singularity;
3. the list of limit periodic sets in the blown-up family of vector fields;
4. calculations of different types of Dulac maps in the neighborhood of the singular points of the blown-up sphere;
5. Poincaré maps and displacement functions;
6. generalized derivation-division methods.

Since the nilpotent singularity can be of codimension 4 in these 4 families of graphics, some generic properties of the related maps fail which brings more difficulties in our study. Therefore, besides the above tools, we also need to make use of some techniques and special properties of the specific graphics for the proof which include:

1. first integral of Hamiltonian systems;

2. calculation of Poincaré first return map and the second derivative of the transition map along the invariant parabola;
3. fixed connection along the equator.

With the above tools, techniques and special properties of the specific graphics, we prove that the 4 families of HH-graphics (I_{12}^1) , (I_{13}^1) , (I_{9b}^1) and (I_{11b}^1) with a triple nilpotent singularity of saddle or elliptic type have finite cyclicity.

The thesis is organized as follows. In Chapter 2, we introduce some basic concepts, theorems and mathematical tools which are fundamental and required for the proof of the finite cyclicity of graphics. In Chapter 3, we prove the finite cyclicity of (I_{12}^1) . The finite cyclicity of (I_{13}^1) is proved in Chapter 4. We prove the finite cyclicity of (I_{9b}^1) in Chapter 5. In Chapter 6, we prove the finite cyclicity of (I_{11b}^1) except the cyclicity of Ehh3e in which the nilpotent elliptic point is of codimension 4. Finishing the proof of the cyclicity of these 4 families of HH-graphics represents one important step towards the proof of the finiteness part of Hilbert's 16th problem for quadratic systems.

2 Preliminaries

In this chapter, we introduce some basic concepts, theorems and mathematical tools which are fundamental and required for the proof of the finite cyclicity of graphics.

2.1 General finite cyclicity theorems

For the graphics with a nilpotent singular point of an analytic vector field, Zhu and Rousseau [53] proved the following theorems.

Theorem 2.1.1. *A convex HH-graphic through a triple nilpotent saddle of codimension 3 has finite cyclicity if the graphic is generic, i.e., the associated Poincaré first return map P satisfies $P'(0) \neq 1$.*

Theorem 2.1.2. *An HH-graphic through a triple nilpotent elliptic point of codimension 3 has finite cyclicity if the graphic is generic, i.e., the associated Poincaré first return map satisfies $P'(0) \neq 1$.*

2.2 Transition maps

2.2.1 Derivative of a regular transition map

Theorem 2.2.1. [1] *Consider the vector field*

$$\mathcal{X} = P(x, y) \frac{\partial}{\partial x} + Q(x, y) \frac{\partial}{\partial y}.$$

Let $\Sigma = \{(x, y) = (f_1(s), g_1(s))\}$ and $\tilde{\Sigma} = \{(x, y) = (f_2(\tilde{s}), g_2(\tilde{s}))\}$ be two arcs transverse to the same orbit $\Gamma(t)$. Let $R(s)$ be the transition map from Σ to $\tilde{\Sigma}$. Then

$$R'(s) = \frac{\Delta(s)}{\tilde{\Delta}(R(s))} \exp \left(\int_0^{T(s)} \operatorname{div} \mathcal{X}(\Gamma(t)) dt \right), \quad (2.2.1)$$

where $T(s)$ is the time to go from $(f_1(s), g_1(s))$ to $(f_2(R(s)), g_2(R(s)))$ along the orbit $\Gamma(t)$ starting at $(f_1(s), g_1(s))$ for $t = 0$, and

$$\Delta(s) = \begin{vmatrix} P(f_1(s), g_1(s)) & f_1'(s) \\ Q(f_1(s), g_1(s)) & g_1'(s) \end{vmatrix}, \quad \tilde{\Delta}(\tilde{s}) = \begin{vmatrix} P(f_2(\tilde{s}), g_2(\tilde{s})) & f_2'(\tilde{s}) \\ Q(f_2(\tilde{s}), g_2(\tilde{s})) & g_2'(\tilde{s}) \end{vmatrix}.$$

2.2.2 Dulac map near a hyperbolic saddle in the plane

Definition 2.2.2. *For a planar vector field, a singular point is elementary if it has at least one nonzero eigenvalue. It is hyperbolic (resp. semi-hyperbolic) if the two eigenvalues are not on the imaginary axis (resp. exactly one eigenvalue is zero).*

Definition 2.2.3. *The hyperbolicity ratio at a hyperbolic saddle is $r = -\frac{\lambda_1}{\lambda_2}$, where $\lambda_1 < 0 < \lambda_2$ are the two eigenvalues.*

Let \mathcal{X}_λ , $\lambda \in \Lambda$, be a C^∞ family of planar vector field defined in a neighborhood of a hyperbolic saddle at the origin, where Λ is the parameter space. Assume that the coordinate axes are the invariant manifolds of the saddle point. Let r_λ be the hyperbolicity ratio of \mathcal{X}_λ at the origin. By normal form theory, for any fixed $k \in \mathbb{N}$, up to a C^k -equivalence, the vector field \mathcal{X}_λ can be written into some explicit expressions of the normal form [27, 48].

- If r_0 is irrational, $\forall k \in \mathbb{N}$, the vector field \mathcal{X}_λ is C^k -equivalent to

$$\begin{cases} \dot{x} = x, \\ \dot{y} = -r(\lambda)y, \end{cases}$$

for λ in a neighborhood W of the origin in parameter space.

- If $r_0 \in \mathbb{Q}$, let $r_0 = \frac{p}{q}$, $(p, q) = 1$. Then $\forall k \in \mathbb{N}$, \mathcal{X}_λ is C^k -equivalent to

$$\begin{cases} \dot{x} = x, \\ \dot{y} = y \left[-r_0 + \sum_{i=0}^{N(k)} \alpha_{i+1}(\lambda) (x^p y^q)^i \right], \end{cases}$$

for λ in a neighborhood W of the origin in parameter space, and $\alpha_1(\lambda) = r(\lambda) - r_0$.

Let $\tilde{\Sigma}_1 = \{y = y_0\}$ and $\tilde{\Sigma}_2 = \{x = x_0\}$ be two sections transverse to the vector field \mathcal{X}_λ as shown in Fig. 2.1, where $x_0, y_0 > 0$ are constants. The flow of \mathcal{X}_λ induces a transition map $D_\lambda(\cdot)$, also called a Dulac map:

$$D_\lambda : \tilde{\Sigma}_1 \longrightarrow \tilde{\Sigma}_2$$

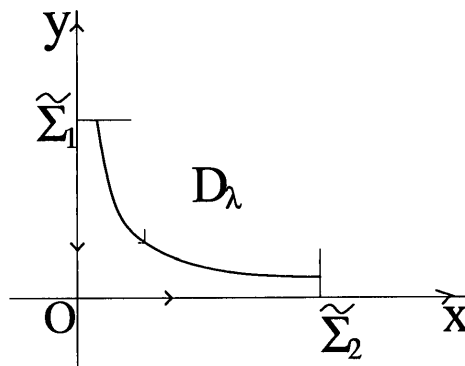


Figure 2.1: Dulac map near a hyperbolic saddle in the plane

for all $\lambda \in W$.

The Dulac map is C^∞ for $x > 0$. The following theorem describes its behavior near $x = 0$.

Proposition 2.2.4. [37] *The Dulac map D_λ can be written as*

$$D_\lambda(x) = x^{r(\lambda)}[c(\lambda) + \psi(x, \lambda)], \quad (2.2.2)$$

where $c(\lambda) = \frac{y_0}{x_0^{r(\lambda)}}$, $\psi(x, \lambda)$ is C^∞ for $(x, \lambda) \in (0, x_0] \times W$. Furthermore, ψ satisfies the following properties (I_0^∞):

$$(I_0^\infty) : \quad \forall n \in \mathbb{N}, \quad \lim_{x \rightarrow 0} x^n \frac{\partial^n \psi}{\partial x^n}(x, \lambda) = 0 \quad \text{uniformly for } \lambda \in W. \quad (2.2.3)$$

Furthermore,

(1) if $r_0 \notin \mathbb{Q}$, then $\psi \equiv 0$;

(2) if $r_0 = 1$, the expression (2.2.2) is in general not fine enough for proving the cyclicity.

Definition 2.2.5. [34, 40] *The Leontovich-Andronova-Ecalle-Roussarie compensator of the vector fields \mathcal{X}_λ is defined as*

$$\omega(x, \alpha_1) = \begin{cases} \frac{x^{-\alpha_1-1}}{\alpha_1} & \text{if } \alpha_1 \neq 0, \\ -\ln x & \text{if } \alpha_1 = 0. \end{cases} \quad (2.2.4)$$

The Dulac map in Proposition 2.2.4 is not fine enough to prove the cyclicity for the case $r_0 = 1$. In [40], using the compensator, Roussarie has an additional refinement:

Proposition 2.2.6. [40] *If $r_0 = 1$, the Dulac map D_λ has a well-ordered asymptotic expansion:*

$$\begin{aligned} D_\lambda(x) &= \alpha_1(\lambda)[x\omega + \dots] + \beta_1(\lambda)x \\ &\quad + \alpha_2(\lambda)[x^2\omega + \dots] + \dots + \alpha_k(\lambda)[x^k\omega + \dots] + \psi_k(x, \lambda), \end{aligned} \quad (2.2.5)$$

where $\alpha_1(\lambda) = r(\lambda) - 1$, $\alpha_i(\lambda)$ and $\beta(\lambda)$ are smooth functions of the parameters λ . ψ_k is a C^k function, k -flat with respect to $x = 0$.

2.2.3 Transition map near a semi-hyperbolic singularity

Let \mathcal{X}_λ be a family of planar vector fields sufficiently differentiable with respect to $((x, y), \lambda) \in \mathbb{R}^2 \times \Lambda$. Suppose that the vector field \mathcal{X}_0 has a semi-hyperbolic singular point at the origin of codimension m and the coordinate axes are its local invariant manifolds. In [27], it was proved that for any $k \geq 2m$, the family \mathcal{X}_λ can be written up

to a C^k equivalence form

$$(\mathcal{X}_\lambda) \begin{cases} \dot{x} = F(x, \lambda), \\ \dot{y} = -y, \end{cases}$$

for λ in a neighborhood W of the origin in parameter space, where

$$F(x, \lambda) = c(\lambda)x^{m+1}(1 + c(\lambda)\alpha_{2m+1}(\lambda)x^m) + \sum_{i=0}^{m-1} \alpha_i(\lambda)x^i.$$

The $\alpha_i(\lambda)$ are smooth functions of the parameters λ with $\alpha_i(0) = 0$ for $0 \leq i \leq m - 1$ and $c(0) \neq 0$. The quantity $\alpha_{2m+1}(0)$ is the formal invariant of the germ of \mathcal{X}_0 at the origin.

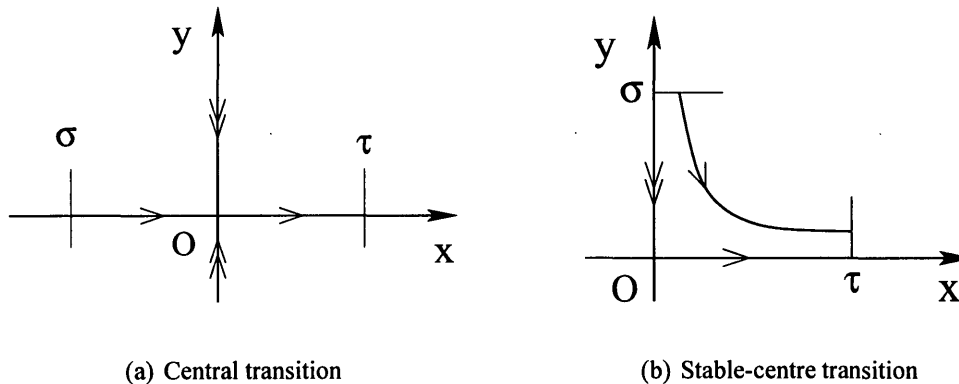


Figure 2.2: Two types of transitions near a semi-hyperbolic point

- *Central transition*

For some values of the parameters, the vector field \mathcal{X}_0 may have no singular points.

This yields possible transitions along the center manifold $\{y = 0\}$ from $\sigma = \{x =$

$-x_0, -y_0 \leq y \leq y_0\}$ to $\tau = \{x = x_0, -y_1 \leq y \leq y_1\}$ where $x_0, y_0, y_1 > 0$ are chosen such that the transition $D_\lambda(y)$ is defined from σ to τ , and $\lambda \in \mathcal{O}_F := \{\lambda \in W \mid F(x, \lambda) \neq 0, \forall x \in [-x_0, x_0]\}$.

Proposition 2.2.7. [14] *The transition map $D_\lambda(y)$ is linear and*

$$D_\lambda(y) = m(\lambda)y \quad \text{with} \quad m(\lambda) = \exp\left(-\int_{-x_0}^{x_0} \frac{dx}{F(x, \lambda)}\right). \quad (2.2.6)$$

The function $m(\lambda)$ is continuous and non-zero on \mathcal{O}_F and has a continuous extension $m(\lambda) = 0$ for $\lambda \in \partial\mathcal{O}_F$.

• *Stable-centre transition*

Take sections $\sigma = \{y = y_0, -x_0 \leq x \leq x_0\}$ and $\tau = \{x = x_0, -y_0 \leq y \leq y_0\}$ where $x_0 > 0$ and $y_0 > 0$. For $\lambda = 0$ and x_0, y_0 sufficiently small, we have a transition $D_0(x)$ from $\sigma^+ = \{(x, y) \in \sigma \mid x > 0\}$ to τ along the trajectories of \mathcal{X}_0 . This transition can be extended for any value of λ for some subinterval $\sigma_\lambda \subset \sigma$ to τ in a transition $D(x, \lambda)$ which is also denoted by $D_\lambda(x)$. The subinterval σ_λ is defined as follows.

(i) If $\lambda \in \mathcal{O}_F$, then $\sigma_\lambda = [-x_0, x_0]$.

(ii) If $\lambda \notin \mathcal{O}_F$ and $z(\lambda)$ is the largest root of $F(x, \lambda) = 0$ with $-x_0 \leq z(\lambda) \leq x_0$ and $z(0) = 0$, then $\sigma_\lambda = [z(\lambda), x_0]$. We extend $D_\lambda(\cdot)$ continuously at $z(\lambda)$ by $D_\lambda(z(\lambda)) = 0$.

The domain of $D_\lambda(x)$ is $\mathcal{C} = \cup_\lambda \{\sigma_\lambda, \lambda\} \subset [-x_0, x_0] \times W$.

The stable-centre transition map $D(x, \lambda)$ satisfies the following flatness property.

Proposition 2.2.8. [14] For the stable-centre transition map $D(x, \lambda)$ defined above,

$\forall p, n \in \mathbb{N}$ and $\forall (i_0, i_1, \dots, i_N)$ with $i_0 + i_1 + \dots + i_N = n$, we have

$$\frac{\partial^n D(x, \lambda)}{\partial x^{i_0} \partial \lambda_1^{i_1} \dots \partial \lambda_N^{i_N}} = O(|x, \lambda|^p), \quad \forall (x, \lambda) \in \mathcal{C}. \quad (2.2.7)$$

2.3 Normal forms near nilpotent singularities of multiplicity 3

A family containing a triple nilpotent singularity of elliptic or saddle type can be written as [17]

$$\begin{cases} \dot{x} = y, \\ \dot{y} = \varepsilon_1 x^3 + \lambda_2 x + \lambda_1 + y(\lambda_3 + bx + \varepsilon_2 x^2 + x^3 h(x, \lambda)) + y^2 Q(x, y, \lambda), \end{cases} \quad (2.3.8)$$

where for the saddle case $\varepsilon_1 = 1$ (Fig. 2.3(a)); for the elliptic case $\varepsilon_1 = -1, b > 2\sqrt{2}$ (Fig. 2.3(b)), $\lambda = (\lambda_1, \lambda_2, \lambda_3)$ are the parameters, $h(x, \lambda)$ is C^∞ in (x, λ) , $Q(x, y, \lambda)$ is C^∞ in (x, y, λ) and of arbitrarily high order in (x, y, λ) . For any value of ε_2 , they have the same topological type.

For the purpose of studying the passages in the neighborhood of the nilpotent singularity, a new normal form to unfold the nilpotent singularity of saddle or elliptic type was developed in [53].

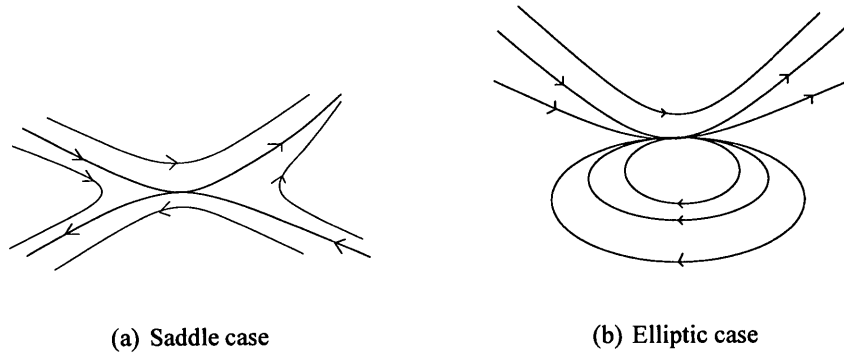


Figure 2.3: The different topological types

Theorem 2.3.1. [53] *The family (2.3.8) is C^∞ -equivalent to*

$$\begin{cases} \dot{X} = Y + \mu_2 + a(\mu)X^2, \\ \dot{Y} = \mu_1 + Y(\mu_3 + X + \bar{\varepsilon}_2 X^2 + X^3 h_1(X, \mu)) + X^4 h_2(X, \mu) + Y^2 Q(X, Y, \mu), \end{cases} \quad (2.3.9)$$

where $\bar{\varepsilon}_2 = -a\varepsilon_1\varepsilon_2$, and

- for the saddle case: $a(0) \in (-\frac{1}{2}, 0)$,

if $a(0) = -\frac{1}{2}$, the unfolding is of codimension 4 which corresponds to the case $b = 0$ in (2.3.8);

- for the elliptic case: $a(0) \in (0, \frac{1}{2})$,

if $a(0) = \frac{1}{3}$, the unfolding is of codimension 4, type 2, which corresponds to the case $\varepsilon_2 = 0$ in (2.3.8).

$\mu = (\mu_1, \mu_2, \mu_3)$ is the parameter, $h_1(X, \mu)$, $h_2(X, \mu) = \bar{\varepsilon}_2 a + O(\mu) + O(X)$ and $Q(X, Y, \mu)$ are C^∞ and $Q(X, Y, \mu)$ is of arbitrary high order in (X, Y, μ) .

We denote $A = [-\frac{1}{2}, 0)$ for the saddle case, and $A = (0, \frac{1}{2})$ for the elliptic case.

2.4 Blow-up of the family

We are interested in the family for $a \in A$ and (x, y, μ) in a neighborhood $U \times \Lambda$ of $((0, 0), (0, 0, 0))$. Taking Λ as a sphere, we make the change of parameters

$$\mu_1 = \nu^3 \bar{\mu}_1, \quad \mu_2 = \nu^2 \bar{\mu}_2, \quad \mu_3 = \nu \bar{\mu}_3, \quad (2.4.10)$$

where $\bar{\mu} = (\bar{\mu}_1, \bar{\mu}_2, \bar{\mu}_3) \in \mathbb{S}^2$ and $\nu \in (0, \nu_0)$. Adding the equation $\dot{\nu} = 0$ to system (2.3.9), we have

$$\widehat{X} : \begin{cases} \dot{x} = y + \nu^2 \bar{\mu}_2 + ax^2, \\ \dot{y} = \nu^3 \bar{\mu}_1 + y \left[\nu \bar{\mu}_3 + x + \varepsilon_2 x^2 + x^3 h_1(x, \nu \bar{\mu}) \right] \\ \quad + x^4 h_2(x, \nu \bar{\mu}) + y^2 Q(x, y, \nu \bar{\mu}), \\ \dot{\nu} = 0. \end{cases} \quad (2.4.11)$$

We then make the weighted blow-up

$$x = r\bar{x}, \quad y = r^2\bar{y}, \quad \nu = r\rho, \quad (2.4.12)$$

where $r > 0$ and $(\bar{x}, \bar{y}, \rho) \in \mathbb{S}^2$.

By the blow-up (2.4.12), we have a C^∞ family $\bar{X} = \frac{1}{r} \widehat{X}$. Note that for each $(a, \bar{\mu})$, the foliation given by $\{\nu = r\rho = \text{const}\}$ is preserved by $\bar{X}_{(a, \bar{\mu})}$:

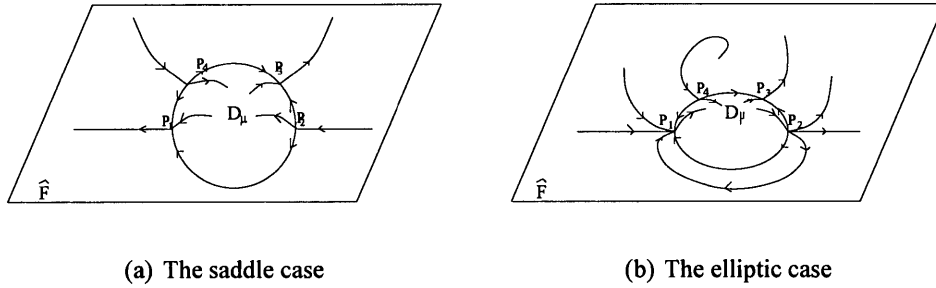


Figure 2.4: The stratified set $\{r\rho = 0\}$ in the blown-up

- For $\{r\rho = \nu\}$ with $\nu > 0$, the leaf is a regular manifold of dimension 2.
- For $\{r\rho = 0\}$, we get a stratified set in the critical locus. As shown in Fig. 2.4, there are two strata of 2-dimensional manifolds:

$$- \hat{F}_{\bar{\mu}} \cong S^1 \times R^+ \quad \text{the blow-up of the fiber } \mu = 0,$$

$$- D_{\bar{\mu}} = \{\bar{x}^2 + \bar{y}^2 + \rho^2 = 1, \rho \geq 0\}.$$

On $\hat{F}_{\bar{\mu}} = \{\rho = 0\}$, (2.4.12) is just the common blow-up of the nilpotent point:

$$x = r\bar{x}, \quad y = r^2\bar{y}. \quad (2.4.13)$$

By the blow-up (2.4.13), we get a vector field with four singular points P_i ($i = 1, 2, 3, 4$). P_3 and P_4 are hyperbolic saddles, P_1 and P_2 are saddles (resp. nodes) in the saddle (resp. elliptic) case as shown in Fig. 2.5.

The four points P_i on the circle $x^2 + y^2 = 1, r = \rho = 0$ are studied in the charts

$$\text{P.R.1 } \bar{x} = -1, (r_1, \rho_1, \bar{y}_1), \quad \text{and} \quad \text{P.R.2 } \bar{x} = 1, (r_2, \rho_2, \bar{y}_2),$$

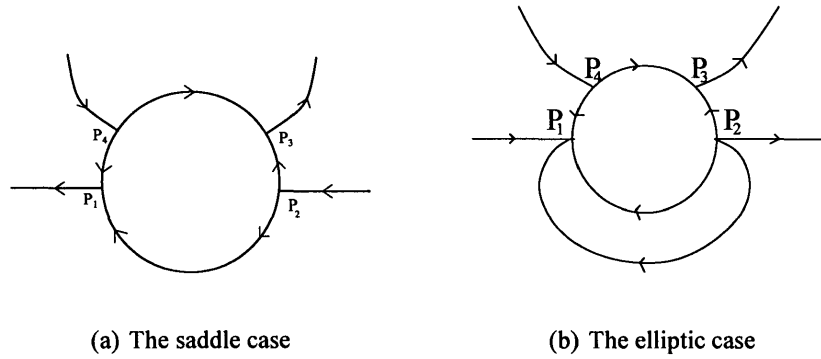


Figure 2.5: Common blow-up of the nilpotent singularity

while the upper part of the sphere $r = 0, \rho > 0$ is studied in the chart

$$\mathbf{F.R.} \quad \rho = 1, (\bar{x}, \bar{y}, r)$$

yielding

$$\begin{cases} \dot{\bar{x}} = \bar{\mu}_2 + \bar{y} + a\bar{x}^2, \\ \dot{\bar{y}} = \bar{\mu}_1 + (\bar{\mu}_3 + \bar{x})\bar{y} + r\bar{h}(\bar{x}, \bar{y}, r, \bar{\mu}), \\ \dot{r} = 0, \end{cases} \quad (2.4.14)$$

where $\bar{h}(\bar{x}, \bar{y}, r, \bar{\mu})$ is C^∞ in $(\bar{x}, \bar{y}, r, \bar{\mu})$. Especially, on $\{r = 0\}$, we have

$$\bar{X}_{\rho=1} : \begin{cases} \dot{\bar{x}} = \bar{\mu}_2 + \bar{y} + a\bar{x}^2, \\ \dot{\bar{y}} = \bar{\mu}_1 + (\bar{\mu}_3 + \bar{x})\bar{y}. \end{cases} \quad (2.4.15)$$

In [53], the complete bifurcation analysis of (2.4.15) was given and phase portraits for the different values of $\bar{\mu} \in \mathbb{S}^2$ were studied and presented. Together with the regular part of the graphics, we have a list of limit periodic sets for which finite cyclicity must be

proved. In [53], Zhu and Rousseau listed all the possible limit periodic sets of HH-type for the saddle case, and PP-type, HP-type and HH-type for the elliptic case. As the limit periodic sets of HH-type for the saddle case and elliptic case will be needed in our proof, so we recall them in the following Table 2.1 and Table 2.2.

family Sxhh1	family Sxhh2	family Sxhh3	family Sxhh4
family Sxhh5	family Sxhh6	family Sxhh7	family Sxhh8
family Sxhh9			family Sxhh10

Table 2.1: Convex limit periodic sets of HH-type for the saddle case [53]

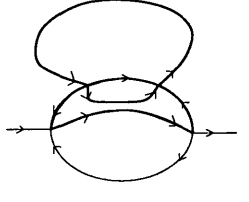
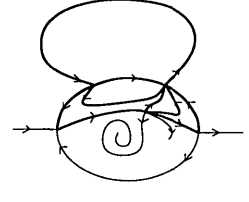
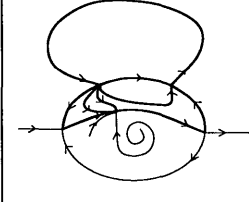
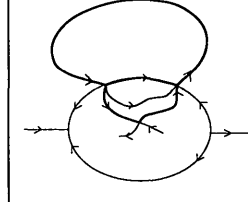
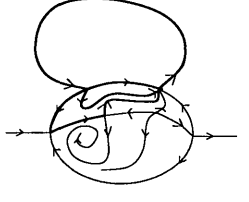
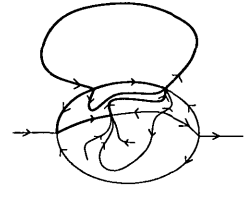
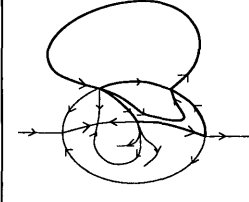
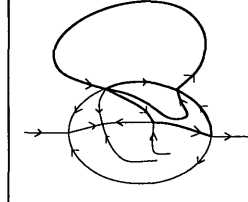
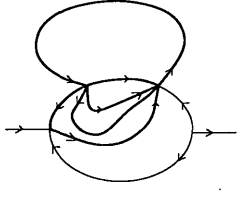
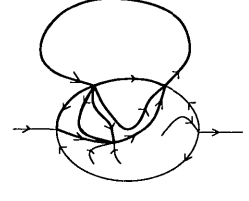
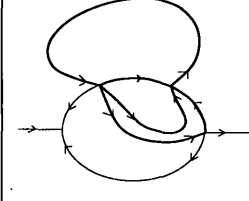
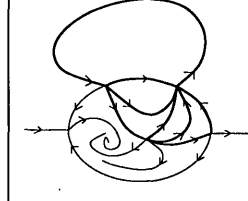
			
family Ehh1	family Ehh2	family Ehh3	family Ehh4
			
family Ehh5	family Ehh6	family Ehh7	family Ehh8
			
family Ehh9	family Ehh10	family Ehh11	family Ehh12

Table 2.2: Limit periodic sets of HH-type for the elliptic case [53]

2.5 Dulac maps near P_i ($i = 1, 2, 3, 4$)

For saddle and elliptic case, the family of vector fields at each point P_i ($i = 1, 2, 3, 4$) has the same form. Due to the special form of the family, after dividing by a C^∞ positive function, the system is linear in r and ρ . If necessary, one can reverse the time ($t \mapsto -t$), so that one will have two negative eigenvalues and the third eigenvalue is positive. So

for the three eigenvalues at each point, there are only two possibilities

$$-1, \quad 1, \quad -\sigma(a)$$

or

$$1, \quad -1, \quad -\sigma(a)$$

$$\text{where } \sigma(a) = \begin{cases} \left| \frac{1-2a}{a} \right|, & \text{at } P_1 \text{ and } P_2, \\ 2(1-2a), & \text{at } P_3 \text{ and } P_4. \end{cases}$$

By exchanging the roles of r and ρ , one only need to consider the following system

$$X_{(a, \bar{\mu})} \begin{cases} \dot{r} = -r, \\ \dot{\rho} = \rho, \\ \dot{\bar{y}} = -\sigma(a)\bar{y} + f_{(a, \bar{\mu})}(r, \rho, \bar{y}), \end{cases} \quad (2.5.16)$$

where

$$\begin{aligned} & f_{(a, \bar{\mu})}(r, \rho, \bar{y}) \\ &= \sigma(a)\bar{y} + \frac{-(1-2a)\bar{y} + 2\bar{y}^2 + \bar{y}[\varepsilon_2 r + \bar{\mu}_3 \rho + 2\bar{\mu}_2 \rho^2 - r^2 h_1(r, r\rho, \bar{\mu})] + \bar{\mu}_1 \rho^3 + r \bar{h}_2(r, r\rho, \bar{\mu}) + \bar{y}^2 \bar{Q}_2(r, \rho, \bar{y}, \bar{\mu})}{a + \bar{y} + \bar{\mu}_2 \rho^2} \end{aligned} \quad (2.5.17)$$

with the parameters $(a, \bar{\mu}) \in A \times \mathbb{S}^2$.

Remark 2.5.1. For the quadratic systems, we have $\bar{h}_2 \equiv 0$ in (2.5.17).

Proposition 2.5.2. [53] Consider the family $X_{(a, \bar{\mu})}$ in the form of (2.5.16) with parameters $(a, \bar{\mu}) \in A \times \mathbb{S}^2$. Then $\forall (a_0, \bar{\mu}) \in A \times \mathbb{S}^2$ and $\forall k \in \mathbb{N}$, there exists $A_0 \subset A$, a

neighborhood of a_0 , $N(k) \in \mathbb{N}$ and a C^k -transformation

$$\Psi_{(a, \bar{\mu})} : (r, \rho, \bar{y}) \longrightarrow (r, \rho, \psi_{(a, \bar{\mu})}(r, \rho, \bar{y})),$$

where

$$\psi_{(a, \bar{\mu})}(r, \rho, \bar{y}) = \bar{y} + o(|(r, \rho, \bar{y})|)$$

such that $\forall (a, \bar{\mu}) \in A_0 \times \mathbb{S}^2$, the map $\psi_{(a, \bar{\mu})}$ transforms $X_{(a, \bar{\mu})}$ into one of the following normal forms:

- if $\sigma(a_0) \notin \mathbb{Q}$

$$\tilde{X}_{(a, \bar{\mu})} \begin{cases} \dot{r} = -r, \\ \dot{\rho} = \rho, \\ \dot{y} = -\bar{\sigma}(a, \bar{\mu}, \nu)y, \end{cases} \quad (2.5.18)$$

- if $\sigma(a_0) = \frac{p}{q} \in \mathbb{Q}$

$$\tilde{X}_{(a, \bar{\mu})} \begin{cases} \dot{r} = -r, \\ \dot{\rho} = \rho, \\ \dot{y} = \kappa r^p + \frac{1}{q} \left[-p + \sum_{i=0}^{N(k)} \alpha_{i+1}(a, \bar{\mu}, \nu) (\rho^p y^q)^i \right] y, \end{cases} \quad (2.5.19)$$

where $\nu = r\rho > 0$ and

$$\begin{aligned} \bar{\sigma}(a, \bar{\mu}, \nu) &= \sigma(a) - \alpha_0(a, \bar{\mu}, \nu), \\ \alpha_0(a, \bar{\mu}, \nu) &= \sum_{i=1}^{N(k)} \gamma_i \nu^i, \\ \alpha_1(a, \bar{\mu}, \nu) &= p - \bar{\sigma}(a, \bar{\mu}, \nu)q, \end{aligned} \quad (2.5.20)$$

where $\gamma_i(a, \bar{\mu})$, α_i and κ are smooth functions defined for $(a, \bar{\mu}) \in A_0 \times \mathbb{S}^2$. Especially, $\kappa = 0$ for $q \geq 2$.

Notation 2.5.3. For convenience in the notation, in the following sections and chapters, let r_0 , ρ_0 and y_0 be positive constants, and we always use

$$\begin{aligned}\Sigma_i &= \{r_i = r_0\}, & i = 1, 2, 3, 4; \\ \Pi_i &= \{\rho_i = \rho_0\}, & i = 1, 2, 3, 4; \\ \tau_i &= \{\tilde{y}_i = y_0\}, & i = 1, 2; \\ \tau_i &= \{\tilde{y}_i = -y_0\}, & i = 3, 4,\end{aligned}\tag{2.5.21}$$

to denote the sections in normal form coordinates $(r_i, \rho_i, \tilde{y}_i)$ in the neighborhood of the singular points P_i ($i = 1, 2, 3, 4$).

In order to study the transition maps near the singular point P_i ($i = 1, 2, 3, 4$), one only need to consider $\tilde{X}_{(a, \bar{\mu})}$ with eigenvalues $-1, 1, -\sigma(a)$ in the normal forms (2.5.18) or (2.5.19) and consider the following two types of Dulac maps:

$$\begin{aligned}\Delta_{(a, \bar{\mu})} &= (d, D) : \Sigma \longrightarrow \Pi, \\ \Theta_{(a, \bar{\mu})} &= (\xi, \Xi) : \tau \longrightarrow \Pi,\end{aligned}$$

where $\Sigma = \{r = r_0\}$, $\Pi = \{\rho = \rho_0\}$ and $\tau = \{y = y_0\}$ are sections in the normal form coordinates.

The properties and explicit expressions of the two types of Dulac maps are given in the following two theorems, which were studied by Zhu and Rousseau in [53].

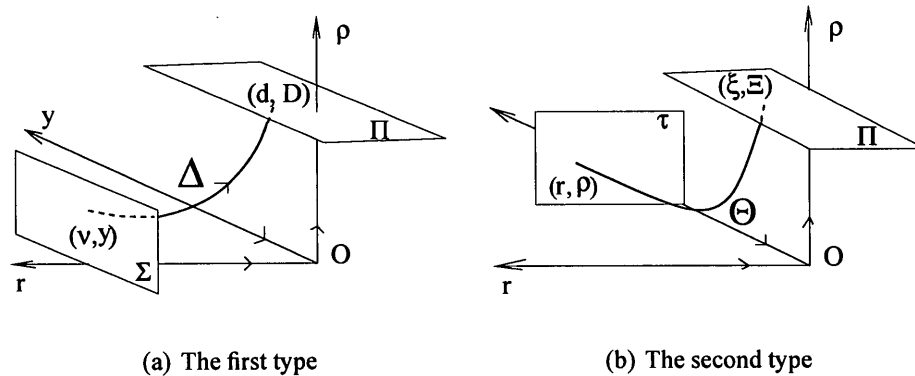


Figure 2.6: Two types of Dulac maps

Remark 2.5.4. *To simplify the notation, for all the maps and vector fields, we will drop the index $(a, \bar{\mu})$. For example, the Dulac map $\Delta(\nu, y)$ means $\Delta_{(a, \bar{\mu})}(\nu, y)$.*

Firstly we study the first type of Dulac map $\Delta = (d, D)$. If we parameterize the sections Σ and Π by (ν, y) with the obvious relation $\rho = \frac{\nu}{r_0}$ on Σ and $r = \frac{\nu}{\rho_0}$ on Π , then we have

Theorem 2.5.5. [53] *For any $a_0 \in A$ and $\bar{\mu} \in \mathbb{S}^2$, consider the family $\tilde{X}_{(a, \bar{\mu})}$ with eigenvalues $-1, 1, \sigma(a_0)$ in normal form (2.5.18) or (2.5.19). Then $\forall Y_0 \in \mathbb{R}$, there exist $A_0 \subset A$, a neighborhood of a_0 , and $\nu_1 > 0$ such that $\forall \nu \in (0, \nu_1)$ and $(a, \bar{\mu}, y) \in A_0 \times \mathbb{S}^2 \times [0, Y_0]$, the Dulac map $\Delta(\nu, y) = (d(\nu, y), D(\nu, y))$ has the form*

$$\begin{cases} d(\nu, y) = \nu, \\ D(\nu, y) = \eta(\nu, \omega(\frac{\nu}{\nu_0}, -\alpha_1)) + \left(\frac{\nu}{\nu_0}\right)^{\bar{\sigma}} \left[y + \phi(\nu, \omega(\frac{\nu}{\nu_0}, -\alpha_1), y) \right], \end{cases} \quad (2.5.22)$$

where $\nu_0 = r_0 \rho_0 > 0$ is a constant and

$$\text{if } \sigma(a_0) \notin \mathbb{Q}, \quad \eta = \phi = 0;$$

$$\text{if } \sigma(a_0) \in \mathbb{Q} \setminus \mathbb{N}, \quad \eta = 0;$$

$$\text{if } \sigma(a_0) = p \in \mathbb{N}, \quad \eta(\nu, \omega(\frac{\nu}{\nu_0}, -\alpha_1)) = \kappa r_0^p \omega(\frac{\nu}{\nu_0}, -\alpha_1) (\frac{\nu}{\nu_0})^{\bar{\sigma}};$$

if $\sigma(a_0) = \frac{p}{q} \in \mathbb{Q}$, $p, q \in \mathbb{N}$ and $(p, q) = 1$, then $\phi(\nu, \omega(\frac{\nu}{\nu_0}, -\alpha_1), y)$ is C^∞ and

$$\phi = O(\nu^{\bar{p}} \omega^{q+1}(\frac{\nu}{\nu_0}, -\alpha_1) \ln \frac{\nu}{\nu_0}),$$

$$\frac{\partial \phi}{\partial y} = O(\nu^{\bar{p}} \omega^q(\frac{\nu}{\nu_0}, -\alpha_1) \ln \frac{\nu}{\nu_0}),$$

$$\frac{\partial^j \phi}{\partial y^j} = O\left(\nu^{\bar{p}(1+\lfloor \frac{j-2}{q} \rfloor)} \omega^{q-j+1+\lfloor \frac{j-2}{q} \rfloor}(\frac{\nu}{\nu_0}, -\alpha_1) \ln \frac{\nu}{\nu_0}\right), \quad j \geq 2,$$

(2.5.23)

where

$$\bar{p} = \begin{cases} q\bar{\sigma}(a, \nu), & \alpha_1 \geq 0, \\ p, & \alpha_1 < 0. \end{cases}$$

Also all the partial derivatives with respect to the parameters $(a, \bar{\mu})$ are of order

$$O\left(\nu^{\bar{p}} \omega^q(\frac{\nu}{\nu_0}, -\alpha_1) \ln \frac{\nu}{\nu_0}\right).$$

Now we consider the second type Dulac map $\Theta = (\xi, \Xi)$. If we parameterize τ by (r, ρ) and Π by (ν, y) with the relation $r\rho = \nu$ and $r = \frac{\nu}{\rho_0}$ on the two sections respectively, then we have

Theorem 2.5.6. [53] For any $a_0 \in A$, consider $\tilde{X}_{(a, \bar{\mu})}$ with eigenvalues $-1, 1, -\sigma(a_0)$ in the normal form (2.5.18) or (2.5.19). Then for $r, \rho > 0$ sufficiently small, there exist

$A_0 \subset A$, a neighborhood of a_0 , and $\nu_1 > 0$ such that $\forall (a, \bar{\mu}) \in A_0 \times \mathbb{S}^2$ and $\nu \in (0, \nu_1)$,

the Dulac map $\Theta(r, \rho)$ has the form

$$\begin{cases} \xi(r, \rho) = \nu, \\ \Xi(r, \rho) = \eta(\nu, \omega(\frac{\rho}{\rho_0}, \alpha_1)) + (\frac{\rho}{\rho_0})^{\bar{\sigma}} [y_0 + \theta(r, \rho, \omega(\frac{\rho}{\rho_0}, -\alpha_1))], \end{cases} \quad (2.5.24)$$

where

- if $\sigma(a_0) \notin \mathbb{N}$, then $\eta = 0$; if $\sigma(a_0) = p \in \mathbb{N}$, then

$$\eta = \frac{\kappa}{\rho_0^p} \nu^p \omega(\frac{\rho}{\rho_0}, \alpha_1);$$

- if $\sigma(a_0) \notin \mathbb{Q}$, then $\theta = 0$; if $\sigma(a_0) = \frac{p}{q} \in \mathbb{Q}$, then $\theta(r, \rho, \omega(\frac{\rho}{\rho_0}, -\alpha_1))$ is C^∞ in $(a, \bar{\mu})$ and $(r, \rho, \omega(\frac{\rho}{\rho_0}, -\alpha_1))$, and also satisfies

$$\begin{aligned} \theta &= O\left(\rho^p \omega(\frac{\rho}{\rho_0}, \alpha_1) \left[1 + \kappa r^p \omega^2(\frac{\rho}{\rho_0}, -\alpha_1)\right]\right), \\ \rho^j \frac{\partial^j \theta}{\partial \rho^j} &= O\left(\rho^p \omega(\frac{\rho}{\rho_0}, \alpha_1) \left[1 + \kappa r^p \omega^2(\frac{\rho}{\rho_0}, -\alpha_1)\right]\right), \quad j \geq 1. \end{aligned} \quad (2.5.25)$$

which are uniformly valid for $(a, \bar{\mu}) \in A_0 \times \mathbb{S}^2$ and $r, \rho > 0$ sufficiently small.

Remark 2.5.7. For the quadratic systems, we have $\eta(\nu, \omega(\frac{\nu}{\nu_0}, -\alpha_1)) \equiv 0$ in (2.5.22) and $\eta(\nu, \omega(\frac{\rho}{\rho_0}, \alpha_1)) \equiv 0$ in (2.5.24). For the second type Dulac map, the inverse of Θ has the same form and properties as (2.5.24) and (2.5.25).

3 Finite cyclicity of (I_{12}^1)

For the graphic (I_{12}^1) , it is an HH-type graphic with a nilpotent saddle of multiplicity 3 at infinity and an invariant parabola as shown in Fig. 3.1.

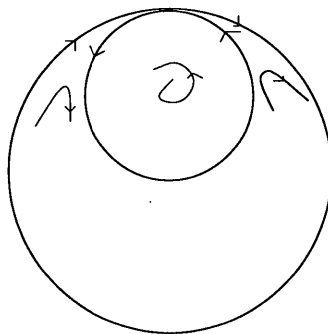


Figure 3.1: The graphic (I_{12}^1) .

In this chapter, firstly we prove the general theorem 3.1.1 for the finite cyclicity of a convex graphic through a nilpotent saddle of multiplicity 3 in section 3.1–3.3. According to the general theorem, to prove the finite cyclicity of (I_{12}^1) , we only need to check that the first return map P along the invariant parabola satisfies $P'(0) \neq 1$, which is given in section 3.4.

3.1 Main theorem

Theorem 3.1.1. *A convex graphic through a nilpotent saddle of multiplicity 3 has finite cyclicity provided that the derivative of the first return map $P'(0) \neq 1$.*

For the nilpotent saddle of multiplicity 3, it can be of codimension 3 or 4. The theorem with codimension 3 nilpotent saddle was proved in [53]. When $a_0 = -\frac{1}{2}$, the nilpotent saddle is of codimension 4. In this special case, only the limit periodic set $Sxhh1$ used the hypothesis $a_0 \neq -\frac{1}{2}$, so we only need to treat the case $Sxhh1$ with $a_0 = -\frac{1}{2}$.

The finite cyclicity of the upper boundary graphic of $Sxhh1$ was proved in [53], and $Cycl(Sxhh1a) \leq 1$. Therefore, we need to prove that the intermediate graphics and the lower boundary graphic of $Sxhh1$ have finite cyclicity, and the proof is given in the section 3.2 and section 3.3.

3.2 Preliminaries

Let Γ be any intermediate or lower boundary graphic of $Sxhh1$. To study its cyclicity, as shown in Fig. 3.2, take sections $\Pi_i = \{\rho_i = \rho_0\}$ in the normal form coordinates $(r_i, \rho_i, \tilde{y}_i)$ in the neighborhood of the singular point $P_i (i = 3, 4)$. We will study the

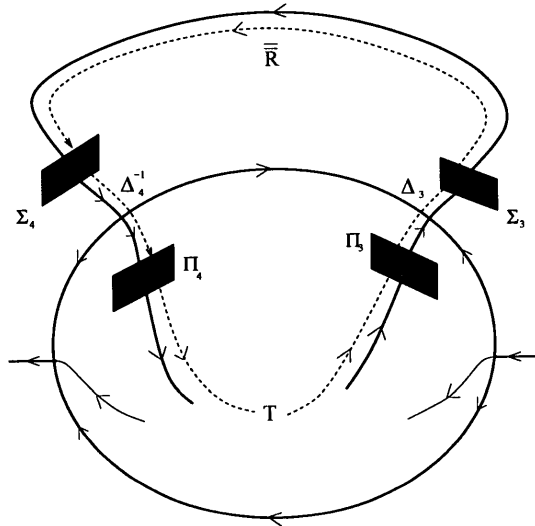


Figure 3.2: Transition maps for the HH-graphics of saddle type

displacement map

$$L : \Pi_4 \longrightarrow \Pi_3$$

$$L = R^{-1} - T,$$

where $R : \Pi_3 \longrightarrow \Pi_4$ is the transition map along the regular orbit in the normal form coordinates, and $T : \Pi_4 \longrightarrow \Pi_3$ is the transition map passing through the blown-up singularity. We will study the maximum number of small roots of $L = 0$.

For the transition map R , it has been studied in [53], and we recall it here as a proposition.

Proposition 3.2.1. [53] *For any $k \in \mathbb{N}$ and $\forall a_0 \in A = (-\frac{1}{2}, 0)$, there exist $A_0 \subset A$, a neighborhood of a_0 and $\nu_1 > 0$ such that $\forall (a, \bar{\mu}) \in A_0 \times \mathbb{S}^2$ and $\forall \nu \in (0, \nu_1)$,*

$R(\nu, \tilde{y}_3) = (R_1(\nu, \tilde{y}_3), R_2(\nu, \tilde{y}_3))$ is C^k and $R_1(\nu, \tilde{y}_3) = \nu$, $R_2(\nu, \tilde{y}_3)$ takes the following form

(1) if $a_0 \notin \mathbb{Q}$,

$$\begin{aligned} R_2(\nu, \tilde{y}_3) &= m_0(\nu) \left(\frac{\nu}{\nu_0}\right)^{-\bar{\sigma}_4} + (\gamma^* + O(\nu \ln \frac{\nu}{\nu_0})) \tilde{y}_3 \\ &\quad + \sum_{i=2}^k O(\nu^{(i-1)\bar{\sigma}_3}) \tilde{y}_3^i + O(\tilde{y}_3^{k+1}); \end{aligned} \quad (3.2.1)$$

2) if $a_0 \in \mathbb{Q}$,

$$R_2(\nu, \tilde{y}_3) = \gamma_0(\nu, \omega(\frac{\nu}{\nu_0}, -\beta_1)) + \sum_{i=1}^k \gamma_i(\nu, \omega(\frac{\nu}{\nu_0}, -\beta_1)) \tilde{y}_3^i + O(\tilde{y}_3^{k+1}), \quad (3.2.2)$$

where

$$\begin{aligned} \gamma_0 &= m_0(\nu) \left(\frac{\nu}{\nu_0}\right)^{-\bar{\sigma}_4} + \kappa_3 r_0^{\bar{p}_3} (\gamma^* - 1) \omega(\frac{\nu}{\nu_0}, -\beta_1) + \kappa_3 O(\nu^{\bar{\sigma}_3} \omega^2(\frac{\nu}{\nu_0}, -\beta_1)), \\ \gamma_1 &= \gamma^* + O(\nu \ln \frac{\nu}{\nu_0}) + O(\nu^{\bar{p}_3} \omega^{q_3}(\frac{\nu}{\nu_0}, -\beta_1) \ln \frac{\nu}{\nu_0}), \\ \gamma_i &= O(\nu \ln \frac{\nu}{\nu_0}) + O(\nu^{\bar{p}_3(1+\lfloor \frac{i-2}{q_3} \rfloor)} \omega^{q_3+1-i+q_3 \lfloor \frac{i-2}{q_3} \rfloor}(\frac{\nu}{\nu_0}, -\beta_1) \ln \frac{\nu}{\nu_0}) \quad i \geq 2. \end{aligned}$$

Here $\gamma^* = P'(0)$ and $\beta_1 = p_3 - \bar{\sigma}_3(a)q_3$. Also $R_2^{-1}(\nu, \tilde{y}_4)$ is C^k and has the same form as R_2 .

Remark 3.2.2. The above proposition was proved in [53] by straightforward calculations of the transition map R , which can be decomposed as

$$R = \Delta_4^{-1} \circ \overline{\overline{R}} \circ \Delta_3,$$

where $\Delta_i : \Pi_i \rightarrow \Sigma_i (i = 3, 4)$ are two Dulac transition maps of the first type in the

normal form coordinates near P_3 and P_4 , respectively. $\overline{R} : \Sigma_3 \rightarrow \Sigma_4$ is the regular transition map, and we can write it as

$$\begin{cases} \overline{R}_1(\nu, \tilde{y}_3) = \nu, \\ \overline{R}_2(\nu, \tilde{y}_3) = m_0(\nu) + m_1(\nu)\tilde{y}_3 + O(\tilde{y}_3^2), \end{cases} \quad (3.2.3)$$

where $m_0(0) = 0$, and $m_1(0) = \gamma^* + O(\nu)$.

In the proof, only the fact $\sigma_3(a) = 2(1 - 2a) > 0$ was used. So as long as $a < \frac{1}{2}$, the three maps Δ_3 , \overline{R} and Δ_4 keep the same expressions as the case for $a_0 \in (-\frac{1}{2}, 0)$. Therefore, the interval $A = (-\frac{1}{2}, 0)$ in the above proposition can be extended to $(-\infty, \frac{1}{2})$. Hence, if $a_0 \in (-\infty, \frac{1}{2})$, $R_2(\nu, \tilde{y}_3)$ has the same form as (3.2.1) or (3.2.2).

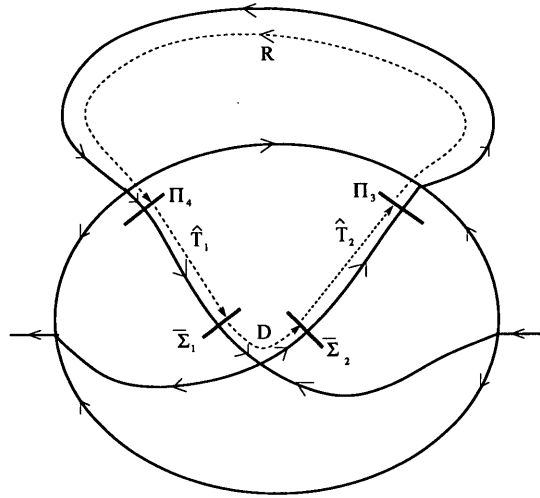


Figure 3.3: Transition maps for the lower boundary graphic Sxhh1c

In this chapter, we use $V \in \mathbb{S}^2$ to denote the set of the parameter $\bar{\mu}$ in which the family Sxhh1 exists. Family Sxhh1 has a lower boundary graphic Sxhh1c which passes

through a hyperbolic saddle point as shown in Fig 3.3. Let λ_0 be the hyperbolicity ratio at this saddle point when $r = 0$ for $\bar{\mu} = \bar{\mu}_0$ and $a = a_0$.

For the case $\lambda_0 \neq 1$, it was treated in [53], so we restrict ourself to the case $\lambda_0 = 1$ i.e., the divergence of system $\bar{X}_{\rho=1}$ in (2.4.15) vanishes. Note that $a_0 = -\frac{1}{2}$, so we have $\bar{\mu}_3 = 0$. Then in this case family Sxhh1 exists if and only $V = \{\bar{\mu} \in \mathbb{S}^2 | \bar{\mu}_3 = 0\}$.

Let the saddle point be (\bar{x}_0, \bar{y}_0) . After translating the singular point to the origin, by a linear transformation and C^k changes of coordinates, we can bring the system (2.4.14) in the neighborhood of the saddle point into a normal form

$$\begin{cases} \dot{\tilde{x}} = \tilde{x}, \\ \dot{\tilde{y}} = \tilde{y} \left[-1 + \sum_{i=0}^{N(k)} \alpha_i(r, \bar{\mu}, a) (\tilde{x}\tilde{y})^i \right], \\ \dot{r} = 0. \end{cases} \quad (3.2.4)$$

Take sections $\bar{\Sigma}_1 = \{\tilde{y} = 1\}$ and $\bar{\Sigma}_2 = \{\tilde{x} = 1\}$ in the normal form coordinates. Let $D(\nu, \tilde{x}) = (D_1(\nu, \tilde{x}), D_2(\nu, \tilde{x})) : \bar{\Sigma}_1 \longrightarrow \bar{\Sigma}_2$ be the transition map. Then $D_1(\nu, \tilde{x}) = \nu$, and $D_2(\nu, \tilde{x})$ is the Dulac map in the neighborhood of the saddle point. There exist V_0 , a neighborhood of $\bar{\mu}_0$, and $\varepsilon > 0$, $\nu_0 > 0$ sufficiently small, such that $\forall a \in (-\frac{1}{2} - \varepsilon, \frac{1}{2} + \varepsilon) \subset A$, $\forall \nu \in (0, \nu_0)$ and $\forall \bar{\mu} \in V_0$, $D(\nu, \tilde{x}) : \bar{\Sigma}_1 \longrightarrow \bar{\Sigma}_2$ can be written as

$$\begin{cases} D_1(\nu, \tilde{x}) = \nu, \\ D_2(\nu, \tilde{x}) = \alpha_1(\nu)[\tilde{x}\omega + \dots] + \tilde{x} + \alpha_2(\nu)[\tilde{x}^2\omega + \dots] + \dots, \end{cases} \quad (3.2.5)$$

where α_i are functions of $(\nu, \bar{\mu}, a)$ given in (3.2.4), $\alpha_1(\nu) = \lambda(\nu) - 1$ and $\omega = \omega(\tilde{x}, \alpha_1(\nu))$ is the *Leontovich-Andronova-Ecalle-Roussarie* compensator defined in (2.2.4).

Let $\widehat{T}_1 : \Pi_4 \longrightarrow \overline{\Sigma}_1$ and $\widehat{T}_2 : \overline{\Sigma}_2 \longrightarrow \Pi_3$. They are the compositions of normal form coordinate changes and regular transition maps. Therefore, $\widehat{T}_1(\nu, \tilde{y}_4)$ can be written as

$$\begin{cases} \widehat{T}_{11}(\nu, \tilde{y}_4) = \nu, \\ \widehat{T}_{12}(\nu, \tilde{y}_4) = e_0(\nu) + e_1(\nu)\tilde{y}_4 + O(\tilde{y}_4^2), \end{cases} \quad (3.2.6)$$

and $\widehat{T}_2(\nu, \tilde{y})$ can be written as

$$\begin{cases} \widehat{T}_{21}(\nu, \tilde{y}) = \nu, \\ \widehat{T}_{22}(\nu, \tilde{y}) = b_0(\nu) + b_1(\nu)\tilde{y} + O(\tilde{y}^2), \end{cases} \quad (3.2.7)$$

where $e_0(0) = 0$, $b_0(0) = 0$, $e_1(0) > 0$ and $b_1(0) > 0$.

In the following, we study the lower boundary graphic Sxhh1c and intermediate graphics Sxhh1b.

3.3 Proof of the main theorem

We treat the lower boundary graphic Sxhh1c and intermediate graphics Sxhh1b separately.

3.3.1 The lower boundary graphic Sxhh1c

For the transition map T , we have

$$T = \widehat{T}_2 \circ D \circ \widehat{T}_1.$$

Performing a change of parametrization on Π_4 , the displacement map $L : \Pi_4 \longrightarrow \Pi_3$

will be defined as

$$L(\nu, \tilde{Y}_4) = R^{-1}(\nu, \tilde{Y}_4 + \zeta(\nu)) - \tilde{T}(\nu, \tilde{Y}_4), \quad (3.3.8)$$

where $\zeta(\nu) = \widehat{T}_{12}^{-1}(\nu, 0)$ with $\zeta(0) = 0$, and $\tilde{T} = \widehat{T}_2 \circ D \circ \widehat{S}_1$. For \widehat{S}_1 , we have

$$\begin{cases} \widehat{S}_{11}(\nu, \tilde{Y}_4) = \nu, \\ \widehat{S}_{12}(\nu, \tilde{Y}_4) = \tilde{e}_1(\nu)\tilde{Y}_4 + \tilde{e}_2(\nu)\tilde{Y}_4^2 + O(\tilde{Y}_4^3), \end{cases} \quad (3.3.9)$$

where $\tilde{e}_1(0) = e_1(0) > 0$.

By (3.2.5), (3.2.7) and (3.3.9), for \tilde{T} we have

$$\begin{cases} \tilde{T}_1(\nu, \tilde{Y}_4) = \nu, \\ \tilde{T}_2(\nu, \tilde{Y}_4) = b_0(\nu) + \tilde{e}_1^{1-\alpha_1}(\nu)b_1(\nu)\alpha_1(\nu)[\tilde{Y}_4\omega(\tilde{Y}_4, \alpha_1) + \dots] \\ \quad + \tilde{e}_1(\nu)b_1(\nu)\tilde{Y}_4 + \dots \end{cases} \quad (3.3.10)$$

By (3.2.2), (3.3.8) and (3.3.10), we have

$$\begin{cases} L_1(\nu, \tilde{Y}_4) = 0, \\ L_2(\nu, \tilde{Y}_4) = c_0(\nu) + c_1(\nu)[\tilde{Y}_4\omega(\tilde{Y}_4, \alpha_1) + \dots] + c_2(\nu)\tilde{Y}_4 + \dots, \end{cases} \quad (3.3.11)$$

where

$$c_0(\nu) = \gamma_0(\nu, \omega(\frac{\nu}{\nu_0}, -\beta_1)) + O(\zeta(\nu)) - b_0(\nu),$$

$$c_1(\nu) = -\tilde{e}_1^{1-\alpha_1}(\nu)b_1(\nu)\alpha_1(\nu),$$

$$c_2(\nu) = \frac{1}{\gamma^*} + O(\nu^{\bar{p}_3}\omega^{q_3}(\frac{\nu}{\nu_0}, -\beta_1) \ln \frac{\nu}{\nu_0}) + O(\zeta(\nu)) - \tilde{e}_1(\nu)b_1(\nu).$$

In order to prove the cyclicity of S_{xhh1c} , we need the follow lemma.

Lemma 3.3.1. $\tilde{e}_1(0)b_1(0) = 1$ for $\nu = 0$, $\bar{\mu}_{30} = 0$ and $a_0 = -\frac{1}{2}$.

Proof. To calculate $\tilde{e}_1(\nu)b_1(\nu)$ for $\nu = 0$, $\bar{\mu}_{30} = 0$ and $a_0 = -\frac{1}{2}$, we can restrict ourself on the blown-up sphere $r = 0$ to study maps $\widehat{T}_1(0, \cdot)$ and $\widehat{T}_2(0, \cdot)$.

Since $a_0 = -\frac{1}{2}$, and $\bar{\mu}_{30} = 0$, in the chart F.R. on $r = 0$, we have system $\overline{X}_{\rho=1}$, which becomes

$$\begin{cases} \dot{\bar{x}} = \bar{\mu}_2 + \bar{y} - \frac{1}{2}\bar{x}^2 := \widehat{P}(\bar{x}, \bar{y}), \\ \dot{\bar{y}} = \bar{\mu}_1 + \bar{x}\bar{y} := \widehat{Q}(\bar{x}, \bar{y}). \end{cases} \quad (3.3.12)$$

We can use the quasi-homogeneous compactification

$$\begin{cases} \bar{x} = \pm \frac{1}{\rho_i}, \\ \bar{y} = \frac{\tilde{y}_i}{\rho_i^2}, \end{cases} \quad (i = 3, 4), \quad (3.3.13)$$

to study the singularities P_3 and P_4 at infinity of system (3.3.12), and obtain the normal forms in the neighborhood of P_3 and P_4 in the chart F.R. on $r = 0$. Near $P_3 = (0, 1)$, we have

$$\begin{cases} \dot{\rho}_3 = -\rho_3, \\ \dot{\tilde{y}}_3 = -4\tilde{y}_3 + \kappa_3\rho_3^4, \end{cases} \quad (3.3.14)$$

where κ_3 is the function of $\bar{\mu}$. Similarly, in the neighborhood of $P_4 = (0, 1)$, we have

$$\begin{cases} \dot{\rho}_4 = \rho_4, \\ \dot{\tilde{y}}_4 = 4\tilde{y}_4 - \kappa_3\rho_4^4. \end{cases} \quad (3.3.15)$$

Let $\pi_i = \{\rho_i = \rho_0\} (i = 3, 4)$ be the two line sections in the chart F. R. on $r = 0$ parameterized by $\tilde{y}_i (i = 3, 4)$, respectively. Let $\bar{\sigma}_1 = \{\tilde{y} = 1\}$ and $\bar{\sigma}_2 = \{\bar{x} = 1\}$ be the

two line sections near the saddle point in the chart F. R. on $r = 0$ parameterized by \tilde{x} and \tilde{y} , respectively. Then we are reduced to study the one dimensional transition maps

$$\hat{T}_{12}(0, \tilde{y}_4) : \pi_4 \longrightarrow \bar{\sigma}_1 \quad \text{and} \quad \hat{T}_{22}(0, \tilde{y}) : \bar{\sigma}_2 \longrightarrow \pi_3.$$

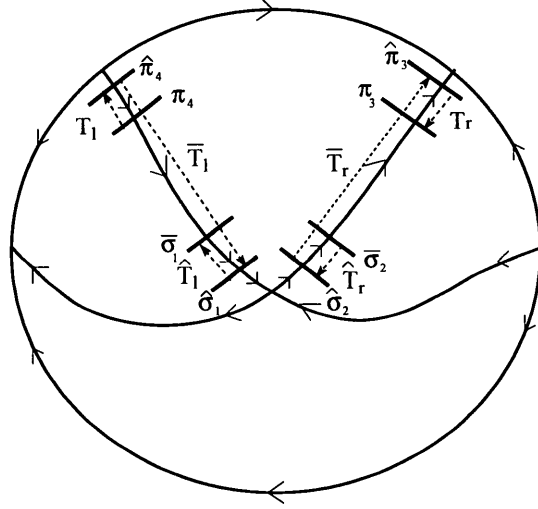


Figure 3.4: Transition maps for Sxhh1c in the chart F.R. on $r = 0$

To calculate the maps $\hat{T}_{12}(0, \tilde{y}_4)$ and $\hat{T}_{22}(0, \tilde{y})$, we introduce two auxiliary line sections $\hat{\pi}_i = \{\rho_i = \rho_{00}\}$ in the normal form coordinates (ρ_i, \tilde{y}_i) near $P_i (i = 3, 4)$ with $0 < \rho_{00} < \rho_0$, which are expressed as follows.

$$\begin{aligned} \hat{\pi}_3 &= \{(\bar{x}, \bar{y}) \mid \bar{x} = f_3(\hat{y}_3) = \frac{1}{\rho_{00}}, \\ &\quad \bar{y} = g_3(\hat{y}_3) = \frac{1}{\rho_{00}^2} (1 + \hat{y}_3 + \phi(\hat{y}_3) + \rho_{00} \psi_3(\rho_{00}, \hat{y}_3)) \}, \\ \hat{\pi}_4 &= \{(\bar{x}, \bar{y}) \mid \bar{x} = f_4(\hat{y}_4) = -\frac{1}{\rho_{00}}, \\ &\quad \bar{y} = g_4(\hat{y}_4) = \frac{1}{\rho_{00}^2} (1 + \hat{y}_4 + \phi(\hat{y}_4) + \rho_{00} \psi_4(\rho_{00}, \hat{y}_4)) \}, \end{aligned} \quad (3.3.16)$$

where $\phi(x) = O(x^2)$, $\psi_3(\rho_{00}, \hat{y}_3) = O(|\rho_{00}, \hat{y}_3|)$ and $\psi_4(\rho_{00}, \hat{y}_4) = O(|\rho_{00}, \hat{y}_4|)$.

We also introduce another two auxiliary line sections $\hat{\sigma}_1 = \{\tilde{y} = d_{00}\}$ and $\hat{\sigma}_2 = \{\tilde{x} = d_{00}\}$ in the normal form coordinates (\tilde{x}, \tilde{y}) with $0 < d_{00} < 1$.

As we know, after translating the singular point to the origin, by a linear transformation $T = \begin{pmatrix} t_1 & t_2 \\ t_3 & t_4 \end{pmatrix}$ and C^k normal change of coordinates, we can bring the system (3.3.12) into normal form near the saddle point (\bar{x}_0, \bar{y}_0) . Hence, on the blown-up sphere $r = 0$, $\hat{\sigma}_1$ and $\hat{\sigma}_2$ can be expressed in the original coordinates (\bar{x}, \bar{y}) as follows.

$$\begin{aligned} \hat{\sigma}_1 &= \{(\bar{x}, \bar{y}) | \bar{x} = f_1(\tilde{x}) = \bar{x}_0 + t_1\tilde{x} + t_2d_{00} + d_{00}O(\tilde{x}, d_{00}) + O(\tilde{x}^2), \\ &\quad \bar{y} = g_1(\tilde{x}) = \bar{y}_0 + t_3\tilde{x} + t_4d_{00} + d_{00}O(\tilde{x}, d_{00}) + O(\tilde{x}^2)\}, \\ \hat{\sigma}_2 &= \{(\bar{x}, \bar{y}) | \bar{x} = f_2(\tilde{y}) = \bar{x}_0 + t_1d_{00} + t_2\tilde{y} + d_{00}O(d_{00}, \tilde{y}) + O(\tilde{y}^2), \\ &\quad \bar{y} = g_2(\tilde{y}) = \bar{y}_0 + t_3d_{00} + t_4\tilde{y} + d_{00}O(d_{00}, \tilde{y}) + O(\tilde{y}^2)\}. \end{aligned}$$

Therefore, the map $\hat{T}_{12}(0, \tilde{y}_4) : \pi_4 \longrightarrow \bar{\sigma}_1$ can be calculated by the decomposition

$$\hat{T}_{12}(0, \tilde{y}_4) = \hat{T}_l \circ \bar{T}_l \circ T_l(\tilde{y}_4),$$

where $T_l : \pi_4 \longrightarrow \hat{\pi}_4$, $\bar{T}_l : \hat{\pi}_4 \longrightarrow \hat{\sigma}_1$ and $\hat{T}_l : \hat{\sigma}_1 \longrightarrow \bar{\sigma}_1$ are one dimensional regular transition maps. The map $\hat{T}_{22}(0, \tilde{y}) : \bar{\sigma}_2 \longrightarrow \pi_3$ can be calculated by the decomposition

$$\hat{T}_{22}(0, \tilde{y}) = T_r \circ \bar{T}_r \circ \hat{T}_r(\tilde{y}),$$

where $\hat{T}_r : \bar{\sigma}_2 \longrightarrow \hat{\sigma}_2$, $\bar{T}_r : \hat{\sigma}_2 \longrightarrow \hat{\pi}_3$ and $T_r : \hat{\pi}_3 \longrightarrow \pi_3$ are one dimensional regular transition maps.

For T_l and T_r , form (3.3.14) and (3.3.15), we have

$$\hat{y}_4 = T_l(\tilde{y}_4) = \left(\frac{\rho_{00}}{\rho_0}\right)^4 \tilde{y}_4 - \kappa_3 \rho_{00}^4 \ln\left(\frac{\rho_{00}}{\rho_0}\right), \quad (3.3.17)$$

$$\tilde{y}_3 = T_r(\hat{y}_3) = \left(\frac{\rho_0}{\rho_{00}}\right)^4 \hat{y}_3 + \kappa_3 \rho_0^4 \ln\left(\frac{\rho_{00}}{\rho_0}\right). \quad (3.3.18)$$

For \hat{T}_l and \hat{T}_r , using the formula in Theorem 2.2.1, we have

$$\hat{T}_l'(0) = d_{00} \text{ and } \hat{T}_r'(0) = d_{00}^{-1}. \quad (3.3.19)$$

Next, we study transition maps $\bar{T}_l : \hat{\pi}_4 \longrightarrow \hat{\sigma}_1$ and $\bar{T}_r : \hat{\sigma}_2 \longrightarrow \hat{\pi}_3$.

Let

$$\Delta_l(0) = \begin{vmatrix} \hat{P}(f_4(0), g_4(0)) & f_4'(0) \\ \hat{Q}(f_4(0), g_4(0)) & g_4'(0) \end{vmatrix} \text{ and } \tilde{\Delta}_l(0) = \begin{vmatrix} \hat{P}(f_1(0), g_1(0)) & f_1'(0) \\ \hat{Q}(f_1(0), g_1(0)) & g_1'(0) \end{vmatrix},$$

by the formula in Theorem 2.2.1, we have

$$\begin{aligned} \bar{T}_l'(0) &= \frac{\Delta_l(0)}{\tilde{\Delta}_l(0)} \exp\left(\int_{T(\hat{\pi}_4 \rightarrow \hat{\sigma}_1)} \text{div} X(\gamma(t)) \Big|_{(3.3.12)} dt\right) \\ &= \frac{\frac{1}{2} \rho_{00}^{-4} [1 + O(\rho_{00})]}{[t_3 t_4 - (t_1 t_4 + t_2 t_3) \bar{x}_0 - t_1 t_4 \bar{y}_0] d_{00} + O(d_{00}^2)} \exp(0), \end{aligned} \quad (3.3.20)$$

where $T(\hat{\pi}_4 \rightarrow \hat{\sigma}_1)$ denotes the time taken to travel along the lower graphic Γ from $\hat{\pi}_4$ to $\hat{\sigma}_1$.

Let

$$\Delta_r(0) = \begin{vmatrix} \hat{P}(f_2(0), g_2(0)) & f_2'(0) \\ \hat{Q}(f_2(0), g_2(0)) & g_2'(0) \end{vmatrix} \text{ and } \tilde{\Delta}_r(0) = \begin{vmatrix} \hat{P}(f_3(0), g_3(0)) & f_3'(0) \\ \hat{Q}(f_3(0), g_3(0)) & g_3'(0) \end{vmatrix}.$$

Similar to $\bar{T}'_l(0)$, for $\bar{T}'_r(0)$ we have

$$\begin{aligned}\bar{T}'_r(0) &= \frac{\Delta_r(0)}{\tilde{\Delta}_r(0)} \exp\left(\int_{T(\hat{\sigma}_2 \rightarrow \hat{\pi}_3)} \left. \operatorname{div} X(\gamma(t)) \right|_{(3.3.12)} dt\right) \\ &= \frac{[t_3 t_4 - (t_1 t_4 + t_2 t_3) \bar{x}_0 - t_1 t_4 \bar{y}_0] d_{00} + O(d_{00}^2)}{\frac{1}{2} \rho_{00}^{-4} [1 + O(\rho_{00})]} \exp(0),\end{aligned}\quad (3.3.21)$$

where $T(\hat{\sigma}_2 \rightarrow \hat{\pi}_3)$ denotes the time taken to travel along the lower graphic Γ from $\hat{\sigma}_2$ to $\hat{\pi}_3$.

From (3.2.6) and (3.2.7), we have

$$\tilde{e}_1(0) b_1(0) = e_1(0) b_1(0) = \frac{\partial \hat{T}_{12}(0, 0)}{\partial \tilde{y}_4} \frac{\partial \hat{T}_{22}(0, 0)}{\partial \tilde{y}}.$$

Therefore, by (3.3.17), (3.3.18), (3.3.19), (3.3.20) and (3.3.21), we have

$$\tilde{e}_1(0) b_1(0) = \lim_{(\rho_{00}, d_{00}) \rightarrow (0, 0)} \hat{T}'_l(0) \bar{T}'_l(0) T'_l(0) T'_r(0) \bar{T}'_r(0) \hat{T}'_r(0) = 1.$$

□

End of proof for Sxhh1c

From (3.3.11), we have

$$\frac{\partial L_2(\nu, \tilde{Y}_4)}{\partial \tilde{Y}_4} = c_1(\nu) [* \omega(\tilde{Y}_4, \alpha_1) + \dots] + c_2(\nu) + \dots.$$

Here we use the symbol $*$ to replace any continuous function of $(\nu, \bar{\mu}, a)$, which is nonzero at $(\nu, \bar{\mu}, a) = (0, \bar{\mu}_0, a_0)$. Let

$$\xi_1(\nu, \tilde{Y}_4) := \frac{\partial L_2(\nu, \tilde{Y}_4)}{\partial \tilde{Y}_4} \frac{\omega^{-1}(\tilde{Y}_4, \alpha_1)}{*1 + \dots} = c_1(\nu) + c_2(\nu) \frac{*1 + \dots}{*1 + \dots} \frac{1}{\omega(\tilde{Y}_4, \alpha_1)} + \dots.$$

The zeros of $\frac{\partial L_2(\nu, \tilde{Y}_4)}{\partial \tilde{Y}_4}$ are zeros of the function $\xi_1(\nu, \tilde{Y}_4)$ in a small neighborhood of $\tilde{Y}_4 = 0$.

Differentiate $\xi_1(\nu, \tilde{Y}_4)$ with respect to \tilde{Y}_4 , and we have

$$\frac{\partial \xi_1(\nu, \tilde{Y}_4)}{\partial \tilde{Y}_4} = *c_2(\nu) \frac{\tilde{Y}_4^{-1-\alpha_1} + \dots}{*1 + \dots} \frac{1}{\omega^2(\tilde{Y}_4, \alpha_1)} + \dots .$$

Let

$$\xi_2(\nu, \tilde{Y}_4) = \omega^2(\tilde{Y}_4, \alpha_1) \frac{*1 + \dots}{*\tilde{Y}_4^{-1-\alpha} + \dots} \frac{\partial \xi_1(\nu, \tilde{Y}_4)}{\partial \tilde{Y}_4},$$

then we have

$$\xi_2(\nu, \tilde{Y}_4) = *c_2(\nu) + \dots . \quad (3.3.22)$$

Since $\gamma^* \neq 1$, so $c_2(0) = \frac{1}{\gamma^*} - \tilde{e}_1(0)b_1(0) = \frac{1}{\gamma^*} - 1 \neq 0$ for $\nu = 0$, $\bar{\mu}_{30} = 0$ and $a_0 = -\frac{1}{2}$. Because the remainder in (3.3.22) is $o(1)$. Hence, there exist A_0 , a neighborhood of a_0 , V_0 , a neighborhood of $\bar{\mu}_0$, and $\nu_1 > 0$, such that $\forall (a, \bar{\mu}) \in A_0 \times V_0$ and $\forall \nu \in (0, \nu_1)$, we have $\xi_2(\nu, \tilde{Y}_4) \neq 0$ in a small neighborhood of $\tilde{Y}_4 = 0$.

By Rolle's Theorem, $\forall (a, \bar{\mu}) \in A_0 \times V_0$ and $\forall \nu \in (0, \nu_1)$, the map $L_2(\nu, \tilde{Y}_4) = 0$ has at most 2 zeros in a small neighborhood of $\tilde{Y}_4 = 0$, i.e., $Cycl(Sxhh1c) \leq 2$.

3.3.2 The intermediate graphics Sxhh1b

For the intermediate graphics Sxhh1b, we can write the regular transition map T as

$$\begin{cases} T_1(\nu, \tilde{y}_4) = \nu, \\ T_2(\nu, \tilde{y}_4) = c_0(\nu) + c_1(\nu)\tilde{y}_4 + O(\tilde{y}_4^2), \end{cases} \quad (3.3.23)$$

where $c_0(0) = 0$ and $c_1(0) \neq 0$.

Hence, by (3.2.2) and (3.3.23), the displacement map $L = R^{-1} - T$ has the following form

$$\begin{cases} L_1(\nu, \tilde{y}_4) = 0, \\ L_2(\nu, \tilde{y}_4) = \gamma_0(\nu, \omega(\frac{\nu}{\nu_0}, -\beta_3)) + \left[\frac{1}{\gamma^*} + O(\nu^{\bar{p}_3} \omega^{q_3}(\frac{\nu}{\nu_0}, -\beta_1) \ln \frac{\nu}{\nu_0}) \right] \tilde{y}_4 \\ \quad + O(\tilde{y}_4^2) - [c_0(\nu) + c_1(\nu) \tilde{y}_4 + O(\tilde{y}_4^2)]. \end{cases} \quad (3.3.24)$$

In order to prove the cyclicity of Sxhh1b, we need the follow lemma.

Lemma 3.3.2. $T_2(0, \tilde{y}_4)$ is an identity for $\nu = 0$, $\bar{\mu}_{30} = 0$ and $a_0 = -\frac{1}{2}$.

Proof. Just as we did for Sxhh1c, let $\pi_i = \{\rho_i = \rho_0\}$ ($i = 3, 4$) be the two line sections in the chart F. R. on $r = 0$ parameterized by \tilde{y}_i ($i = 3, 4$), respectively. Then we are reduced to study the one dimensional transition map

$$T_2(0, \tilde{y}_4) : \pi_4 \longrightarrow \pi_3.$$

To calculate the map $T_2(0, \tilde{y}_4)$, again we introduce two auxiliary sections $\hat{\pi}_i = \{\rho_i = \rho_{00}\}$ ($i = 3, 4$) in the normal form coordinates in the chart F.R. on $r = 0$ with $0 < \rho_{00} < \rho_0$. Then the map $T_2(0, \tilde{y}_4)$ can be calculated by the decomposition

$$T_2(0, \tilde{y}_4) = T_r \circ \bar{T} \circ T_l(\tilde{y}_4),$$

where $T_l : \pi_4 \longrightarrow \hat{\pi}_4$, $\bar{T} : \hat{\pi}_4 \longrightarrow \hat{\pi}_3$ and $T_r : \hat{\pi}_3 \longrightarrow \pi_3$ are one dimensional regular transition maps as shown in Fig 3.5.

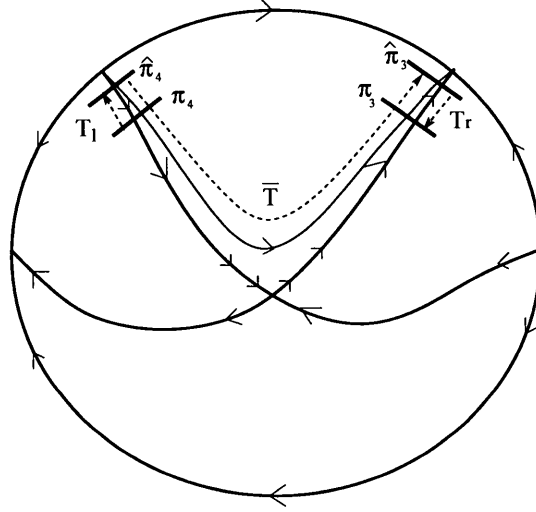


Figure 3.5: Transition maps for the family Sxhh1b in the chart F.R. on $r = 0$

The transition maps T_l and T_r have been explicitly given in (3.3.17) and (3.3.18).

Next, we study the transition map $\bar{T} : \hat{\pi}_4 \longrightarrow \hat{\pi}_3$. For sections $\hat{\pi}_3$ and $\hat{\pi}_4$, we can write them in the original coordinates (\bar{x}, \bar{y}) with $\hat{\pi}_3 = \{\bar{x} = f_3(\hat{y}_3), \bar{y} = g_3(\hat{y}_3)\}$, $\hat{\pi}_4 = \{\bar{x} = f_4(\hat{y}_4), \bar{y} = g_4(\hat{y}_4)\}$. Here, $f_3(\hat{y}_3)$, $g_3(\hat{y}_3)$, $f_4(\hat{y}_4)$ and $g_4(\hat{y}_4)$ are given in (3.3.16).

System (3.3.12) is Hamiltonian with the first integral

$$H(\bar{x}, \bar{y}) = -\bar{\mu}_1 \bar{x} + \bar{\mu}_2 \bar{y} + \frac{1}{2} \bar{y}^2 - \frac{1}{2} \bar{x}^2 \bar{y},$$

so we have $H(f_4(\hat{y}_4), g_4(\hat{y}_4)) = H(f_3(\hat{y}_3), g_3(\hat{y}_3))$. Let $\rho_{00} \rightarrow 0$, then we have

$$(1 + \hat{y}_4 + \phi(\hat{y}_4))(\hat{y}_4 + \phi_3(\hat{y}_4)) = (1 + \hat{y}_3 + \phi(\hat{y}_3))(\hat{y}_3 + \phi_3(\hat{y}_3)).$$

By implicit function theorem, when \hat{y}_4 is in a small neighborhood of $\hat{y}_4 = 0$, we have

$$\hat{y}_3 = \bar{T}(\hat{y}_4) = \hat{y}_4. \quad (3.3.25)$$

Therefore, by (3.3.17), (3.3.18) and (3.3.25), we have

$$T_2(0, \tilde{y}_4) = T_r \circ \bar{T} \circ T_l(\tilde{y}_4) = \tilde{y}_4.$$

So $T_2(0, \tilde{y}_4)$ is an identity for $\nu = 0$, $\bar{\mu}_3 = 0$ and $a_0 = -\frac{1}{2}$.

□

End of proof for Sxhh1b

Hence, for the displacement map $L = R^{-1} - T$, by (3.3.24), we have

$$\frac{\partial L_2(\nu, \tilde{y}_4)}{\partial \tilde{y}_4} = \frac{1}{\gamma^*} - c_1(\nu) + O(\nu, \nu^{\bar{p}_3} \omega^{q_3}(\frac{\nu}{\nu_0}, -\beta_1) \ln \frac{\nu}{\nu_0}) + O(\tilde{y}_4).$$

From Lemma 3.3.2, we have $c_1(0) = 1$ for $\nu = 0$, $\bar{\mu}_{30} = 0$ and $a_0 = -\frac{1}{2}$. Since $\gamma^* \neq 1$, so there exist A_0 , a neighborhood of a_0 , V_0 , a neighborhood of $\bar{\mu}_0$, and $\nu_1 > 0$, such that $\forall (a, \bar{\mu}) \in A_0 \times V_0$ and $\forall \nu \in (0, \nu_1)$, we have $\frac{\partial L_2(\nu, \tilde{y}_4)}{\partial \tilde{y}_4} \neq 0$ in a small neighborhood of $\tilde{y}_4 = 0$.

By Rolle's Theorem, $\forall (a, \bar{\mu}) \in A_0 \times V_0$ and $\forall \nu \in (0, \nu_1)$, the map $L_2(\nu, \tilde{y}_4) = 0$ has at most one zero in a small neighborhood of $\tilde{y}_4 = 0$, i.e., $Cycl(Sxhh1b) \leq 1$.

Altogether, we obtain that all the generic convex graphics with a nilpotent saddle point of multiplicity 3 have finite cyclicity, thus completing the proof of Theorem 3.1.1.

3.4 Finite cyclicity of (I_{12}^1)

Theorem 3.4.1. *The graphic (I_{12}^1) has finite cyclicity.*

Proof. For (I_{12}^1) , it is an HH-type graphic with a nilpotent saddle of multiplicity 3 at infinity and an invariant parabola as shown in Fig 3.1.

To prove the finite cyclicity of (I_{12}^1) , we only need to check that the first return map P along the invariant parabola satisfies $P'(0) \neq 1$. By [15], the graphic (I_{12}^1) occurs in the family

$$\begin{cases} \dot{x} = \lambda x - y + \varepsilon_1 x^2, \\ \dot{y} = x + \lambda y + \delta_1 x^2 + \delta_2 xy, \end{cases} \quad (3.4.26)$$

where $\lambda \neq 0$, $0 < \delta_2 < \varepsilon_1$, $\delta_1 = \lambda(3\varepsilon_1 - \delta_2) > 0$ and $4\varepsilon_1\lambda^2 - (1 + \lambda^2)\delta_2 < 0$. By rescaling we can assume that $\varepsilon_1 = 1$. Then (3.4.26) becomes

$$\begin{cases} \dot{x} = \lambda x - y + x^2, \\ \dot{y} = x + \lambda y + \lambda(3 - \delta_2)x^2 + \delta_2 xy, \end{cases} \quad (3.4.27)$$

with $\Delta_0 = (1 + \lambda^2)\delta_2 - 4\lambda^2 > 0$ and $\lambda \neq 0$. System (3.4.27) has an invariant parabola

$$y = \left(1 - \frac{\delta_2}{2}\right)x^2 - \lambda x - \frac{1}{2}(1 + \lambda^2). \quad (3.4.28)$$

Along the invariant parabola (3.4.28), we have

$$\begin{aligned}
 P'(0) &= \exp \left(\int_{-\infty}^{\infty} \operatorname{div} X(\gamma(t)) \Big|_{(3.4.27)} dt \right) \\
 &= \lim_{x_0 \rightarrow \infty} \exp \left(2 \int_{-x_0}^{x_0} \frac{2\lambda + (2 + \delta_2)x}{\delta_2 x^2 + 4\lambda x + 1 + \lambda^2} dx \right) \\
 &= \lim_{x_0 \rightarrow \infty} \left[\left(\frac{\delta_2 x_0^2 + 4\lambda x_0 + 1 + \lambda^2}{\delta_2 x_0^2 - 4\lambda x_0 + 1 + \lambda^2} \right)^{\frac{2+\delta_2}{\delta_2}} \exp \left(-\frac{16\lambda}{\delta_2 \sqrt{\Delta_0}} \arctan \frac{\delta_2 x + 2\lambda}{\sqrt{\Delta_0}} \right) \Big|_{-x_0}^{x_0} \right] \\
 &= \exp \left(-\frac{16\lambda\pi}{\delta_2 \sqrt{\Delta_0}} \right) \\
 &\neq 1.
 \end{aligned}$$

Therefore, we finish the proof.

□

4 Finite cyclicity of (I_{13}^1)

For the graphic (I_{13}^1) , it is an HH-type graphic with a nilpotent saddle at infinity. Compared to the graphic (I_{12}^1) , there is an additional attracting saddle-node on the invariant parabola for the graphic (I_{13}^1) as shown in Fig. 4.1 .

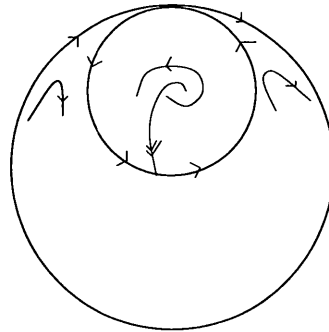


Figure 4.1: The graphic (I_{13}^1) .

In this chapter, firstly we will give a main theorem that the graphic (I_{13}^1) has finite cyclicity in section 4.1, and then we prove the main theorem by showing that all the upper boundary graphics have finite cyclicity in section 4.2, and all the lower boundary graphics and intermediate graphics have finite cyclicity in section 4.3.

4.1 Main theorem

Theorem 4.1.1. *The graphic (I_{13}^1) has finite cyclicity inside quadratic systems.*

Since the graphics (I_{13}^1) has a nilpotent singular point at infinity, we can limit ourselves to the limit periodic sets which have an invariant line ($\bar{\mu}_1 = 0$). Moreover the connection along this line is fixed. Therefore, we only need to look to the limit periodic sets Sxhh1, Sxhh4–Sxhh8.

To prove the finite cyclicity of graphic (I_{13}^1) , we have to prove that all the upper boundary graphics, the intermediate graphics and lower boundary graphics of Sxhh1, Sxhh4–Sxhh8 have finite cyclicity.

We begin with the upper boundary graphics.

4.2 The upper boundary graphic

Proposition 4.2.1. *For the graphic (I_{13}^1) , $Cycl(Sxhhia) \leq 1, i = 1, 2, \dots, 10$.*

Proof. As shown in Fig. 4.2, let $\bar{\Sigma}_3 = \{\tilde{X}_3 = 1\}$ and $\bar{\Sigma}_4 = \{\tilde{X}_3 = -1\}$ be the two sections transversal to the graphics in the normal form coordinates $(\tilde{X}_3, \tilde{Y}_3)$ near the saddle-node point.

We consider the Poincaré first return map P defined on the section Σ_4 :

$$P : \Sigma_4 \longrightarrow \Sigma_4,$$

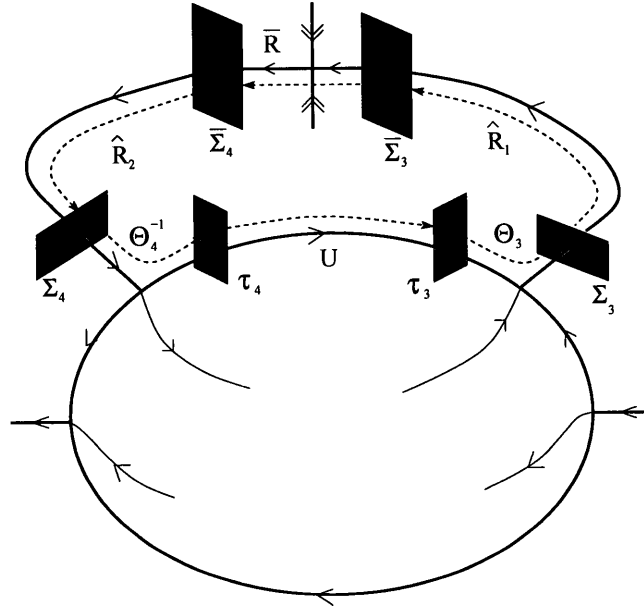


Figure 4.2: Upper boundary graphics of saddle type

which can be calculated by the composition

$$P = \hat{R}_2 \circ \bar{R} \circ \hat{R}_1 \circ \Theta_3 \circ U \circ \Theta_4^{-1}, \quad (4.2.1)$$

where

- $\Theta_i : \tau_i \longrightarrow \Sigma_i$ are the second type of Dulac maps in the neighborhood of P_i ($i = 3, 4$). The second type of Dulac maps $\Theta_i = (\xi_i, \Xi_i)$ ($i = 3, 4$) have the expression

$$\begin{cases} \xi_i(r_i, \rho_i) = \nu, \\ \Xi_i(r_i, \rho_i) = \eta_i(\nu, \omega(\frac{r_i}{r_0}, \beta_1)) + (\frac{r_i}{r_0})^{\bar{\sigma}_i} [y_0 + \theta_i(r_i, \rho_i, \omega(\frac{r_i}{r_0}, -\beta_1))], \end{cases} \quad (4.2.2)$$

where $\beta_1 = p_3 - \bar{\sigma}_3(a)q_3$.

- $U : \tau_4 \longrightarrow \tau_3$ is a regular transition map which can be written as

$$\begin{cases} U_1(r_4, \rho_4) = r_4(j(\nu) + O(|r_4, \rho_4|)), \\ U_2(r_4, \rho_4) = \rho_4(\hat{j}(\nu) + O(|r_4, \rho_4|)), \end{cases} \quad (4.2.3)$$

where $j(0) = 1$ was calculated in Proposition 5.8 of [53] and $\hat{j}(0) = j(0)^{-1} = 1$.

- $\hat{R}_1 : \Sigma_3 \longrightarrow \bar{\Sigma}_3$ is a regular transition map which can be written as

$$\begin{cases} \hat{R}_{11}(\nu, \tilde{y}_3) = \nu, \\ \hat{R}_{12}(\nu, \tilde{y}_3) = l_0(\nu) + l_1(\nu)\tilde{y}_3 + O(\tilde{y}_3^2), \end{cases} \quad (4.2.4)$$

where $l_0(0) = 0$ and $l_1(0) > 0$.

- $\bar{R} : \bar{\Sigma}_3 \longrightarrow \bar{\Sigma}_4$ is a central transition map near the attracting saddle-node point in the normal form coordinates $(\tilde{X}_3, \tilde{Y}_3)$, which can be written as

$$\begin{cases} \bar{R}_1(\nu, \tilde{Y}_3) = \nu, \\ \bar{R}_2(\nu, \tilde{Y}_3) = m(\nu)\tilde{Y}_3, \end{cases} \quad (4.2.5)$$

where $m(\nu) \rightarrow 0$ as $\nu \rightarrow 0$.

- $\hat{R}_2 : \bar{\Sigma}_4 \longrightarrow \Sigma_4$ is a regular transition map which can be written as

$$\begin{cases} \hat{R}_{21}(\nu, \tilde{Y}_4) = \nu, \\ \hat{R}_{22}(\nu, \tilde{Y}_4) = n_0(\nu) + n_1(\nu)\tilde{Y}_4 + O(\tilde{Y}_4^2), \end{cases} \quad (4.2.6)$$

where $n_0(0) = 0$ and $n_1(0) > 0$.

Define

$$\begin{aligned}\tilde{U} : \Sigma_4 &\longrightarrow \Sigma_3 \\ (\nu, \tilde{y}_4) &\longrightarrow (\nu, \tilde{U}_2(\nu, \tilde{y}_4)) \\ \tilde{U} &= \Theta_3 \circ U \circ \Theta_4^{-1}.\end{aligned}\tag{4.2.7}$$

For its first component of \tilde{U} , we have $\tilde{U}_1(\nu, \tilde{y}_4) = \nu$. For the second component $\tilde{U}_2(\nu, \tilde{y}_4)$, it has already been shown in [53] that

$$\frac{\partial \tilde{U}_2(0, 0)}{\partial \tilde{y}_4} = 1.\tag{4.2.8}$$

Define

$$\begin{aligned}\tilde{R} : \Sigma_3 &\longrightarrow \Sigma_4 \\ (\nu, \tilde{y}_3) &\longrightarrow (\nu, \tilde{R}_2(\nu, \tilde{y}_3)) \\ \tilde{R} &= \hat{R}_2 \circ \bar{R} \circ \hat{R}_1\end{aligned}\tag{4.2.9}$$

For $\tilde{R}(\nu, \tilde{y}_3)$, by (4.2.4), (4.2.5) and (4.2.6), we have

$$\begin{cases} \tilde{R}_1(\nu, \tilde{y}_3) = \nu, \\ \tilde{R}_2(\nu, \tilde{y}_3) = \hat{n}_0(\nu) + m(\nu)[\hat{n}_1(\nu)\tilde{y}_3 + O(\tilde{y}_3^2)], \end{cases}$$

where

$$\hat{n}_0(\nu) = n_0(\nu) + O(m(\nu)l_0(\nu)),$$

$$\hat{n}_1(\nu) = l_1(\nu)n_1(\nu) + O(m(\nu)l_0(\nu)).$$

Therefore,

$$\frac{\partial \tilde{R}_2(\nu, \tilde{y}_3)}{\partial \tilde{y}_3} = m(\nu)[l_1(\nu)n_1(\nu) + O(m(\nu)l_0(\nu))] + O(\tilde{y}_3).\tag{4.2.10}$$

So there exist A_0 , a neighborhood of a_0 and $\nu_1 > 0$, such that $\forall (a, \bar{\mu}, \nu) \in A_0 \times \mathbb{S}^2 \times (0, \nu_1)$, $\frac{\partial \tilde{R}_2(\nu, \tilde{y}_3)}{\partial \tilde{y}_3}$ is sufficiently small in a small neighborhood of $\tilde{y}_3 = 0$.

For the first return map P defined by (4.2.1), by the definition \tilde{R} and \tilde{U} , we have

$$P(\nu, \tilde{y}_4) = \tilde{R} \circ \tilde{U}(\nu, \tilde{y}_4).$$

The first component of P satisfies $P_1(\nu, \tilde{y}_4) = \nu$. Let $\tilde{y}_3 = \tilde{U}_2(\nu, \tilde{y}_4)$, then for the second component $P_2(\nu, \tilde{y}_4)$, we have

$$\frac{\partial P_2(\nu, \tilde{y}_4)}{\partial \tilde{y}_4} = \frac{\partial R_2(\nu, \tilde{y}_3)}{\partial \tilde{y}_3} \frac{\partial \tilde{U}_2(\nu, \tilde{y}_4)}{\partial \tilde{y}_4}.$$

By (4.2.8) and (4.2.10), we have that $\forall (a, \bar{\mu}, \nu) \in A_0 \times \mathbb{S}^2 \times (0, \nu_1)$, $\frac{\partial P_2(\nu, \tilde{y}_4)}{\partial \tilde{y}_4}$ is sufficiently small in a small neighborhood of $\tilde{y}_4 = 0$. Hence, by Rolle's theorem, the first return map P has at most 1 fixed point in the neighborhood of $(\nu, \tilde{y}_4) = (0, 0)$, i.e., $Cycl(Sxhhia) \leq 1, i = 1, 2, \dots, 10$.

□

Remark 4.2.2. *In the proof of Proposition 4.2.1, we only use the fact $\sigma_3(a) = 2(1 - 2a) > 0$, so for the elliptic case with $a \in (0, \frac{1}{2})$, the same proof gives that for upper boundary HH-graphic of elliptic type, $Cycl(Ehhia) \leq 1, i = 1, 2, \dots, 12$.*

4.3 The intermediate and lower boundary graphics

Let Γ be any intermediate or lower boundary graphic. To study its cyclicity, as shown in Fig. 4.3, take sections $\Pi_i = \{\rho_i = \rho_0\}$ in the normal form coordinates $(r_i, \rho_i, \tilde{y}_i)$ in the

neighborhood of the singular point P_i ($i=3, 4$). We will study the displacement map

$$L : \Pi_3 \longrightarrow \Pi_4$$

$$L = R - T^{-1},$$

where $R : \Pi_3 \longrightarrow \Pi_4$ is the transition map along the regular orbit in the normal form coordinates, and $T : \Pi_4 \longrightarrow \Pi_3$ is the transition map passing through the blown-up singularity. We study the number of small roots of $L = 0$. The maximum number of roots bounds the cyclicity.

We begin with the transition map R .

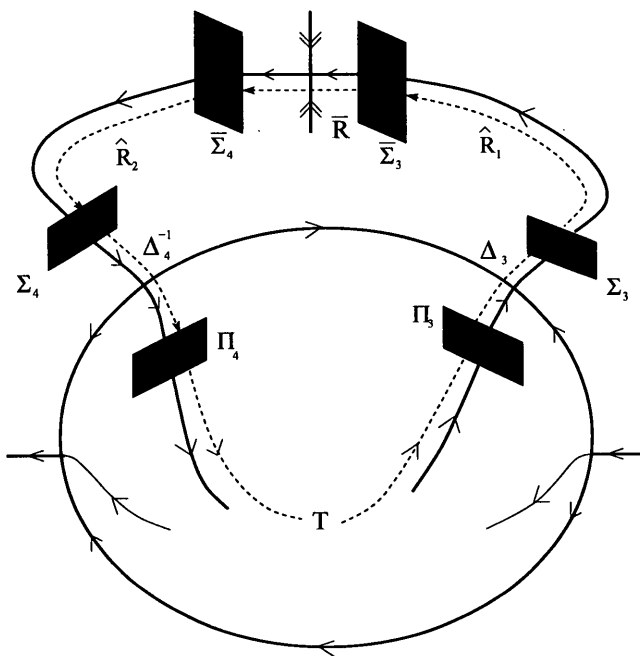


Figure 4.3: Transition maps for the HH-graphics of saddle type

Proposition 4.3.1. For any $k \in \mathbb{N}$ and $\forall a_0 \in A = (-\infty, \frac{1}{2})$, there exist $A_0 \subset A$, a neighborhood of a_0 and $\nu_1 > 0$ such that $\forall (a, \bar{\mu}) \in A_0 \times \mathbb{S}^2$ and $\forall \nu \in (0, \nu_1)$, $R(\nu, \tilde{y}_3) = (R_1(\nu, \tilde{y}_3), R_2(\nu, \tilde{y}_3))$ is C^k and $R_1(\nu, \tilde{y}_3) = \nu$, $R_2(\nu, \tilde{y}_3)$ takes the following form

(1) if $a_0 \notin \mathbb{Q}$,

$$\begin{aligned} R_2(\nu, \tilde{y}_3) &= \left(n_0(\nu) + O(m) \right) \left(\frac{\nu}{\nu_0} \right)^{-\bar{\sigma}_4} \\ &\quad + m(\nu) \left[l_1(\nu) n_1(\nu) + O(\nu \ln \frac{\nu}{\nu_0}) + O(m) \right] \tilde{y}_3 \\ &\quad + m(\nu) \left[\sum_{i=2}^k O(\nu^{(i-1)\bar{\sigma}_3}) \tilde{y}_3^i + O(\tilde{y}_3^{k+1}) \right]; \end{aligned}$$

2) if $a_0 \in \mathbb{Q}$,

$$\begin{aligned} R_2(\nu, \tilde{y}_3) &= \gamma_0(\nu, \omega(\frac{\nu}{\nu_0}, -\beta_1), m(\nu)) \\ &\quad + m(\nu) \left[\sum_{i=1}^k \gamma_i(\nu, \omega(\frac{\nu}{\nu_0}, -\beta_1), m(\nu)) \tilde{y}_3^i + O(\tilde{y}_3^{k+1}) \right], \end{aligned} \quad (4.3.11)$$

where

$$\begin{aligned} \gamma_0 &= (n_0(\nu) + O(m)) \left(\frac{\nu}{\nu_0} \right)^{-\bar{\sigma}_4} + \kappa_3 O(r_0^{\bar{p}_3} \omega(\frac{\nu}{\nu_0}, -\beta_1)), m \nu^{\bar{\sigma}_3} \omega^2(\frac{\nu}{\nu_0}, -\beta_1), \\ \gamma_1 &= l_1(\nu) n_1(\nu) + O(m(\nu)) + O(\nu \ln \frac{\nu}{\nu_0}) + O(\nu^{\bar{p}_3} \omega^{q_3}(\frac{\nu}{\nu_0}, -\beta_1) \ln \frac{\nu}{\nu_0}), \\ \gamma_i &= O(m(\nu)) + O(\nu \ln \frac{\nu}{\nu_0}) + O(\nu^{\bar{p}_3(1 + \lfloor \frac{i-2}{q_3} \rfloor)} \omega^{q_3+1-i+q_3 \lfloor \frac{i-2}{q_3} \rfloor}(\frac{\nu}{\nu_0}, -\beta_1) \ln \frac{\nu}{\nu_0}) \quad i \geq 2. \end{aligned}$$

Proof. We only consider the second case $a_0 \in \mathbb{Q}$. The transition map R can be calculated by the composition

$$R = \Delta_4^{-1} \circ \widehat{R}_2 \circ \bar{R} \circ \widehat{R}_1 \circ \Delta_3, \quad (4.3.12)$$

where

- $\Delta_i : \Pi_i \longrightarrow \Sigma_i$ are the first type of Dulac maps in the neighborhood of P_i ($i = 3, 4$). The first type of Dulac maps $\Delta_i = (d_i, D_i)$ ($i = 3, 4$) have the expressions

$$\begin{cases} d_i(\nu, \tilde{y}_i) = \nu, \\ D_i(\nu, \tilde{y}_i) = \eta_i(\nu, \omega(\frac{\nu}{\nu_0}, -\beta_1)) + (\frac{\nu}{\nu_0})^{\bar{\sigma}_i} [\tilde{y}_i + \psi_i(\nu, \tilde{y}_i, \omega(\frac{\nu}{\nu_0}, -\beta_1))], \end{cases} \quad (4.3.13)$$

where $\beta = p_3 - \bar{\sigma}_3(a)q_3$ and ψ_i ($i = 3, 4$) have the property (2.5.23).

- The transition maps \widehat{R}_1 , \bar{R} and \widehat{R}_2 are given by (4.2.4), (4.2.5) and (4.2.6).
- $\Delta_4^{-1} : \Sigma_4 \longrightarrow \Pi_4$ is the inverse of the first type of Dulac map in the neighborhood of P_4 . It has the expression

$$\begin{cases} d_4^{-1}(\nu, \tilde{y}_4) = \nu, \\ D_4^{-1}(\nu, \tilde{y}_4) = \hat{y}_4 + \hat{\psi}_4(\nu, \omega(\frac{\nu}{\nu_0}, -\beta_1), \hat{y}_4), \end{cases} \quad (4.3.14)$$

where $\hat{y}_4 = (\frac{\nu}{\nu_0})^{-\bar{\sigma}_4}(\tilde{y}_4 - \eta_4(\nu, \omega(\frac{\nu}{\nu_0}, -\beta_1)))$, and $\hat{\psi}_4$ satisfies property (2.5.23).

Hence, for the second component of transition map R , by (4.2.4), (4.2.5), (4.2.6), (4.3.12), (4.3.13), (4.3.14), and Lemma 4.13 in [53], a straightforward calculation yields the result.

□

For each family of graphic Sxhhi ($i = 1, 3, 4, 5, 6, 7, 8$), we use $V_i \subset \mathbb{S}^2$ to denote the set of $\bar{\mu} = (\bar{\mu}_1, \bar{\mu}_2, \bar{\mu}_3)$ in which the family Sxhhi exists, and use V_{i0} to denote a small neighborhood of $\bar{\mu}_0$, where $\bar{\mu}_0 \in V_i$.

4.3.1 Family Sxhh1

Family Sxhh1 has a lower boundary graphic Sxhh1c which passes through a hyperbolic saddle point as shown in Fig 4.4. Let λ_0 be the hyperbolicity ratio at this saddle point when $r = 0$ for $\bar{\mu} = \bar{\mu}_0$ and $a = a_0 \in A$. In the chart F.R., by translating the saddle point to the origin, a linear transformation and C^k changes of coordinates, we can bring the system (2.4.14) in the neighborhood of the saddle point into a normal form.

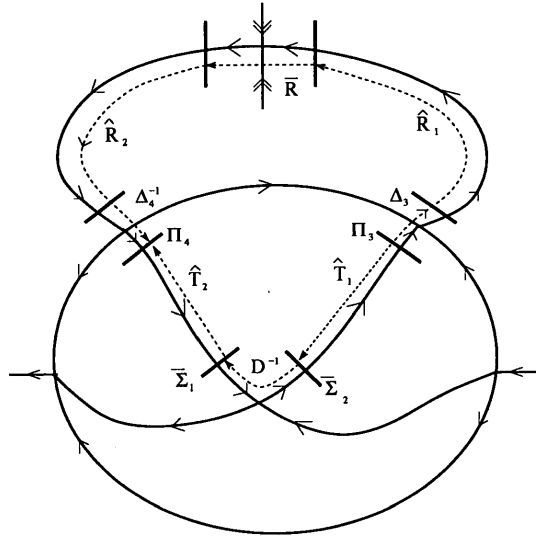


Figure 4.4: Transition maps for the family Sxhh1

Take sections $\bar{\Sigma}_1 = \{\tilde{y} = 1\}$ and $\bar{\Sigma}_2 = \{\tilde{x} = 1\}$ in the normal form coordinates near the saddle point. Let $D(\nu, \tilde{x}) = (D_1(\nu, \tilde{x}), D_2(\nu, \tilde{x})) : \bar{\Sigma}_1 \rightarrow \bar{\Sigma}_2$ be the Dulac map near the saddle point. There exist A_0 , a neighborhood of a_0 , V_{10} , a neighborhood of $\bar{\mu}_0$, and $\nu_1 > 0$, such that $\forall (a, \bar{\mu}) \in A_0 \times V_{10}$ and $\forall \nu \in (0, \nu_1)$, the inverse of the Dulac map

$D(\nu, \tilde{x}) : \bar{\Sigma}_1 \longrightarrow \bar{\Sigma}_2$ can be written as

$$D^{-1} : \bar{\Sigma}_2 \longrightarrow \bar{\Sigma}_1$$

$$(\nu, \tilde{y}) \longrightarrow (D_1^{-1}(\nu, \tilde{y}), D_2^{-1}(\nu, \tilde{y})),$$

which has the following form

$$D_1^{-1}(\nu, \tilde{y}) = \nu,$$

$$D_2^{-1}(\nu, \tilde{y}) = \begin{cases} \tilde{y}^{\frac{1}{\lambda(\nu)}} (1 + \phi(\tilde{y}, \nu)), & \text{if } \lambda_0 \neq 1, \\ \bar{\alpha}_1(\nu)[\tilde{y}\omega + \dots] + \tilde{y} + \bar{\alpha}_2(\nu)[\tilde{y}^2\omega + \dots] + \dots, & \text{if } \lambda_0 = 1, \end{cases}$$

(4.3.15)

where $\phi(\tilde{y}, \nu) \in I_0^\infty$, $\lambda(\nu)$ and $\bar{\alpha}_i(\nu)$ are functions of $(\nu, \bar{\mu}, a)$, $\bar{\alpha}_1(\nu) = 1 - \frac{1}{\lambda(\nu)}$ and $\omega = \omega(\tilde{y}, \bar{\alpha}_1(\nu))$ is the *Leontovich-Andronova-Ecalle-Roussarie* compensator defined in (2.2.4).

Let $\hat{T}_1 : \Pi_3 \longrightarrow \bar{\Sigma}_2$ and $\hat{T}_2 : \bar{\Sigma}_1 \longrightarrow \Pi_4$. They are the compositions of normal form coordinate changes and a regular transition map. $\hat{T}_1(\nu, \tilde{y}_3)$ can be written as

$$\begin{cases} \hat{T}_{11}(\nu, \tilde{y}_3) = \nu, \\ \hat{T}_{12}(\nu, \tilde{y}_3) = e_0(\nu) + e_1(\nu)\tilde{y}_3 + O(\tilde{y}_3^2), \end{cases}$$

(4.3.16)

and $\hat{T}_2(\nu, \tilde{x})$ can be written as

$$\begin{cases} \hat{T}_{21}(\nu, \tilde{x}) = \nu, \\ \hat{T}_{22}(\nu, \tilde{x}) = b_0(\nu) + b_1(\nu)\tilde{x} + O(\tilde{x}^2), \end{cases}$$

(4.3.17)

where $e_0(0) = 0$, $b_0(0) = 0$, $e_1(0) > 0$ and $b_1(0) > 0$. Then for $T^{-1} : \Pi_3 \longrightarrow \Pi_4$, we have

$$T^{-1} = \widehat{T}_2 \circ D^{-1} \circ \widehat{T}_1.$$

We treat two cases $\lambda_0 \neq 1$ and $\lambda_0 = 1$ separately.

4.3.1.1 $\lambda_0 \neq 1$

Firstly, we study the lower boundary graphic S_{xhh1c} . By (4.3.15), (4.3.16) and (4.3.17),

we have

$$\begin{cases} T_1^{-1}(\nu, \tilde{y}_3) = \nu, \\ T_2^{-1}(\nu, \tilde{y}_3) = \varepsilon_1(\nu) + h(\nu)(\varepsilon_2(\nu) + \tilde{y}_3)^{\frac{1}{\lambda(\nu)}} [1 + \phi_0(\tilde{y}_3, \nu)], \end{cases} \quad (4.3.18)$$

where $\varepsilon_i(0) = 0$ ($i = 1, 2$), $h(0) = e_1(0)^{\frac{1}{\lambda_0}} b_1(0) \neq 0$ and $\phi_0 \in I_0^\infty$. Therefore, from (4.3.11) and (4.3.18), the displacement map L has the following form

$$\begin{cases} L_1(\nu, \tilde{y}_3) = 0, \\ L_2(\nu, \tilde{y}_3) = \gamma_0(\nu, \omega(\frac{\nu}{\nu_0}, -\beta_1), m(\nu)) + m(\nu) \left[\sum_{i=1}^k \gamma_i(\nu, \omega(\frac{\nu}{\nu_0}, -\beta_1), m(\nu)) \tilde{y}_3^i \right. \\ \left. + O(\tilde{y}_3^{k+1}) \right] - \left[\varepsilon_1(\nu) + h(\nu)(\varepsilon_2(\nu) + \tilde{y}_3)^{\frac{1}{\lambda(\nu)}} (1 + \phi_0(\tilde{y}_3, \nu)) \right]. \end{cases}$$

Then

$$\begin{aligned} \frac{\partial L_2(\nu, \tilde{y}_3)}{\partial \tilde{y}_3} &= m(\nu) [\gamma_1(\nu, \omega(\frac{\nu}{\nu_0}, -\beta_1), m(\nu)) + O(\tilde{y}_3)] \\ &\quad - \frac{h(\nu)}{\lambda(\nu)} (\varepsilon_2(\nu) + \tilde{y}_3)^{\frac{1}{\lambda(\nu)} - 1} [1 + \phi_1(\tilde{y}_3, \nu)], \end{aligned} \quad (4.3.19)$$

where $\phi_1 \in I_0^\infty$.

- $\lambda_0 > 1$.

Since $\gamma_1(\nu, \omega(\frac{\nu}{\nu_0}, -\beta_3), m(\nu))$ is bounded and $m(\nu) \rightarrow 0$ as $\nu \rightarrow 0$, so

$$\lim_{(\nu, \tilde{y}_3, \bar{\mu}, a) \rightarrow (0, 0, \bar{\mu}_0, a_0)} m(\nu) [\gamma_1(\nu, \omega(\frac{\nu}{\nu_0}, -\beta_3), m(\nu)) + O(\tilde{y}_3)] = 0.$$

For $(\nu, \bar{\mu}, a)$ in a small neighborhood of $(0, \bar{\mu}_0, a_0)$, we have $\frac{1}{\lambda(\nu)} - 1 < 0$, $r(\nu)$ and $h(\nu)$ are all bounded and bounded from zero. Hence,

$$\lim_{(\nu, \tilde{y}_3, \bar{\mu}, a) \rightarrow (0, 0, \bar{\mu}_0, a_0)} -\frac{h(\nu)}{\lambda(\nu)} (\varepsilon_2(\nu) + \tilde{y}_3)^{\frac{1}{\lambda(\nu)} - 1} [1 + \phi_1(\tilde{y}_3, \nu)] = \infty.$$

Hence, there exist A_0 , a neighborhood of a_0 , V_{10} , a neighborhood of $\bar{\mu}_0$, and $\nu_1 > 0$, such that $\forall (a, \bar{\mu}) \in A_0 \times V_{10}$ and $\forall \nu \in (0, \nu_1)$, we have $\frac{\partial L_2(\nu, \tilde{y}_3)}{\partial \tilde{y}_3} \neq 0$ in a small neighborhood of $\tilde{y}_3 = 0$.

By Rolle's Theorem, $\forall (a, \bar{\mu}) \in A_0 \times V_{10}$ and $\forall \nu \in (0, \nu_1)$, the map $L_2(\nu, \tilde{y}_3) = 0$ has at most one zero in a small neighborhood of $\tilde{y}_3 = 0$, i.e., $Cycl(Sxhh1c) \leq 1$.

- $\lambda_0 < 1$.

By (4.3.19), zeros of $\frac{\partial L_2(\nu, \tilde{y}_3)}{\partial \tilde{y}_3}$ are the same zeros of

$$\begin{aligned} \bar{L}_2(\nu, \tilde{y}_3) &= m(\nu)^{\frac{\lambda(\nu)}{1-\lambda(\nu)}} [1 + O(\tilde{y}_3)]^{\frac{\lambda(\nu)}{1-\lambda(\nu)}} \\ &\quad - \left(\frac{h(\nu)}{\lambda(\nu)\gamma_1(\nu)} \right)^{\frac{\lambda(\nu)}{1-\lambda(\nu)}} (\varepsilon_2(\nu) + \tilde{y}_3) [1 + \phi_2(\tilde{y}_3, \nu)], \end{aligned}$$

where $\phi_2 \in I_0^\infty$.

Differentiate $\bar{L}_2(\nu, \tilde{y}_3)$ with respect to \tilde{y}_3 , and we have

$$\frac{\partial \bar{L}_2(\nu, \tilde{y}_3)}{\partial \tilde{y}_3} = m(\nu)^{\frac{\lambda(\nu)}{1-\lambda(\nu)}} O(1) - \left(\frac{h(\nu)}{\lambda(\nu)\gamma_1(\nu)} \right)^{\frac{\lambda(\nu)}{1-\lambda(\nu)}} (1 + \phi_3(\tilde{y}_3, \nu)),$$

where $\phi_3 \in I_0^\infty$. Since $\frac{\lambda_0}{1-\lambda_0} > 0$ and $m(\nu) \rightarrow 0$ as $\nu \rightarrow 0$, so

$$\lim_{(\nu, \tilde{y}_3, \bar{\mu}, a) \rightarrow (0, 0, \bar{\mu}_0, a_0)} \frac{\partial \bar{L}_2(\nu, \tilde{y}_3)}{\partial \tilde{y}_3} = - \left(\frac{e_1(0)^{\frac{1}{\lambda_0}} b_1(0)}{\lambda_0 l_1(0) n_1(0)} \right)^{\frac{\lambda_0}{1-\lambda_0}} \neq 0.$$

Therefore, there exist A_0 , a neighborhood of a_0 , V_{10} , a neighborhood of $\bar{\mu}_0$, and $\nu_1 > 0$, such that $\forall (a, \bar{\mu}) \in A_0 \times V_{10}$ and $\forall \nu \in (0, \nu_1)$, we have $\frac{\partial \bar{L}_2(\nu, \tilde{y}_3)}{\partial \tilde{y}_3} \neq 0$ for \tilde{y}_3 in a small neighborhood of $\tilde{y}_3 = 0$.

By Rolle's theorem, $\forall (a, \bar{\mu}) \in A_0 \times V_{10}$ and $\forall \nu \in (0, \nu_1)$, $L_2(\nu, \tilde{y}_3) = 0$ has at most two roots in a small neighborhood of $\tilde{y}_3 = 0$, i.e., $Cycl(Sxhh1c) \leq 2$.

Now we study the intermediate graphics Sxhh1b for $\lambda_0 \neq 1$. Note that for $\nu = 0$, $a = a_0$ and $\bar{\mu} = \bar{\mu}_0$, from (4.3.18) we have

$$T_2^{-1}(0, \tilde{y}_3) = h(0) \tilde{y}_3^{\frac{1}{\lambda_0}} [1 + o(1)].$$

Since $h(0) = e_1(0)^{\frac{1}{\lambda_0}} b_1(0) \neq 0$ and $\lambda_0 \neq 1$, so for $\forall (a, \bar{\mu}) \in A_0 \times V_{10}$, $T_2^{-1}(0, \tilde{y}_3)$ is nonlinear. By analytic extension principle [11, 52, 53], $T_2^{-1}(0, \tilde{y}_3)$ is nonlinear in its analytic extension domain.

From proposition 4.3.1, we know that any i^{th} derivative of the second component of transition map $R(\nu, \tilde{y}_3)$ is close to zero. Suppose that $T_2^{-1}(0, \tilde{y}_3)$ has its n^{th} derivative

nonvanishing, then by Rolle's theorem, $\forall(a, \bar{\mu}) \in A_0 \times V_{10}$ and $\nu > 0$ sufficiently small, $L_2(\nu, \tilde{y}_3) = 0$ has at most n roots in a small neighborhood of $\tilde{y}_3 = 0$ i.e., $Cycl(Sxhh1b) \leq n$.

4.3.1.2 $\lambda_0 = 1$

Performing a change of parametrization on Π_3 , the displacement map L will be defined as

$$L(\nu, \tilde{Y}_3) = R(\nu, \tilde{Y}_3 + \zeta(\nu)) - \tilde{T}^{-1}(\nu, \tilde{Y}_3), \quad (4.3.20)$$

where $\zeta(\nu) = \hat{T}_{12}^{-1}(\nu, 0)$ with $\zeta(0) = 0$, and $\tilde{T}^{-1} = \hat{T}_2 \circ D^{-1} \circ \hat{S}_1$. The maps D^{-1} and \hat{T}_2 are given by (4.3.15) and (4.3.17), respectively. For \hat{S}_1 , we have

$$\begin{cases} \hat{S}_{11}(\nu, \tilde{Y}_3) = \nu, \\ \hat{S}_{12}(\nu, \tilde{Y}_3) = \tilde{e}_1(\nu)\tilde{Y}_3 + \tilde{e}_2(\nu)\tilde{Y}_3^2 + O(\tilde{Y}_3^3), \end{cases} \quad (4.3.21)$$

where $\tilde{e}_1(0) = e_1(0) > 0$.

By (4.3.15), (4.3.17) and (4.3.21), for \tilde{T}^{-1} we have

$$\begin{cases} \tilde{T}_1^{-1}(\nu, \tilde{Y}_3) = \nu, \\ \tilde{T}_2^{-1}(\nu, \tilde{Y}_3) = b_0(\nu) + \tilde{e}_1^{1-\bar{\alpha}_1}(\nu)b_1(\nu)\bar{\alpha}_1(\nu)[\tilde{Y}_3\omega(\tilde{Y}_3, \bar{\alpha}_1) + \dots] \\ \quad \tilde{e}_1(\nu)b_1(\nu)\tilde{Y}_3 + \tilde{e}_1^{2-\bar{\alpha}_1}(\nu)b_1(\nu)\bar{\alpha}_2(\nu)[\tilde{Y}_3^2\omega(\tilde{Y}_3, \bar{\alpha}_1) + \dots] + \dots \end{cases} \quad (4.3.22)$$

Therefore, for the displacement map $L(\nu, \tilde{Y}_3)$, by (4.3.11), (4.3.20) and (4.3.22), we have

$$\begin{cases} L_1(\nu, \tilde{Y}_3) = 0, \\ L_2(\nu, \tilde{Y}_3) = c_0(\nu) + c_1(\nu)[\tilde{Y}_3\omega(\tilde{Y}_3, \bar{\alpha}_1) + \dots] \\ \quad + c_2(\nu)\tilde{Y}_3 + c_3(\nu)[\tilde{Y}_3^2\omega(\tilde{Y}_3, \bar{\alpha}_1) + \dots] + \dots, \end{cases} \quad (4.3.23)$$

where

$$c_0(\nu) = \gamma_0(\nu, \omega(\frac{\nu}{\nu_0}, -\beta_1), m(\nu)) + O(\zeta(\nu)) - b_0(\nu),$$

$$c_1(\nu) = -\tilde{e}_1^{1-\bar{\alpha}_1}(\nu)b_1(\nu)\bar{\alpha}_1(\nu),$$

$$c_2(\nu) = m(\nu)\gamma_1(\nu, \omega(\frac{\nu}{\nu_0}, -\beta_1), m(\nu)) + O(\zeta(\nu)) - \tilde{e}_1(\nu)b_1(\nu),$$

$$c_3(\nu) = -\tilde{e}_1^{2-\bar{\alpha}_1}(\nu)b_1(\nu)\bar{\alpha}_2(\nu).$$

We will treat the following three cases separately depending on the parameters $(a, \bar{\mu})$.

- $a_0 \neq -\frac{1}{2}$ and $\bar{\mu}_{30} = 0$.

Since $\bar{\mu}_{10} = 0$, if $\bar{\mu}_{30} = 0$, then in the chart F.R. on the blown-up sphere $r = 0$, system $\bar{X}_{\rho=1}$ in (2.4.15) is symmetric with respect to the y-axis, so we have $\tilde{e}_1(0)b_1(0) = 1$.

Differentiate $L_2(\nu, \tilde{Y}_3)$ with respect to \tilde{Y}_3 , and we have

$$\frac{\partial L_2(\nu, \tilde{Y}_3)}{\partial \tilde{Y}_3} = c_1(\nu)[*\omega(\tilde{Y}_3, \bar{\alpha}_1) + \dots] + c_2(\nu) + c_3(\nu)[*\tilde{Y}_3\omega(\tilde{Y}_3, \bar{\alpha}_1) + \dots] + \dots.$$

Let

$$\xi_1(\nu, \tilde{Y}_3) := \frac{\partial L_2(\nu, \tilde{Y}_3)}{\partial \tilde{Y}_3} \frac{\omega^{-1}(\tilde{Y}_3, \bar{\alpha}_1)}{*1 + \dots} = c_1(\nu) + c_2(\nu) \frac{*1 + \dots}{*1 + \dots} \frac{1}{\omega(\tilde{Y}_3, \bar{\alpha}_1)} + \dots.$$

The zeros of $\frac{\partial L_2(\nu, \tilde{Y}_3)}{\partial \tilde{Y}_3}$ are zeros of the function $\xi_1(\nu, \tilde{Y}_3)$ in some neighborhood of $\tilde{Y}_3 = 0$.

Differentiate $\xi_1(\nu, \tilde{Y}_3)$ with respect to \tilde{Y}_3 , and we have

$$\frac{\partial \xi_1(\nu, \tilde{Y}_3)}{\partial \tilde{Y}_3} = *c_2(\nu) \frac{\tilde{Y}_3^{-1-\bar{\alpha}_1} + \dots}{*1 + \dots} \frac{1}{\omega^2(\tilde{Y}_3, \bar{\alpha}_1)} + \dots .$$

Let

$$\xi_2(\nu, \tilde{Y}_3) := \omega^2(\tilde{Y}_3, \bar{\alpha}_1) \frac{*1 + \dots}{*\tilde{Y}_3^{-1-\bar{\alpha}} + \dots} \frac{\partial \xi_1(\nu, \tilde{Y}_3)}{\partial \tilde{Y}_3},$$

then we have

$$\xi_2(\nu, \tilde{Y}_3) = *c_2(\nu) + \dots .$$

Since $c_2(0) = -\bar{e}_1(0)b_1(0) = -1 \neq 0$, and the remainder is $o(1)$, so there exist A_0 , a neighborhood of a_0 , V_{10} , a neighborhood of $\bar{\mu}_0$, and $\nu_1 > 0$, such that $\forall (a, \bar{\mu}) \in A_0 \times V_{10}$ and $\forall \nu \in (0, \nu_1)$, $\xi_2(\nu, \tilde{Y}_3) \neq 0$ in some neighborhood of $\tilde{Y}_3 = 0$. By Rolle's Theorem, $\forall (a, \bar{\mu}) \in A_0 \times V_{10}$ and $\forall \nu \in (0, \nu_1)$, the displacement map $L(\nu, \tilde{Y}_3)$ has at most 2 zeros in some neighborhood of $\tilde{Y}_3 = 0$, i.e., $Cycl(Sxhh1c) \leq 2$.

For the intermediate graphics, if $\bar{\mu}_{10} = 0$ and $\bar{\mu}_{30} = 0$, because of the symmetry, $T_2^{-1}(0, \tilde{y}_3)$ is an identity. From proposition 4.3.1, we know that any i^{th} derivative of the second component of transition map $R(\nu, \tilde{y}_3)$ with respect to \tilde{y}_3 is close to zero. By Rolle's theorem, $\forall (a, \bar{\mu}) \in A_0 \times V_{10}$ and $\nu > 0$ sufficiently small, $L(\nu, \tilde{y}_3)$ has at most one root in a small neighborhood of $\tilde{y}_3 = 0$, i.e., $Cycl(Sxhh1b) \leq 1$.

- $a_0 \neq -\frac{1}{2}$ and $\bar{\mu}_{30} \neq 0$.

For $a_0 \neq -\frac{1}{2}$ and $\bar{\mu}_{30} \neq 0$, it has been calculated in [53] that the first saddle quantity

$$\bar{\alpha}_2 = \frac{2a_0(a_0 - 1)(1 + 2a_0)^2}{a_0(4a_0 - 1)\bar{\mu}_{30}^2 - (1 + 2a_0)^2\bar{\mu}_{20}} \bar{\mu}_{30} \neq 0.$$

Differentiate $L_2(\nu, \tilde{Y}_3)$ with respect to \tilde{Y}_3 , and we have

$$\frac{\partial L_2(\nu, \tilde{Y}_3)}{\partial \tilde{Y}_3} = c_1(\nu)[*\omega(\tilde{Y}_3, \bar{\alpha}_1) + \dots] + c_2(\nu) + \dots.$$

Let

$$\xi_1(\nu, \tilde{Y}_3) := \frac{\partial L_2(\nu, \tilde{Y}_3)}{\partial \tilde{Y}_3} \frac{\omega^{-1}(\tilde{Y}_3, \bar{\alpha}_1)}{*\mathbf{1} + \dots} = c_1(\nu) + c_2(\nu) \frac{*\mathbf{1} + \dots}{*\mathbf{1} + \dots} \frac{1}{\omega(\tilde{Y}_3, \bar{\alpha}_1)} + \dots.$$

The zeros of $\frac{\partial L_2(\nu, \tilde{Y}_3)}{\partial \tilde{Y}_3}$ are zeros of the function $\xi_1(\nu, \tilde{Y}_3)$ in some neighborhood of $\tilde{Y}_3 = 0$.

Differentiate $\xi_1(\nu, \tilde{Y}_3)$ with respect to \tilde{Y}_3 , and we have

$$\frac{\partial \xi_1(\nu, \tilde{Y}_3)}{\partial \tilde{Y}_3} = *c_2(\nu) \frac{\tilde{Y}_3^{-1-\bar{\alpha}_1} + \dots}{*\mathbf{1} + \dots} \frac{1}{\omega^2(\tilde{Y}_3, \bar{\alpha}_1)} + \dots.$$

Let

$$\xi_2(\nu, \tilde{Y}_3) := \omega^2(\tilde{Y}_3, \bar{\alpha}_1) \frac{*\mathbf{1} + \dots}{*\tilde{Y}_3^{-1-\bar{\alpha}_1} + \dots} \frac{\partial \xi_1(\nu, \tilde{Y}_3)}{\partial \tilde{Y}_3},$$

then we have

$$\xi_2(\nu, \tilde{Y}_3) = *c_2(\nu) + \dots.$$

Since $c_2(0) = -\bar{e}_1(0)b_1(0) \neq 0$ and the remainder is $o(1)$, so there exist A_0 , a neighborhood of a_0 , V_{10} , a neighborhood of $\bar{\mu}_0$, and $\nu_1 > 0$, such that $\forall (a, \bar{\mu}) \in A_0 \times V_{10}$ and $\forall \nu \in (0, \nu_1)$, $\xi_2(\nu, \tilde{Y}_3) \neq 0$ in some neighborhood of $\tilde{Y}_3 = 0$.

By Rolle's Theorem, $\forall(a, \bar{\mu}) \in A_0 \times V_{10}$ and $\forall \nu \in (0, \nu_1)$ the displacement map $L(\nu, \tilde{Y}_3)$ has at most 2 zeros in some neighborhood of $\tilde{Y}_3 = 0$, i.e., $Cycl(Sxhh1c) \leq 2$.

For the intermediate graphics, since $\bar{\alpha}_2 \neq 0$, from (4.3.22), we have $\frac{\partial^2 \tilde{T}_2^{-1}(0, \tilde{Y}_3)}{\partial \tilde{Y}_3^2} \neq 0$. Hence, $\tilde{T}_2^{-1}(0, \tilde{Y}_3)$ is nonlinear. By analytic extension principle [11, 52, 53], $\tilde{T}_2^{-1}(0, \tilde{Y}_3)$ is nonlinear in its analytic extension domain.

From proposition 4.3.1, we know that any i^{th} derivative of the second component of transition map $R(\nu, \tilde{Y}_3 + \zeta(\nu))$ with respect to \tilde{Y}_3 is close to zero. If $\tilde{T}_2^{-1}(0, \tilde{Y}_3)$ has its n^{th} derivative nonvanishing, then by Rolle's theorem, $\forall(a, \bar{\mu}) \in A_0 \times V_{10}$ and $\nu > 0$ sufficiently small, $L(\nu, \tilde{Y}_3)$ has at most n roots in a small neighborhood of $\tilde{Y}_3 = 0$, i.e., $Cycl(Sxhh1b) \leq n$.

- $a_0 = -\frac{1}{2}$.

Since $\lambda_0 = 1$, so the divergence of $\bar{X}_{\rho=1}$ vanishes, i.e., $(1 + 2a_0)\tilde{x}_0 + \bar{\mu}_{30} = 0$. If $a_0 = -\frac{1}{2}$, then $\bar{\mu}_{30} = 0$. Note that $\bar{\mu}_{10} = 0$, so again system $\bar{X}_{\rho=1}$ is symmetric with respect to the y-axis. Exactly as we did for the case $a_0 \neq -\frac{1}{2}$ and $\bar{\mu}_{30} = 0$, we can prove that $Cycl(Sxhh1b) \leq 1$ and $Cycl(Sxhh1c) \leq 2$.

4.3.2 Families Sxhh4 and Sxhh6

The family Sxhh4 exists if and only if

$$V_4 = \{\bar{\mu} \in \mathbb{S}^2 \mid \bar{\mu}_1 = 0, \bar{\mu}_3 > 0, \bar{\mu}_2 > a\bar{\mu}_3^2\},$$

and the family Sxhh6 exists if and only if

$$V_6 = \{\bar{\mu} \in \mathbb{S}^2 \mid \bar{\mu}_1 = 0, \bar{\mu}_3 < 0, \bar{\mu}_2 > a\bar{\mu}_3^2\}.$$

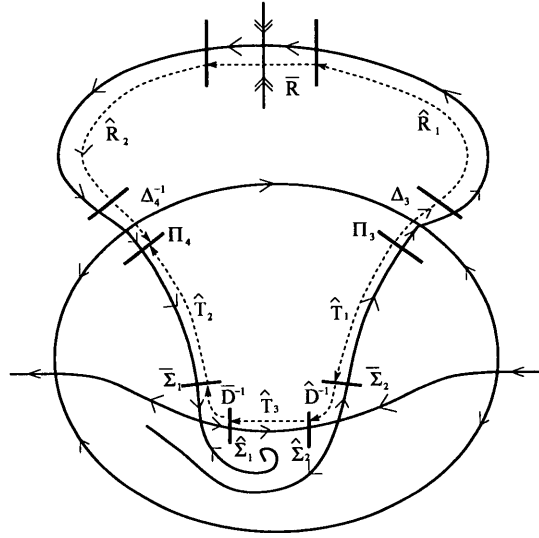


Figure 4.5: Transition maps for the family Sxhh4

For families Sxhh4 and Sxhh6, the lower boundary graphic has a saddle connection S_1S_2 as shown Fig. 4.5. At S_1 and S_2 , the hyperbolicity ratios are

$$S_1 : \lambda_1 = \frac{\bar{\mu}_3 - \sqrt{-\frac{\bar{\mu}_2}{a}}}{2a\sqrt{-\frac{\bar{\mu}_2}{a}}}; \quad S_2 : \lambda_2 = \frac{-2a\sqrt{-\frac{\bar{\mu}_2}{a}}}{\bar{\mu}_3 + \sqrt{-\frac{\bar{\mu}_2}{a}}}.$$

We first consider the lower boundary graphics.

In the chart F.R., in the neighborhood of S_1 , take sections $\bar{\Sigma}_1 = \{\tilde{y}_1 = 1\}$ and $\hat{\Sigma}_1 = \{\tilde{x}_1 = 1\}$ in the normal form coordinates. In the neighborhood of S_2 , take sections

$\bar{\Sigma}_2 = \{\tilde{x}_2 = 1\}$ and $\hat{\Sigma}_2 = \{\tilde{y}_2 = 1\}$ in the normal form coordinates.

The transition map $T^{-1} : \Pi_3 \longrightarrow \Pi_4$ can be calculated by the composition

$$T^{-1} = \hat{T}_2 \circ \bar{D}^{-1} \circ \hat{T}_3 \circ \hat{D}^{-1} \circ \hat{T}_1,$$

where

- $\hat{T}_1 : \Pi_3 \longrightarrow \bar{\Sigma}_2$ is a composition of normal form coordinate changes and a regular transition map, which can be written as

$$\begin{cases} \hat{T}_{11}(\nu, \tilde{y}_3) = \nu, \\ \hat{T}_{12}(\nu, \tilde{y}_3) = e_0(\nu) + e_1(\nu)\tilde{y}_3 + O(\tilde{y}_3^2), \end{cases} \quad (4.3.24)$$

where $e_0(0) = 0$ and $e_1(0) > 0$.

- $\hat{D}^{-1} : \bar{\Sigma}_2 \longrightarrow \hat{\Sigma}_2$ is the Dulac map in the neighborhood of S_2 , which has the expression

$$\begin{cases} \hat{D}_1^{-1}(\nu, \tilde{y}_2) = \nu, \\ \hat{D}_2^{-1}(\nu, \tilde{y}_2) = \tilde{y}_2^{\frac{1}{\lambda_2(\nu)}} [1 + \hat{\phi}(\tilde{y}_2, \nu)], \end{cases} \quad (4.3.25)$$

where $\hat{\phi} \in I_0^\infty$.

- $\hat{T}_3 : \hat{\Sigma}_2 \longrightarrow \hat{\Sigma}_1$ is the composition of normal form coordinates changes and a transition map. Since \bar{x} axis is fixed for $\bar{X}_{\rho=1}$, so \hat{T}_3 can be written as

$$\begin{cases} \hat{T}_{31}(\nu, \tilde{x}_2) = \nu, \\ \hat{T}_{32}(\nu, \tilde{x}_2) = k_1(\nu)\tilde{x}_2 + O(\tilde{x}_2^2), \end{cases} \quad (4.3.26)$$

where $k_1(0) > 0$.

- $\bar{D}^{-1} : \widehat{\Sigma}_1 \longrightarrow \bar{\Sigma}_1$ is the Dulac map in the neighborhood of S_1 , which has the expression

$$\begin{cases} \bar{D}_1^{-1}(\nu, \tilde{y}_1) = \nu, \\ \bar{D}_2^{-1}(\nu, \tilde{y}_1) = \tilde{y}_1^{\frac{1}{\lambda_1(\nu)}} [1 + \bar{\phi}(\tilde{y}_1, \nu)], \end{cases} \quad (4.3.27)$$

where $\bar{\phi} \in I_0^\infty$.

- $\widehat{T}_2 : \bar{\Sigma}_1 \longrightarrow \Pi_4$ is a composition of normal form coordinate changes and a regular transition map, which can be written as

$$\begin{cases} \widehat{T}_{21}(\nu, \tilde{x}) = \nu, \\ \widehat{T}_{22}(\nu, \tilde{x}) = b_0(\nu) + b_1(\nu)\tilde{x} + O(\tilde{x}^2), \end{cases} \quad (4.3.28)$$

where $b_0(0) = 0$, and $b_1(0) > 0$.

Then by (4.3.24), (4.3.25), (4.3.26), (4.3.27) and (4.3.28), for the transition map T^{-1} , we

have

$$\begin{cases} T_1^{-1}(\nu, \tilde{y}_3) = \nu, \\ T_2^{-1}(\nu, \tilde{y}_3) = \varepsilon_1(\nu) + h(\nu)(\varepsilon_2(\nu) + \tilde{y}_3)^{\frac{1}{\lambda_1(\nu)\lambda_2(\nu)}} [1 + \psi_0(\tilde{y}_3, \nu)], \end{cases} \quad (4.3.29)$$

where $\varepsilon_i(0) = 0$ ($i = 1, 2$), $h(0) = e_1(0)^{\frac{1}{\lambda_1(0)\lambda_2(0)}} k_1(0)^{\frac{1}{\lambda_1(0)}} b_1(0) \neq 0$ and $\psi_0 \in I_0^\infty$.

Let $\lambda(\nu) = \lambda_1(\nu)\lambda_2(\nu)$ in (4.3.29). Since $\lambda_1(0)\lambda_2(0) = \frac{\sqrt{-\frac{\bar{\mu}_{20}}{\alpha_0} - \bar{\mu}_{30}}}{\sqrt{-\frac{\bar{\mu}_{20}}{\alpha_0} + \bar{\mu}_{30}}}$, then

1. If $\bar{\mu}_0 \in V_4$, then $\lambda_1(0)\lambda_2(0) < 1$. Exactly as we did for the case $\lambda_0(\bar{\mu}_0) < 1$ of graphic *Sxhh1*, we have $Cycl(Sxhh4b) \leq n$ and $Cycl(Sxhh4c) \leq 2$.
2. If $\bar{\mu}_0 \in V_6$, we have $\lambda_1(0)\lambda_2(0) > 1$. Exactly as we did for the case $\lambda_0(\bar{\mu}_0) > 1$ of graphic *Sxhh1*, we have $Cycl(Sxhh6b) \leq n$ and $Cycl(Sxhh6c) \leq 1$.

4.3.3 Family *Sxhh5*

The family *Sxhh5* exists if and only if $\bar{\mu}_0 = (0, 1, 0)$. Then system $\bar{X}_{\rho=1}$ is symmetric with respect to y-axis as shown in Fig 4.6.

4.3.3.1 *Sxhh5b*

For the intermediate graphics, the transition map $T_2^{-1}(0, \tilde{y}_3)$ is an identity for $\bar{\mu}_0 = (0, 1, 0)$. Since the derivative of the second component of transition map $R(\nu, \tilde{y}_3)$ with respect to \tilde{y}_3 is close to zero, so by Rolle's theorem, we have $Cycl(Sxhh5b) \leq 1$.

4.3.3.2 *Sxhh5c*

Now we consider the graphic *Sxhh5c*. The hyperbolicity ratio λ_1 and λ_2 satisfy $\lambda_1 = -\frac{1}{2a}$, $\lambda_2 = -2a$ and $\lambda_1\lambda_2 = 1$.

In the chart F.R., in the neighborhood of S_1 , take sections $\bar{\Sigma}_1 = \{\tilde{y}_1 = 1\}$ and $\hat{\Sigma}_1 = \{\tilde{x}_1 = 1\}$ in the normal form coordinates. In the neighborhood of S_2 , take sections

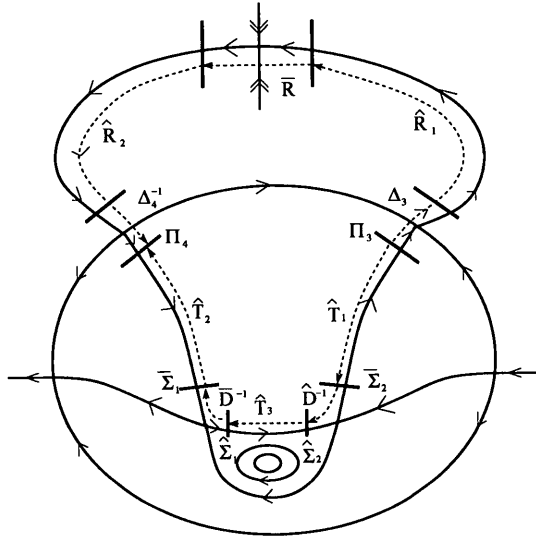


Figure 4.6: Transition maps for the family Sxhh5

$\bar{\Sigma}_2 = \{\tilde{x}_2 = 1\}$ and $\hat{\Sigma}_2 = \{\tilde{y}_2 = 1\}$ in the normal form coordinates.

The transition map $T^{-1} : \Pi_3 \rightarrow \Pi_4$ can be calculated by the composition

$$T^{-1} = \hat{T}_2 \circ \bar{D}^{-1} \circ \hat{T}_3 \circ \hat{D}^{-1} \circ \hat{T}_1,$$

where the transition maps \hat{T}_1 , \hat{D}^{-1} , \hat{T}_3 , \bar{D}^{-1} and \hat{T}_2 have the same definitions and expressions as those in Family Sxhh4.

Performing a change of parametrization on Π_3 , the displacement map L will be defined as

$$L(\nu, \tilde{Y}_3) = R(\nu, \tilde{Y}_3 + \zeta(\nu)) - \tilde{T}^{-1}(\nu, \tilde{Y}_3), \quad (4.3.30)$$

where $\zeta(\nu) = \hat{T}_{12}^{-1}(\nu, 0)$ with $\zeta(0) = 0$, and $\tilde{T}^{-1} = \hat{T}_2 \circ \bar{D}^{-1} \circ \hat{T}_3 \circ \hat{D}^{-1} \circ \hat{S}_1$.

For \widehat{S}_1 , we have

$$\begin{cases} \widehat{S}_{11}(\nu, \tilde{Y}_3) = \nu, \\ \widehat{S}_{12}(\nu, \tilde{Y}_3) = \tilde{e}_1(\nu)\tilde{Y}_3 + \tilde{e}_2(\nu)\tilde{Y}_3^2 + O(\tilde{Y}_3^3), \end{cases} \quad (4.3.31)$$

where $\tilde{e}_1(0) = e_1(0) > 0$.

By (4.3.25), (4.3.26), (4.3.27), (4.3.28), (4.3.30) and (4.3.31), for \tilde{T}^{-1} we have

$$\begin{cases} \tilde{T}_1^{-1}(\nu, \tilde{Y}_3) = \nu, \\ \tilde{T}_2^{-1}(\nu, \tilde{Y}_3) = b_0(\nu) + \bar{h}(\nu)\tilde{Y}_3^{\frac{1}{\lambda_1\lambda_2}} [1 + \psi_0(\tilde{Y}_3, \nu)], \end{cases} \quad (4.3.32)$$

where $\bar{h}(0) = \tilde{e}_1(0)^{\frac{1}{\lambda_1(0)\lambda_2(0)}} k_1(0)^{\frac{1}{\lambda_1(0)}} b_1(0) \neq 0$ and $\psi_0 \in I_0^\infty$.

As $\lambda_1(0)\lambda_2(0) = 1$, if we let $\frac{1}{\lambda_1(\nu)\lambda_2(\nu)} = 1 - \hat{\alpha}(\nu)$, then $\hat{\alpha}(0) = 0$. We introduce a

compensator ω defined as follows.

$$\omega(\tilde{Y}_3, \nu) = \begin{cases} \frac{\tilde{Y}_3^{-\hat{\alpha}(\nu)} - 1}{\hat{\alpha}(\nu)}, & \text{if } \hat{\alpha}(\nu) \neq 0, \\ -\ln \tilde{Y}_3, & \text{if } \hat{\alpha}(\nu) = 0. \end{cases}$$

This yields

$$\tilde{Y}_3^{\frac{1}{\lambda_1\lambda_2}} = \tilde{Y}_3^{1-\hat{\alpha}} = [1 + \hat{\alpha}(\nu)\omega(\tilde{Y}_3, \nu)]\tilde{Y}_3. \quad (4.3.33)$$

By (4.3.32) and (4.3.33), \tilde{T}^{-1} has the form

$$\begin{cases} \tilde{T}_1^{-1}(\nu, \tilde{Y}_3) = \nu, \\ \tilde{T}_2^{-1}(\nu, \tilde{Y}_3) = b_0(\nu) + \hat{\alpha}\bar{h}(\nu)\tilde{Y}_3\omega(\tilde{Y}_3, \nu)[1 + \psi_0(\tilde{Y}_3, \nu)] \\ \quad + \bar{h}(\nu)\tilde{Y}_3[1 + \psi_0(\tilde{Y}_3, \nu)]. \end{cases} \quad (4.3.34)$$

For $R(\nu, \tilde{Y}_3 + \zeta(\nu))$, by (4.3.11), we have

$$\begin{cases} R(\nu, \tilde{Y}_3 + \zeta(\nu)) = \nu, \\ R(\nu, \tilde{Y}_3 + \zeta(\nu)) = \gamma_0 + O(m(\nu)) + m(\nu)[(\gamma_1(\nu) + O(\zeta))\tilde{Y}_3 + O(\tilde{Y}_3^2)]. \end{cases} \quad (4.3.35)$$

By (4.3.30), (4.3.32) and (4.3.35), we have

$$\begin{cases} L_1(\nu, \tilde{Y}_3) = 0, \\ L_2(\nu, \tilde{Y}_3) = \gamma_0 + O(m(\nu)) - b_0(\nu) - \hat{\alpha}(\nu)\bar{h}(\nu)\tilde{Y}_3\omega(\tilde{Y}_3, \nu)[1 + \psi_0(\tilde{Y}_3, \nu)] \\ \quad - \bar{h}(\nu)\tilde{Y}_3[1 - \frac{m(\nu)}{\bar{h}(\nu)}(\gamma_1(\nu) + O(\zeta)) + \Psi_0(\tilde{Y}_3, \nu)], \end{cases}$$

where $\Psi_0 \in I_0^\infty$.

Differentiating $L_2(\nu, \tilde{Y}_3)$ with respect to \tilde{Y}_3 , we have

$$\begin{aligned} \frac{\partial L_2(\nu, \tilde{Y}_3)}{\partial \tilde{Y}_3} &= -\hat{\alpha}(\nu)\bar{h}(\nu)[*\omega(\tilde{Y}_3, \nu) + \psi_1(\tilde{Y}_3, \nu)] \\ &\quad - \bar{h}(\nu)[1 - \frac{m(\nu)}{\bar{h}(\nu)}(\gamma_1(\nu) + O(\zeta)) + \Psi_1(\tilde{Y}_3, \nu)], \end{aligned}$$

where $\psi_1, \Psi_1 \in I_0^\infty$. Let

$$\begin{aligned} \xi_1(\nu, \tilde{Y}_3) &:= \frac{\partial L_2(\nu, \tilde{Y}_3)}{\partial \tilde{Y}_3} \frac{\omega^{-1}(\tilde{Y}_3, \nu)}{*1 + \dots} \\ &= -\hat{\alpha}(\nu)\bar{h}(\nu) + *\bar{h}(\nu)[1 - \frac{m(\nu)}{\bar{h}(\nu)}(\gamma_1(\nu) + O(\zeta)) + \Psi_2(\tilde{Y}_3, \nu)]\omega^{-1}(\tilde{Y}_3, \nu), \end{aligned}$$

where $\Psi_2 \in I_0^\infty$. The zeros of $\frac{\partial L_2(\nu, \tilde{Y}_3)}{\partial \tilde{Y}_3}$ are zeros of the function $\xi_1(\nu, \tilde{Y}_3)$ in some

neighborhood of $\tilde{Y}_3 = 0$. Differentiate $\xi_1(\nu, \tilde{Y}_3)$ with respect to \tilde{Y}_3 , and we have

$$\frac{\partial \xi_1(\nu, \tilde{Y}_3)}{\partial \tilde{Y}_3} = *\bar{h}(\nu) \left[1 - \frac{m(\nu)}{\bar{h}(\nu)}(\gamma_1(\nu) + O(\zeta)) + \Psi_3(\tilde{Y}_3, \nu) \right] \frac{\tilde{Y}_3^{-1-\hat{\alpha}}}{\omega^2(\tilde{Y}_3, \nu)} + \dots,$$

where $\Psi_3 \in I_0^\infty$. Let

$$\xi_2(\nu, \tilde{Y}_3) := \omega^2(\tilde{Y}_3, \hat{\alpha}) \tilde{Y}_3^{1+\hat{\alpha}} \frac{\partial \xi_1(\nu, \tilde{Y}_3)}{\partial \tilde{Y}_3},$$

then the roots of $\xi_2(\nu, \tilde{Y}_3)$ are the same roots of $\frac{\partial \xi_1(\nu, \tilde{Y}_3)}{\partial \tilde{Y}_3}$ in a small neighborhood of $\tilde{Y}_3 = 0$, and we have

$$\begin{aligned} \xi_2(\nu, \tilde{Y}_3) &= * \bar{h}(\nu) \left[1 - \frac{m(\nu)}{\bar{h}(\nu)} (\gamma_1(\nu) + O(\zeta)) + \Psi_3(\tilde{Y}_3, \nu) \right] + \dots \\ &\rightarrow * e_1(0)^{\frac{1}{\lambda_1(0)\lambda_2(0)}} k(0)^{\frac{1}{\lambda_1(0)}} b_1(0) \neq 0 \end{aligned}$$

when $(\tilde{Y}_3, \nu, \bar{\mu}, a) \rightarrow (0, 0, \bar{\mu}_0, a_0)$.

Hence, there exist A_0 , a neighborhood of a_0 , V_{50} , a neighborhood of $\bar{\mu}_0$, and $\nu_1 > 0$, such that $\forall (a, \bar{\mu}) \in A_0 \times V_{50}$ and $\forall \nu \in (0, \nu_1)$, $\xi_2(\nu, \tilde{Y}_3) \neq 0$ in a small neighborhood of $\tilde{Y}_3 = 0$. By Rolle's Theorem, $\forall (a, \bar{\mu}) \in A_0 \times V_{50}$ and $\forall \nu \in (0, \nu_1)$, the map $L(\nu, \tilde{Y}_3)$ has at most 2 zeros in a small neighborhood of $\tilde{Y}_3 = 0$, i.e., $Cycl(Sxhh5c) \leq 2$.

4.3.4 Family Sxhh7

For the graphics Sxhh7, as shown in Fig. 4.7, there is a repelling saddle-node S_1 and a saddle point S_2 on the lower boundary graphic Sxhh7c. Graphics Sxhh7 exists if and only if

$$V_7 = \{ \bar{\mu} \in \mathbb{S}^2 \mid \bar{\mu}_1 = 0, \bar{\mu}_2 > 0, \bar{\mu}_3 = \sqrt{-\frac{\bar{\mu}_2}{a}} \}.$$

The hyperbolicity ratio of the saddle S_2 is $\lambda_2 = -a \leq \frac{1}{2}$.

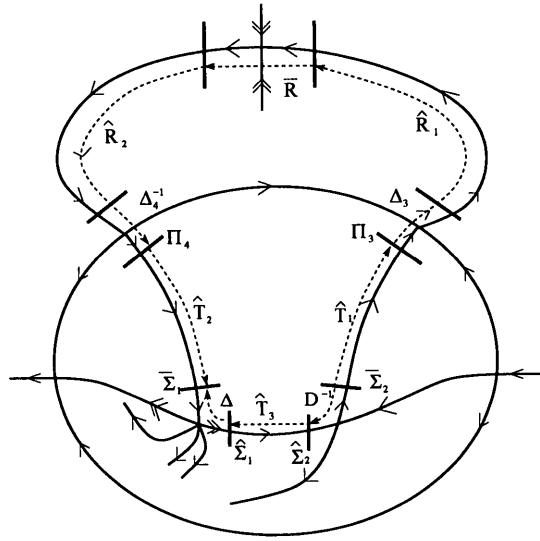


Figure 4.7: Transition maps for the family Sxhh7

4.3.4.1 Sxhh7c

We first consider the lower boundary graphic Sxhh7c.

In the chart F.R., in the neighborhood of the saddle-node point, take sections $\bar{\Sigma}_1 = \{\tilde{y}_1 = 1\}$ and $\hat{\Sigma}_1 = \{\tilde{x}_1 = 1\}$ in the normal form coordinates $(\tilde{x}_1, \tilde{y}_1)$. In the neighborhood of saddle point S_2 , take sections $\bar{\Sigma}_2 = \{\tilde{x}_2 = 1\}$ and $\hat{\Sigma}_2 = \{\tilde{y}_2 = 1\}$ in the normal form coordinates $(\tilde{x}_2, \tilde{y}_2)$. We study the displacement map

$$\bar{L}: \bar{\Sigma}_2 \longrightarrow \bar{\Sigma}_1 \tag{4.3.36}$$

$$\bar{L} = \bar{W} - \widehat{W}.$$

For the transition map \widehat{W} , we calculate it by making the following decomposition

$$\widehat{W} = \hat{T}_2 \circ R \circ \hat{T}_1,$$

where

- $\widehat{T}_1 : \bar{\Sigma}_2 \longrightarrow \Pi_3$, which is the compositions of normal form coordinate changes and a regular transition map. It can be written as

$$\begin{cases} \widehat{T}_{11}(\nu, \tilde{y}_2) = \nu, \\ \widehat{T}_{12}(\nu, \tilde{y}_2) = e_0(\nu) + e_1(\nu)\tilde{y}_2 + O(\tilde{y}_2^2), \end{cases} \quad (4.3.37)$$

where $e_0(0) = 0$ and $e_1(0) > 0$.

- $R : \Pi_3 \longrightarrow \Pi_4$ is a transition map, which is given in Proposition 4.3.1.
- $\widehat{T}_2 : \Pi_4 \longrightarrow \bar{\Sigma}_1$ is the composition of normal form coordinates changes and a regular transition map, which is given as follows

$$\begin{cases} \widehat{T}_{21}(\nu, \tilde{y}_4) = \nu, \\ \widehat{T}_{22}(\nu, \tilde{y}_4) = b_0(\nu) + b_1(\nu)\tilde{y}_4 + O(\tilde{y}_4^2), \end{cases} \quad (4.3.38)$$

where $b_0(0) = 0$ and $b_1(0) > 0$.

Then by straightforward calculation from (4.3.11), (4.3.37) and (4.3.38), for \widehat{W} , we

have

$$\begin{cases} \widehat{W}_1(\nu, \tilde{y}_2) = \nu, \\ \widehat{W}_2(\nu, \tilde{y}_2) = \zeta_0(\nu) + m(\nu)[\zeta_1(\nu)\tilde{y}_2 + \zeta_2(\nu)\tilde{y}_2^2 + O(\tilde{y}_2^3)], \end{cases} \quad (4.3.39)$$

where

$$\zeta_0(\nu) = b_0(\nu) + O(\gamma_0(\nu)) + O(m(\nu)),$$

$$\zeta_1(\nu) = e_1(\nu)b_1(\nu)\gamma_1(\nu) + O(e_0(\nu)) + O(\gamma_0(\nu)) + O(m(\nu)),$$

$$\zeta_2(\nu) = e_2(\nu)b_1(\nu)\gamma_1(\nu) + e_1^2(\nu)b_1(\nu)\gamma_2(\nu) + O(e_0(\nu)) + O(\gamma_0(\nu)) + O(m(\nu)).$$

For the transition map \overline{W} , we calculate it by making the following decomposition

$$\overline{W} = \Delta \circ \widehat{T}_3 \circ D^{-1},$$

where

- $D^{-1} : \overline{\Sigma}_2 \longrightarrow \widehat{\Sigma}_2$ is the Dulac map in the neighborhood of S_2 , which has the expression

$$\begin{cases} D_1^{-1}(\nu, \tilde{y}_2) = \nu, \\ D_2^{-1}(\nu, \tilde{y}_2) = \tilde{y}_2^{\frac{1}{\lambda_2(\nu)}} [1 + \hat{\phi}_0(\tilde{y}_2, \nu)], \end{cases} \quad (4.3.40)$$

where $\hat{\phi}_0 \in I_0^\infty$.

- $\widehat{T}_3 : \widehat{\Sigma}_2 \longrightarrow \widehat{\Sigma}_1$ is the composition of normal form coordinates changes and a regular transition map. Since \bar{x} axis is fixed for $\overline{X}_{\rho=1}$, so \widehat{T}_3 can be written as

$$\begin{cases} \widehat{T}_{31}(\nu, \tilde{x}_2) = \nu, \\ \widehat{T}_{32}(\nu, \tilde{x}_2) = k_1(\nu)\tilde{x}_2 + O(\tilde{x}_2^2), \end{cases} \quad (4.3.41)$$

where $k_1(0) > 0$.

- $\Delta : \widehat{\Sigma}_1 \longrightarrow \overline{\Sigma}_1$ is the stable-centre transition map in the neighborhood of the saddle-node S_1 . Obviously, the first component $\Delta_1(\nu, \tilde{y}_1) = \nu$. For the second component $\Delta_2(\nu, \tilde{y}_1)$, the graph $\tilde{x}_1 = \Delta_2(\nu, \tilde{y}_1)$ is a solution of the following differential equation

$$\Omega = F(\tilde{y}_1, \nu, \bar{\mu}, a)d\tilde{x}_1 - \tilde{x}_1 d\tilde{y}_1 = 0, \quad (4.3.42)$$

where $F(\tilde{y}_1, \nu, \bar{\mu}, a) = O(\nu) + \varpi(\nu)\tilde{y}_1^2 + O(\tilde{y}_1^3)$ and $\varpi(\nu) = -\frac{1}{2a}\sqrt{-\frac{a}{\bar{\mu}_2}} + O(\nu)$.

Hence, by (4.3.40), (4.3.41) and (4.3.42), the transition map \overline{W} has the following form

$$\begin{cases} \overline{W}_1(\nu, \tilde{y}_2) = \nu, \\ \overline{W}_2(\nu, \tilde{y}_2) = \Delta_2(\nu, \tilde{y}_1), \end{cases} \quad (4.3.43)$$

where

$$\tilde{y}_1 = k_1(\nu)\tilde{y}_2^{\frac{1}{\lambda_2(\nu)}} [1 + \hat{\phi}_1(\tilde{y}_2, \nu)]$$

and $\hat{\phi}_1(\tilde{y}_2, \nu) \in I_0^\infty$.

Now we study the displacement map $\overline{L} = \overline{W} - \widehat{W}$. Obviously, we see $\overline{L}_1(\nu, \tilde{x}_2) = 0$. By (4.3.36), (4.3.39) and (4.3.43), the equation $\overline{L}_2(\nu, \tilde{x}_2) = 0$ is equivalent to the following system

$$\begin{cases} \tilde{x}_1 = \Delta_2(\nu, \tilde{y}_1), \\ \tilde{x}_1 = \widehat{W}_2(\nu, \tilde{y}_2). \end{cases} \quad (4.3.44)$$

Since $\Delta_2(\nu, \tilde{y}_1)$ is a connected graph, the Khovanskii procedure [32] shows that the number of solutions of (4.3.44) is at most 1 plus the number of solutions of the following

system

$$\begin{cases} \tilde{x}_1 = \widehat{W}_2(\nu, \tilde{y}_2), \\ \Omega \wedge d\widehat{W}_2(\nu, \tilde{y}_2) = 0. \end{cases}$$

This above system is equivalent to

$$\begin{cases} \tilde{x}_1 = \widehat{W}_2(\nu, \tilde{y}_2), \\ \det \begin{pmatrix} \frac{\partial \widehat{W}_2(\nu, \tilde{y}_2)}{\partial \tilde{y}_2} & -1 \\ -\tilde{x}_1 & F(\tilde{y}_1, \nu, \bar{\mu}, a) \end{pmatrix} = 0. \end{cases} \quad (4.3.45)$$

Eliminating \tilde{x}_1 from the equations (4.3.45), we have an equivalent equation

$$\bar{\bar{L}}_2 = \widehat{W}_2(\nu, \tilde{y}_2) - F(\tilde{y}_1, \nu, \bar{\mu}, a) \frac{\partial \widehat{W}_2(\nu, \tilde{y}_2)}{\partial \tilde{y}_2}. \quad (4.3.46)$$

Differentiating (4.3.46) with respect to \tilde{x}_2 , we have

$$\begin{aligned} \frac{\partial \bar{\bar{L}}_2}{\partial \tilde{y}_2} &= \left(1 - \frac{\partial F(\tilde{y}_1, \nu, \bar{\mu}, a)}{\partial \tilde{y}_2}\right) \frac{\partial \widehat{W}_2(\nu, \tilde{y}_2)}{\partial \tilde{y}_2} - F(\tilde{y}_1, \nu, \bar{\mu}, a) \frac{\partial^2 \widehat{W}_2(\nu, \tilde{y}_2)}{\partial \tilde{y}_2^2} \\ &= m(\nu) \left[\left(1 - 2\varpi(\nu)k_1^2(\nu) \frac{1}{\lambda_2(\nu)} \tilde{y}_2^{\frac{2}{\lambda_2} - 1} (1 + \hat{\phi}_2(\tilde{y}_2, \nu))\right) (\zeta_1(\nu) + O(\tilde{y}_2)) \right. \\ &\quad \left. - \left(O(\nu) + \varpi(\nu)k_1^2(\nu) \tilde{y}_2^{\frac{2}{\lambda_2}(\nu)} (1 + \hat{\phi}_3(\tilde{y}_2, \nu))\right) (2\zeta_2(\nu) + O(\tilde{y}_2)) \right] \\ &= m(\nu) \left[\zeta_1(\nu) - O(\nu)\zeta_2(\nu) + O(\tilde{y}_2) \right], \end{aligned}$$

which has the same number of small roots as of

$$\widehat{L}_2 := \frac{1}{m(\nu)} \frac{\partial \bar{\bar{L}}_2}{\partial \tilde{y}_2} = \zeta_1(\nu) - O(\nu)\zeta_2(\nu) + O(\tilde{y}_2).$$

Since $\zeta_1(0) = e_1(0)b_1(0)l_1(0)n_1(0) \neq 0$ and $\zeta_2(\nu)$ is bounded for $(\nu, \bar{\mu}, a)$ in a small neighborhood of $(0, \bar{\mu}_0, a_0)$. Therefore, there exist A_0 , a neighborhood of a_0 , V_{70} ,

a neighborhood of $\bar{\mu}_0$, and $\nu_1 > 0$, such that $\forall(a, \bar{\mu}) \in A_0 \times V_{70}$ and $\forall \nu \in (0, \nu_1)$, $\widehat{L}_2(\nu, \tilde{y}_2) \neq 0$ in a small neighborhood of $\tilde{y}_2 = 0$.

Therefore, by Rolle's theorem, $\forall(a, \bar{\mu}) \in A_0 \times V_{70}$ and $\forall \nu \in (0, \nu_1)$, equation $\bar{L}_2(\nu, \tilde{y}_2) = 0$ has at most 2 small zeroes, i.e., $Cycl(Sxhh7c) \leq 2$.

4.3.4.2 Sxhh7b

We study the transition map $T^{-1} : \Pi_3 \longrightarrow \Pi_4$. In the chart F. R. on $r = 0$, Π_3 and Π_4 are two line sections parameterized by $\tilde{y}_i (i = 3, 4)$, respectively. The second component $T_2^{-1}(0, \tilde{y}_3)$ maps $(0, +\infty)$ to $(0, +\infty)$.

If $T_2^{-1}(0, \tilde{y}_3)$ is in the neighborhood of the graphic Sxhh7c, since the Dulac map D^{-1} is attracting and the map Δ has flatness property, then we have $\lim_{\tilde{y}_3 \rightarrow 0} \frac{\partial T_2^{-1}}{\partial \tilde{y}_3}(0, \tilde{y}_3) = 0$. If $T_2^{-1}(0, \tilde{y}_3)$ is in the neighborhood of the graphic Sxhh7a, then by (4.2.3), we have $\lim_{\tilde{y}_3 \rightarrow +\infty} \frac{\partial T_2^{-1}}{\partial \tilde{y}_3}(0, \tilde{y}_3) = 1$. so $T_2^{-1}(0, \tilde{y}_3)$ has to be nonlinear. Therefore, it is nonlinear for $\tilde{y}_3 \in \mathbb{R}^+$.

From proposition 4.3.1, we know that any i^{th} derivative of the second component of transition map $R(\nu, \tilde{y}_3)$ is close to zero. If $T_2^{-1}(0, \tilde{y}_3)$ has its n^{th} derivative nonvanishing, then by Rolle's theorem, $\forall(a, \bar{\mu}) \in A_0 \times V_{70}$ and $\nu > 0$ sufficiently small, $L(\nu, \tilde{y}_3)$ has at most n roots in a small neighborhood of $\tilde{y}_3 = 0$, i.e., we have $Cycl(Sxhh7b) \leq n$.

4.3.5 Family Sxhh8

As shown in Fig. 4.8, there is a saddle point S_1 and an attracting saddle node S_2 on the lower boundary graphic Sxhh8c. In this case

$$V_8 = \{\bar{\mu} \in \mathbb{S}^2 \mid \bar{\mu}_1 = 0, \bar{\mu}_2 > 0, \bar{\mu}_3 = -\sqrt{-\frac{\bar{\mu}_2}{a}}\}.$$

The hyperbolicity ratio at S_1 is $\lambda_1 = -\frac{1}{a} \geq 2$.

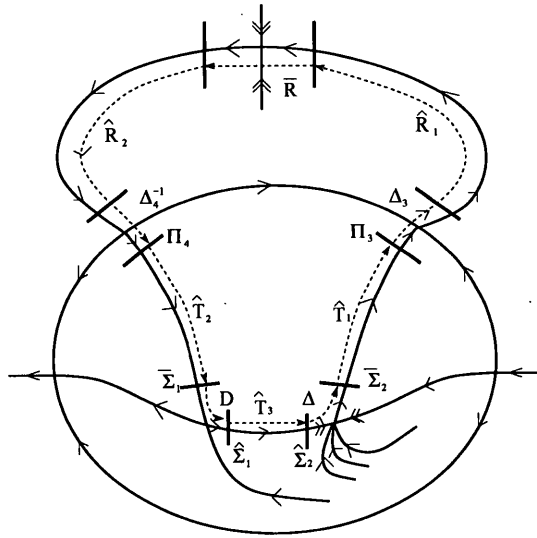


Figure 4.8: Transition maps for the family Sxhh8

4.3.5.1 Sxhh8c

We first consider the lower boundary graphic Sxhh8c. In the chart F.R., in the neighborhood of S_1 , take sections $\bar{\Sigma}_1 = \{\tilde{y}_1 = 1\}$ and $\hat{\Sigma}_1 = \{\tilde{x}_1 = 1\}$ in the normal form

coordinates. In the neighborhood of saddle-node point, take sections $\bar{\Sigma}_2 = \{\tilde{y}_2 = 1\}$ and $\hat{\Sigma}_2 = \{\tilde{x}_2 = -1\}$ in the normal form coordinates. We study the first return map

$$P : \bar{\Sigma}_2 \longrightarrow \bar{\Sigma}_2.$$

For the Poincaré return map P , we calculate it by making the following decomposition

$$P = \Delta \circ \hat{T}_3 \circ D \circ \hat{T}_2 \circ R \circ \hat{T}_1,$$

where

- $\hat{T}_1 : \bar{\Sigma}_2 \longrightarrow \Pi_3$, which is the compositions of normal form coordinate changes and a regular transition map. It can be written as

$$\begin{cases} \hat{T}_{11}(\nu, \tilde{x}_2) = \nu, \\ \hat{T}_{12}(\nu, \tilde{x}_2) = e_0(\nu) + e_1(\nu)\tilde{x}_2 + O(\tilde{x}_2^2), \end{cases} \quad (4.3.47)$$

where $e_0(0) = 0$ and $e_1(0) > 0$.

- $R : \Pi_3 \longrightarrow \Pi_4$ is a transition map, which is given by Proposition 4.3.1.
- $\hat{T}_2 : \Pi_4 \longrightarrow \bar{\Sigma}_1$ is the composition of normal form coordinate changes and a regular transition map, which is given as follows

$$\begin{cases} \hat{T}_{21}(\nu, \tilde{y}_4) = \nu, \\ \hat{T}_{22}(\nu, \tilde{y}_4) = b_0(\nu) + b_1(\nu)\tilde{y}_4 + O(\tilde{y}_4^2), \end{cases} \quad (4.3.48)$$

where $b_0(0) = 0$ and $b_1(0) > 0$.

- $D : \bar{\Sigma}_1 \longrightarrow \hat{\Sigma}_1$ is the Dulac map near the attracting saddle S_1 , which is given as follows

$$\begin{cases} D_1(\nu, \tilde{x}_1) = \nu, \\ D_2(\nu, \tilde{x}_1) = \tilde{x}_1^{\lambda_1(\nu)} [1 + \hat{\phi}(\tilde{x}_1, \nu)], \end{cases} \quad (4.3.49)$$

where $\hat{\phi} \in I_0^\infty$.

- $\hat{T}_3 : \hat{\Sigma}_1 \longrightarrow \hat{\Sigma}_2$ is the composition of normal form coordinates changes and a regular transition map. Since \bar{x} axis is fixed for $\bar{X}_{\rho=1}$, so \hat{T}_3 can be written as

$$\begin{cases} \hat{T}_{31}(\nu, \tilde{y}_1) = \nu, \\ \hat{T}_{32}(\nu, \tilde{y}_1) = k_1(\nu)\tilde{y}_1 + O(\tilde{y}_1^2), \end{cases} \quad (4.3.50)$$

where $k_1(0) > 0$.

- $\Delta : \hat{\Sigma}_2 \longrightarrow \bar{\Sigma}_2$ is the stable-centre transition map near saddle-node point S_2 . Obviously, the first component $\Delta_1(\nu, \tilde{y}_2) = \nu$. For the second component $\Delta_2(\nu, \tilde{y}_2)$, $\forall p, q \in \mathbb{N}$, we have the flatness property:

$$\frac{\partial^p \Delta_2(\nu, \tilde{y}_2)}{\partial \tilde{y}_2^p} = O(\tilde{y}_2^q). \quad (4.3.51)$$

Then by (4.3.11), (4.3.47), (4.3.48), (4.3.49) and (4.3.50), for the return map P , we have

$$\begin{cases} P_1(\nu, \tilde{x}_2) = \nu, \\ P_2(\nu, \tilde{x}_2) = \Delta_2 \circ \hat{T}_{32} \circ D_2 \circ \hat{T}_{22} \circ R_2 \circ \hat{T}_{12}(\nu, \tilde{x}_2). \end{cases} \quad (4.3.52)$$

Let $\tilde{y}_3 = \widehat{T}_{12}(\nu, \tilde{x}_2)$, $\tilde{y}_4 = R_2(\nu, \tilde{y}_3)$, $\tilde{x}_1 = \widehat{T}_{22}(\nu, \tilde{y}_4)$, $\tilde{y}_1 = D_2(\nu, \tilde{x}_1)$, $\tilde{y}_2 = \widehat{T}_{32}(\nu, \tilde{y}_1)$ and $\tilde{x}_2 = \Delta_2(\nu, \tilde{y}_2)$. Then

$$\begin{aligned} \frac{\partial P_2(\nu, \tilde{x}_2)}{\partial \tilde{x}_2} &= \frac{\partial \Delta_2(\nu, \tilde{y}_2)}{\partial \tilde{y}_2} \frac{\partial \widehat{T}_{32}(\nu, \tilde{y}_1)}{\partial \tilde{y}_1} \frac{\partial D_2(\nu, \tilde{x}_1)}{\partial \tilde{x}_1} \frac{\partial \widehat{T}_{22}(\nu, \tilde{y}_4)}{\partial \tilde{y}_4} \\ &\quad \times \frac{\partial R_2(\nu, \tilde{y}_3)}{\partial \tilde{y}_3} \frac{\partial \widehat{T}_{12}(\nu, \tilde{x}_2)}{\partial \tilde{x}_2}. \end{aligned} \quad (4.3.53)$$

From proposition 4.3.1, we know that any i^{th} derivative of the second component of transition map $R(\nu, \tilde{y}_3)$ is close to zero for $\nu > 0$ sufficiently small and $(\nu, \bar{\mu})$ sufficiently near $(a, \bar{\mu}) = (a_0, \bar{\mu}_0)$. D is the Dulac map near an attracting saddle, and Δ is the stable-centre transition map with flatness property (4.3.51).

Therefore, for any $0 < \varepsilon \ll 1$, there exist A_0 , a neighborhood of a_0 , V_{80} , a neighborhood of $\bar{\mu}_0$, $\nu_1 > 0$, neighborhoods $U_0(\tilde{x}_i)$ of $\tilde{x}_i = 0$ ($i = 1, 2$) and neighborhoods $U_0(\tilde{y}_i)$ of $\tilde{y}_i = 0$ ($i = 1, 2, 3, 4$), such that if $(a, \bar{\mu}) \in A_0 \times V_{80}$ and $\nu \in (0, \nu_1)$, and $\tilde{x}_2 \in U_0(\tilde{x}_2)$, then we have $\tilde{x}_1 \in U_0(\tilde{x}_1)$, $\tilde{y}_i \in U_0(\tilde{y}_i)$ ($i = 1, 2, 3, 4$) and

$$\left| \frac{\partial \Delta_2(\nu, \tilde{y}_2)}{\partial \tilde{y}_2} \right| < \varepsilon, \quad \left| \frac{\partial D_2(\nu, \tilde{x}_1)}{\partial \tilde{x}_1} \right| < \varepsilon, \quad \left| \frac{\partial R_2(\nu, \tilde{y}_3)}{\partial \tilde{y}_3} \right| < \varepsilon. \quad (4.3.54)$$

Also, if $(a, \bar{\mu}) \in A_0 \times V_{80}$ and $\nu \in (0, \nu_1)$, $U_0(\tilde{x}_i)$ and $U_0(\tilde{y}_i)$ are sufficiently small, there exist a $M > 0$ such that

$$0 < \left| \frac{\partial \widehat{T}_{32}(\nu, \tilde{y}_1)}{\partial \tilde{y}_1} \right|, \quad \left| \frac{\partial \widehat{T}_{22}(\nu, \tilde{y}_4)}{\partial \tilde{y}_4} \right|, \quad \left| \frac{\partial \widehat{T}_{12}(\nu, \tilde{x}_2)}{\partial \tilde{x}_2} \right| < M. \quad (4.3.55)$$

Hence, by (4.3.53), (4.3.54) and (4.3.55), we have $\left| \frac{\partial P_2(\nu, \tilde{x}_2)}{\partial \tilde{x}_2} \right| \ll 1$. Therefore, by Rolle's theorem, $\forall (a, \bar{\mu}) \in A_0 \times V_{80}$ and $\forall \nu \in (0, \nu_1)$, the first return map P has at most 1 fixed point in a small neighborhood of $\tilde{x}_2 = 0$, i.e., $\text{Cycl}(Sxhh8c) \leq 1$.

4.3.5.2 Sxhh8b

We study the transition map $T : \Pi_4 \longrightarrow \Pi_3$. In the chart F. R. on $r = 0$, Π_3 and Π_4 are two line sections parameterized by \tilde{y}_i ($i = 3, 4$), respectively. The second component $T_2(0, \tilde{y}_4)$ maps $(0, +\infty)$ to $(0, +\infty)$.

If $T_2(0, \tilde{y}_4)$ is in the neighborhood of the graphic Sxhh8c, since the Dulac map D is attracting and the map Δ is flat, then we have $\lim_{\tilde{y}_4 \rightarrow 0} \frac{\partial T_2}{\partial \tilde{y}_4}(0, \tilde{y}_4) = 0$. If $T_2(0, \tilde{y}_4)$ is in the neighborhood of the graphic Sxhh8a, by (4.2.3), we have $\lim_{\tilde{y}_4 \rightarrow +\infty} \frac{\partial T_2}{\partial \tilde{y}_4}(0, \tilde{y}_4) = 1$. Since $T_2(0, \tilde{y}_4)$ is analytic, there exists a constant $M_0 > 0$, such that $|\frac{\partial T_2}{\partial \tilde{y}_4}(0, \tilde{y}_4)| < M_0$ for $\tilde{y}_4 \in (0, \infty)$.

Define the Poincaré return map

$$\begin{aligned} \bar{P} : \Pi_3 &\longrightarrow \Pi_3 \\ (\nu, \tilde{y}_3) &\longrightarrow (\nu, \bar{P}_2(\nu, \tilde{y}_3)) \\ \bar{P} &= T \circ R. \end{aligned} \tag{4.3.56}$$

For the first component \bar{P}_1 , we have $\bar{P}_1(\nu, \tilde{y}_3) = \nu$. For the second component \bar{P}_2 , we have $\bar{P}_2(\nu, \tilde{y}_3) = T_2 \circ R_2(\nu, \tilde{y}_3)$.

Since the derivative of $T_2(0, \tilde{y}_4)$ is bounded for $\tilde{y}_4 \in (0, \infty)$, and any i^{th} derivative of $R_2(\nu, \tilde{y}_3)$ is close to zero, so $\forall (a, \bar{\mu}) \in A_0 \times V_{80}$ and $\nu > 0$ sufficiently small, $\frac{\partial \bar{P}_2}{\partial \tilde{y}_3}(\nu, \tilde{y}_3)$ is sufficiently small in a small neighborhood of $\tilde{y}_3 = 0$. Therefore, the first return map \bar{P} has at most 1 fixed point, i.e., $Cycl(Sxhh8b) \leq 1$.

Altogether, we finish the proof of Theorem 4.1.1.

5 Finite cyclicity of (I_{9b}^1)

For the graphic (I_{9b}^1) , it is an HH-type graphic with a nilpotent elliptic point of multiplicity 3 at infinity and an invariant parabola as shown in Fig 5.1, and this nilpotent elliptic point could be of codimension 3 or 4.

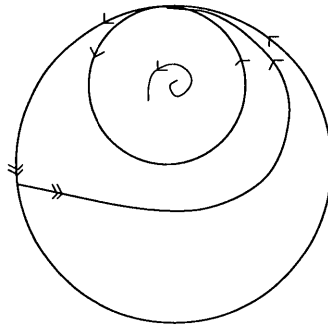


Figure 5.1: The graphic (I_{9b}^1) .

In this chapter, firstly we identify the codimension of the nilpotent singularity point of the graphic (I_{9b}^1) in section 5.1. If the nilpotent elliptic point is of codimension 3, then we only need to verify the generic condition of Theorem 2.1.2. If the nilpotent elliptic point is of codimension 4, by calculation of the second derivative of the transition map

along the invariant parabola we prove that the graphic (I_{9b}^1) has finite cyclicity in section 5.2 and section 5.3.

5.1 Lemmas

Lemma 5.1.1. *The graphic (I_{9b}^1) occurs in the family*

$$\begin{cases} \dot{x} = \lambda x - y + x^2 := \bar{P}(x, y), \\ \dot{y} = x + \lambda y + \delta_1 x^2 + \delta_2 xy := \bar{Q}(x, y), \end{cases} \quad (5.1.1)$$

where $\lambda \neq 0$, $1 < \delta_2 < 2$, $\delta_1 = \lambda(3 - \delta_2) > 0$ and $4\lambda^2 - (1 + \lambda^2)\delta_2 < 0$.

1. If $\delta_2 \neq \frac{3}{2}$, the nilpotent elliptic point is of codimension 3.
2. If $\delta_2 = \frac{3}{2}$, the nilpotent elliptic point is of codimension 4, type 2.

Proof. For the family (5.1.1), the triple nilpotent singular point is at infinity, so we introduce the coordinates $(v, z) = (\frac{x}{y}, \frac{1}{y})$. Then we have

$$\begin{cases} \dot{v} = -z + (1 - \delta_2)v^2 - \lambda(3 - \delta_2)v^3 - v^2z, \\ \dot{z} = -\delta_2vz - \lambda z^2 - \lambda(3 - \delta_2)v^2z - vz^2. \end{cases}$$

By a near-identity transformation

$$\begin{cases} v = v_1, \\ z = z_1 + (1 - \delta_2)v_1^2 + \lambda v_1 z_1 + O(|v_1, z_1|^3), \end{cases} \quad (5.1.2)$$

and change of coordinates $v_1 \rightarrow -v_1$ and $z_1 \rightarrow z_1$, we have

$$\begin{cases} \dot{v}_1 = z_1, \\ \dot{z}_1 = \delta_2(1 - \delta_2)v_1^3 + (3\delta_2 - 2)v_1z_1 + \lambda(9\delta_2 - 16)v_1^2z_1 + O(|v_1, z_1|^4). \end{cases} \quad (5.1.3)$$

Let

$$v_1 = \frac{v_2}{\sqrt{|\delta_2(\delta_2 - 1)|}}, \quad z_1 = \frac{z_2}{\sqrt{|\delta_2(\delta_2 - 1)|}}, \quad (5.1.4)$$

we rescale the system (5.1.3) into

$$\begin{cases} \dot{v}_2 = z_2, \\ \dot{z}_2 = -v_2^3 + \frac{(3\delta_2 - 2)}{\sqrt{|\delta_2(\delta_2 - 1)|}}v_2z_2 - \frac{\lambda(9\delta_2 - 16)}{|\delta_2(\delta_2 - 1)|}v_2^2z_2 + O(|v_2, z_2|^4). \end{cases} \quad (5.1.5)$$

By a near-identity transformation

$$\begin{cases} v_2 = v_3(1 + \frac{\lambda(5\delta_2^2 - 11\delta_2 + 4)}{5\sqrt{|\delta_2(\delta_2 - 1)|^3}}v_3 + O(v_3^2)), \\ z_2 = z_3, \end{cases} \quad (5.1.6)$$

and rescaling the time, we bring system (5.1.5) into a “standard form”

$$\begin{cases} \dot{v}_3 = z_3, \\ \dot{z}_3 = -v_3^3 + z_3[bv_3 + \varepsilon_2v_3^2] + z_3^2O(|(v_3, z_3)|^2), \end{cases} \quad (5.1.7)$$

where

$$b = \frac{3\delta_2 - 2}{\sqrt{|\delta_2(\delta_2 - 1)|}},$$

$$\varepsilon_2 = \frac{2\lambda(2\delta_2 - 3)(\delta_2 - 4)}{5|\delta_2(\delta_2 - 1)|^2}.$$

So for $\lambda \neq 0$ and $\delta_2 \in (1, 2)$, if $\delta_2 \neq \frac{3}{2}$, the nilpotent elliptic point is of codimension

3; if $\delta_2 = \frac{3}{2}$, the nilpotent elliptic point is of codimension 4, type 2. \square

Lemma 5.1.2. *Inside quadratic systems, the graphics (I_{9b}^1) have finite cyclicity if the nilpotent singular point is of codimension 3.*

Proof. If the nilpotent singular point is of codimension 3 [i.e., $\delta_2 \in (1, 2)$ and $\delta_2 \neq \frac{3}{2}$ in family (5.1.1)], to prove that the graphic (I_{9b}^1) has finite cyclicity, by Theorem 2.1.2, we only need to check that for the first return map P along the invariant parabola, it satisfies $P'(0) \neq 1$.

The equation of the invariant parabola is given as follows.

$$y = \left(1 - \frac{\delta_2}{2}\right)x^2 - \lambda x - \frac{1}{2}(1 + \lambda^2). \quad (5.1.8)$$

Along the graphic (the invariant parabola), we have

$$\begin{aligned} P'(0) &= \exp \left(\int_{-\infty}^{\infty} \operatorname{div} X(\Gamma(t)) \Big|_{(5.1.1), (5.1.8)} dt \right) \\ &= \lim_{x_0 \rightarrow \infty} \exp \left(\int_{-x_0}^{x_0} \frac{4\lambda + 2(2 + \delta_2)x}{\delta_2 x^2 + 4\lambda x + 1 + \lambda^2} dx \right) \\ &= \lim_{x_0 \rightarrow \infty} \left[\left(\frac{\delta_2 x_0^2 + 4\lambda x_0 + 1 + \lambda^2}{\delta_2 x_0^2 - 4\lambda x_0 + 1 + \lambda^2} \right)^{\frac{2+\delta_2}{2\delta_2}} \exp \left(-\frac{16\lambda}{\delta_2 \sqrt{\Delta_0}} \arctan \frac{\delta_2 x_0 + 2\lambda}{\sqrt{\Delta_0}} \right) \Big|_{-x_0}^{x_0} \right] \\ &= \exp \left(-\frac{16\lambda\pi}{\delta_2 \sqrt{\Delta_0}} \right) \\ &\neq 1. \end{aligned}$$

where $\Delta_0 = (1 + \lambda^2)\delta_2 - 4\lambda^2 > 0$ and $\lambda \neq 0$.

So, the graphics (I_{9b}^1) have finite cyclicity if the nilpotent point has codimension 3.

□

5.2 Main theorem

Theorem 5.2.1. *The graphics $(I_{\delta b}^1)$ have finite cyclicity inside quadratic systems.*

By Lemma 5.1.2, we only need to prove that $(I_{\delta b}^1)$ have finite cyclicity when the nilpotent singular point is of codimension 4 [i.e., $\delta_2 = \frac{3}{2}$ in family (5.1.1)], which corresponds to $a_0 = \frac{1}{3}$ in (2.4.15).

If the nilpotent singular point is of codimension 4, the finite cyclicity of the limit periodic sets Ehh1a, Ehh2–Ehh12 is the direct consequence of Theorem 2.1.2 and the fact $P'(0) \neq 0$ in Lemma 5.1.2, except the case Ehh1b and Ehh1c, for which the hypothesis $a_0 \neq \frac{1}{3}$ is used.

Therefore, we only need to prove that the intermediate graphic Ehh1b and lower boundary graphic Ehh1c have finite cyclicity when $a_0 = \frac{1}{3}$ [i.e., $\delta_2 = \frac{3}{2}$ in family (5.1.1)].

5.3 Proof of the main theorem

We begin with the lower boundary graphic Ehh1c. We study the displacement maps defined on the sections τ_1 and τ_2 with images on the sections Π_1 and Σ_4 as shown in Fig. 5.2.

The procedure of the proof is the same as the proof for the case Ehh1c of codimension 3, which consists of several steps, so we recall the common steps **(I)–(IV)** as follows.

(I) Parameterization of sections τ_1 and τ_2

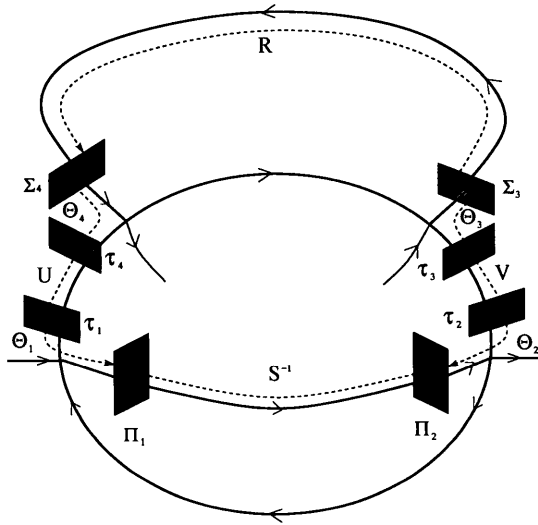


Figure 5.2: Transition maps for the graphic Ehh1c of (I_{9b}^1)

On τ_1 , the coordinates are (r_1, ρ_1) with $r_1\rho_1 = \nu$ for $\nu > 0$ small. Now we want to cover the domain $|r_1| < \varepsilon, |\rho_1| < \varepsilon$ for $\varepsilon > 0$ small. Then $\nu \leq \varepsilon^2$. So $\forall u \in (0, 1)$, on the curve $\nu = u\varepsilon^2$, we have $r_1\rho_1 = u\varepsilon^2$. Hence $r_1, \rho_1 \in (u\varepsilon, \varepsilon)$. Let

$$r_1 = \nu^{1-c}, \quad \rho_1 = \nu^c,$$

then we parameterize the section τ_1 with the coordinates $(\nu, c) \in (0, \varepsilon^2) \times I_\nu$ where

$$I_\nu = \left(\frac{\ln \varepsilon}{\ln \nu}, \frac{\ln u\varepsilon}{\ln \nu} \right) \subset (0, 1).$$

Similarly, on the section τ_2 , we have

$$r_2 = \nu^{1-d}, \quad \rho_2 = \nu^d,$$

and we use coordinates $(\nu, d) \in (0, \varepsilon^2) \times I_\nu$ to parameterize the section τ_2 .

For graphic Ehh1, we use $\bar{V}_1 \subset \mathbb{S}^2$ to denote the set of $\bar{\mu} = (\bar{\mu}_1, \bar{\mu}_2, \bar{\mu}_3)$ in which the family Ehh1 exists, and use \bar{V}_{10} to denote a small neighborhood of $\bar{\mu}_0$, where $\bar{\mu}_0 \in \bar{V}_1$. We use A_0 to denote a small neighborhood of a_0 , where $a_0 \in (0, \frac{1}{2})$.

We will study the number of roots of the following system

$$\begin{cases} T_1(\nu, c) = T_2(\nu, d), \\ T_3(\nu, c) = T_4(\nu, d), \end{cases} \quad (5.3.9)$$

for $(a, \bar{\mu}) \in A_0 \times \bar{V}_{10}$ with $(c, d) \in I_\nu \times I_\nu$ and ν, ε sufficiently small. The transition maps $T_i (i = 1, 2, 3, 4)$ will be developed in the next step.

(II) Transition maps T_i ($i = 1, 2, 3, 4$)

(II-1) The transition map T_1

The map $T_1 : \tau_1 \rightarrow \Pi_1$ is the second type of Dulac map near P_1 . For $r_1 = \nu^{1-c}$ and $\rho_1 = \nu^c$, it has the following expression

$$\begin{cases} T_{11}(\nu, c) = \nu, \\ T_{12}(\nu, c) = \eta_1(\nu, \omega(\frac{\nu^c}{\rho_0}, \alpha_1)) + \nu^{\bar{\sigma}_1 c} \left[l_1 + \theta_1(\nu, \nu^c, \omega(\frac{\nu^c}{\rho_0}, -\alpha_1)) \right], \end{cases} \quad (5.3.10)$$

where $l_1 = \frac{y_0}{\rho_0^{\bar{\sigma}_1}} > 0$, $\alpha_1 = p_1 - \bar{\sigma}_1(a)q_1$, $\eta_1(\nu, \omega(\frac{\nu^c}{\rho_0}, \alpha_1)) = \frac{\kappa_1}{\rho_0^{\bar{\sigma}_1}} \nu^{p_1} \omega(\frac{\nu^c}{\rho_0}, \alpha_1)$ and $\theta_1(\nu, \nu^c, \omega(\frac{\nu^c}{\rho_0}, -\alpha_1))$ is C^k and satisfies the following properties:

$$\begin{aligned} \theta_1(\nu, \nu^c, \omega(\frac{\nu^c}{\rho_0}, -\alpha_1)) &= O\left(\nu^{p_1 c} \omega(\frac{\nu^c}{\rho_0}, -\alpha_1)\right), \\ \frac{\partial^i \theta_1}{\partial c^i}(\nu, \nu^c, \omega(\frac{\nu^c}{\rho_0}, -\alpha_1)) &= O\left(\nu^{p_1 c} \omega(\frac{\nu^c}{\rho_0}, -\alpha_1) (\ln \nu)^i\right), \quad i \geq 1. \end{aligned} \quad (5.3.11)$$

(II-2) The transition map T_2

The transition map $T_2 : \tau_2 \longrightarrow \Pi_1$ can be factorized as

$$T_2 = S^{-1} \circ \Theta_2,$$

where

- $\Theta_2 : \tau_2 \longrightarrow \Pi_2$ is the second type of Dulac map in the neighborhood of P_2 . For

$r_2 = \nu^{1-d}$ and $\rho_2 = \nu^d$, it has the following expression

$$\begin{cases} \Theta_{11}(\nu, d) = \nu, \\ \Theta_{12}(\nu, d) = \eta_2(\nu, \omega(\frac{\nu^d}{\rho_0}, \alpha_1)) + \nu^{\bar{\sigma}_1 d} \left[l_1 + \theta_2(\nu, \nu^d, \omega(\frac{\nu^d}{\rho_0}, -\alpha_1)) \right], \end{cases}$$

where $l_1 = \frac{y_0}{\rho_0^{\bar{\sigma}_1}} > 0$, $\eta_2(\nu, \omega(\frac{\nu^d}{\rho_0}, \alpha_1)) = \frac{\kappa_1}{\rho_0^{\bar{\sigma}_1}} \nu^{\rho_1} \omega(\frac{\nu^d}{\rho_0}, \alpha_1)$ and $\theta_2(\nu, \nu^d, \omega(\frac{\nu^d}{\rho_0}, -\alpha_1))$

is C^k and satisfies the same properties as of θ_1 in (5.3.11).

- $S^{-1} : \Pi_2 \longrightarrow \Pi_1$ is a regular transition map, which can be written as

$$\begin{cases} S_1^{-1}(\nu, \tilde{y}_2) = \nu, \\ S_2^{-1}(\nu, \tilde{y}_2) = k_0(\nu) + k_1(\nu)\tilde{y}_2 + k_2(\nu)\tilde{y}_2^2 + O(\tilde{y}_2^3), \end{cases}$$

where $k_0(0) = 0$, $k_1(0) = e^{-\frac{\pi \bar{\mu}_{30}}{\sqrt{\alpha_0 \mu_{20}}}}$, and $k_2(0) = * \bar{\mu}_{30}$ by Proposition 6.1 in [53].

Therefore, for T_2 , we have

$$\begin{cases} T_{21}(\nu, d) = \nu, \\ T_{22}(\nu, d) = m_{20}(\nu, \omega(\frac{\nu^d}{\rho_0}, \alpha_1)) + \nu^{\bar{\sigma}_1 d} \left[m_{21}(\nu, \omega(\frac{\nu^d}{\rho_0}, \alpha_1)) + \sum_{i=2}^k m_{2i}(\nu, \omega(\frac{\nu^d}{\rho_0}, \alpha_1)) \nu^{(i-1)\bar{\sigma}_1 d} + \theta_{21}(\nu, \nu^d, \omega(\frac{\nu^d}{\rho_0}, -\alpha_1)) \right], \end{cases} \quad (5.3.12)$$

where

$$m_{20}(\nu, \omega(\frac{\nu^d}{\rho_0}, \alpha_1)) = k_0(\nu) + \kappa_1 \left[\frac{n_1(\nu)}{\rho_0^{p_1}} \nu^{p_1} \omega(\frac{\nu^d}{\rho_0}, \alpha_1) + O(\nu^{2p_1} \omega^2(\frac{\nu^d}{\rho_0}, \alpha_1)) \right],$$

$$m_{2i}(\nu, \omega(\frac{\nu^d}{\rho_0}, \alpha_1)) = k_i(\nu) l_1^i + \kappa_1 O(\nu^{p_1} \omega(\frac{\nu^d}{\rho_0}, \alpha_1)), \quad i \geq 1$$

and θ_{21} is C^k and has the same properties as of θ_1 in (5.3.11).

(II-3) The transition map T_3

The transition map $T_3 : \tau_2 \rightarrow \Sigma_4$ can be factorized as

$$T_3 = R \circ \Theta_3 \circ V,$$

where

- $V : \tau_2 \rightarrow \tau_3$ is a regular transition map, which can be written as

$$\begin{cases} r_3 = V_1(\nu^{1-d}, \nu^d) \\ \quad = \nu^{1-d} [m_{141}(\nu) + m_{142}(\nu) \nu^{1-d} + m_{143}(\nu) \nu^d + O(\nu^{2(1-d)}, \nu^{2d})], \\ \rho_3 = V_2(\nu^{1-d}, \nu^d) \\ \quad = \nu^c [\hat{m}_{141}(\nu) + \hat{m}_{142}(\nu) \nu^{1-d} + \hat{m}_{143}(\nu) \nu^d + O(\nu^{2(1-d)}, \nu^{2d})], \end{cases} \quad (5.3.13)$$

where $m_{141}(0) > 0$, $\hat{m}_{141}(0) > 0$, $m_{142}(0) = * \varepsilon_2$, $\hat{m}_{142}(0) = * \varepsilon_2$, $m_{143}(0) = * \bar{\mu}_{30}$ and $\hat{m}_{143}(0) = * \bar{\mu}_{30}$. The symbol $*$ denotes any continuous function of $(\nu, \bar{\mu}, a)$, which is nonzero at $(\nu, \bar{\mu}, a) = (0, \bar{\mu}_0, a_0)$.

- $\Theta_3 : \tau_3 \rightarrow \Pi_3$ is the second type of Dulac map in the neighborhood of P_3 with $\bar{\sigma} = \bar{\sigma}_3$.

- The regular transition map $R : \Sigma_3 \rightarrow \Sigma_4$ is C^k , which can be written as

$$\begin{cases} R_1(\nu, \tilde{y}_3) = \nu, \\ R_2(\nu, \tilde{y}_3) = \hat{m}_0(\nu) + \sum_{j=1}^{N(k)} \hat{m}_j(\nu) \tilde{y}_3 + O(\tilde{y}_3^{N(k)+1}), \end{cases} \quad (5.3.14)$$

where $\hat{m}_0(0) = 0$, $\hat{m}_1(0) > 0$.

Therefore, for T_3 , we have

$$\begin{cases} T_{31}(\nu, d) = \nu, \\ T_{32}(\nu, d) = m_{30}(\nu, \omega(r_3, \beta_1)) + \nu^{\bar{\sigma}_3(1-d)} \left[m_{31}(\nu, \omega(\frac{m_{141}}{r_0} \nu^{1-d}, \beta_1)) \right. \\ \quad + m_{32}(\nu) \nu^{1-d} + m_{33}(\nu) \nu^d + O(\nu^{2(1-d)}, \nu^{2d}) \\ \quad + \sum_{j=1}^{N(k)} \bar{m}_j(\nu) \nu^{\bar{\sigma}_3(1-d)j} + O(\nu^{\bar{\sigma}_3(1-d)(N(k)+1)}) \\ \quad \left. + \theta_{31}(\nu, \nu^{1-d}, \omega(\frac{m_{141}}{r_0} \nu^{1-d}, -\beta_1)) \right], \end{cases} \quad (5.3.15)$$

where

$$\begin{aligned} m_{30} &= \hat{m}_0(\nu) + \kappa_3 \left[\frac{m_1(\nu)}{r_0^{p_3}} \nu^{p_3} \omega\left(\frac{r_3}{r_0}, \beta_1\right) + O(\nu^{2p_3} \omega^2\left(\frac{r_3}{r_0}, \beta_1\right)) \right], \\ m_{31} &= \frac{m_{141}^{\bar{\sigma}_3} \hat{m}_1 y_0}{r_0^{\bar{\sigma}_3}} + \kappa_3 O(\nu^{p_3} \omega\left(\frac{m_{141}}{r_0} \nu^{1-d}, \beta_1\right)), & m_{31}(0) &\neq 0, \\ m_{32} &= \frac{\bar{\sigma}_3 m_{142} y_0}{r_0^{\bar{\sigma}_3} m_{141}^{1-\bar{\sigma}_3}} + \kappa_3 O(\nu^{p_3} \omega\left(\frac{m_{141}}{r_0} \nu^{1-d}, \beta_1\right)), & m_{32}(0) &= * \varepsilon_2, \\ m_{33} &= \frac{\bar{\sigma}_3 m_{143} y_0}{r_0^{\bar{\sigma}_3} m_{141}^{1-\bar{\sigma}_3}} + \kappa_3 O(\nu^{p_3} \omega\left(\frac{m_{141}}{r_0} \nu^{1-d}, \beta_1\right)), & m_{33}(0) &= * \bar{\mu}_{30}, \\ \bar{m}_1 &= \frac{m_{141}^{2\bar{\sigma}_3} \hat{m}_2 y_0^2}{r_0^{2\bar{\sigma}_3}} + \kappa_3 O(\nu^{p_3} \omega\left(\frac{m_{141}}{r_0} \nu^{1-d}, \beta_1\right)), & \bar{m}_1(0) &= * \hat{m}_2(0), \end{aligned}$$

and θ_{31} is C^k and has the same properties as of θ_1 in (5.3.11).

(II-4) The transition map T_4

The transition map $T_4 : \tau_1 \longrightarrow \Sigma_4$ can be factorized as

$$T_4 = \Theta_4 \circ U,$$

where

- $U : \tau_1 \longrightarrow \tau_4$ is a regular transition map, which can be written as

$$\left\{ \begin{array}{l} r_4 = U_1(\nu^{1-c}, \nu^c) \\ \quad = \nu^{1-c} [m_{141}(\nu) + m_{142}(\nu)\nu^{1-c} + m_{143}(\nu)\nu^c + O(\nu^{2(1-c)}, \nu^{2c})], \\ \rho_4 = U_2(\nu^{1-c}, \nu^c) \\ \quad = \nu^c [\hat{m}_{141}(\nu) + \hat{m}_{142}(\nu)\nu^{1-c} + \hat{m}_{143}(\nu)\nu^c + O(\nu^{2(1-c)}, \nu^{2c})], \end{array} \right. \quad (5.3.16)$$

where $m_{141}(\nu)$, $\hat{m}_{141}(\nu)$, $m_{142}(\nu)$, $\hat{m}_{142}(\nu)$, $m_{143}(\nu)$ and $\hat{m}_{143}(\nu)$ are defined in (5.3.13).

- $\Theta_4 : \tau_4 \longrightarrow \Sigma_4$ is the second type of Dulac map in the neighborhood of P_4 with

$$\bar{\sigma} = \bar{\sigma}_3.$$

Therefore, for T_4 , we have

$$\left\{ \begin{array}{l} T_{41}(\nu, c) = \nu, \\ T_{42}(\nu, c) = \eta_4(\nu, \omega(\frac{r_4}{r_0}, \beta_1)) + \nu^{\bar{\sigma}_3(1-c)} [m_{41}(\nu) + m_{42}(\nu)\nu^{1-c} \\ \quad + m_{43}(\nu)\nu^c + O(\nu^{2(1-c)}, \nu^{2c}) + \theta_{41}(\nu, \nu^{1-c}, \omega(\frac{m_{141}}{r_0}\nu^{1-c}, -\beta_1))], \end{array} \right.$$

where $m_{41}(\nu) = -\frac{y_0}{r_0^{\sigma_3}} m_{141}(\nu)^{\bar{\sigma}_3}$, $m_{42}(0) = * \varepsilon_2$ and $m_{43}(0) = * \bar{\mu}_{30}$. θ_{41} is C^k and has the same property as of θ_1 in (5.3.11).

(III) study $F_\nu(c, d)$ and $G_\nu(c, d)$

To obtain the cyclicity of Ehh1c, one needs to study the number of roots for the following system

$$\begin{cases} F_\nu(c, d) := T_{12}(\nu, c) - T_{22}(\nu, d) = 0, \\ G_\nu(c, d) := T_{42}(\nu, c) - T_{32}(\nu, d) = 0, \end{cases} \quad (5.3.17)$$

for $(a, \bar{\mu}) \in A_0 \times \bar{V}_{10}$ with $(c, d) \in \mathcal{D}_\nu$ where $\mathcal{D}_\nu = \mathcal{I}_\nu \times \mathcal{I}_\nu$ and ν, ε sufficiently small.

For $0 < \nu < \varepsilon^2$, $F_\nu(c, d)$ and $G_\nu(c, d)$ are continuous on $\bar{\mathcal{D}}_\nu$ and smooth in \mathcal{D}_ν . For $\forall (c, d) \in \mathcal{D}_\nu$ with $\varepsilon > 0$ sufficiently small, it has been proved in [53] that

$$\frac{\partial}{\partial c} F_\nu(c, d) \neq 0, \quad \frac{\partial}{\partial d} F_\nu(c, d) \neq 0, \quad \frac{\partial}{\partial c} G_\nu(c, d) \neq 0, \quad \frac{\partial}{\partial d} G_\nu(c, d) \neq 0.$$

Denote the number of roots of $F_\nu(c, d) = 0$ and $G_\nu(c, d) = 0$ in the region \mathcal{D}_ν by $\#(F, G)$, and let

$$J[F, G] = \frac{\partial}{\partial d} F_\nu(c, d) \frac{\partial}{\partial c} G_\nu(c, d) - \frac{\partial}{\partial c} F_\nu(c, d) \frac{\partial}{\partial d} G_\nu(c, d).$$

Then for $0 < \nu < \varepsilon^2$ and $\forall (c, d) \in \mathcal{D}_\nu$ with $\varepsilon > 0$ sufficiently small, by generalized

Rolle's Theorem (Theorem 6. 11 in [53]), one can have

$$\begin{aligned}
\#(F, G) &\leq \#(F, J[F, G]) + 1 \\
&= \#(F, G_2) + 1 \\
&\leq \#(G_2, J[F, G_2]) + 2 \\
&= \#(G_2, G_3) + 2,
\end{aligned} \tag{5.3.18}$$

where

$$\begin{aligned}
G_2(\nu, c, d) &= \frac{\bar{\sigma}_3 \nu^{\bar{\sigma}_3}}{\bar{\sigma}_1} \left[\left(\frac{\partial F}{\partial c} \right)^{\frac{1}{\bar{\sigma}_1 + \bar{\sigma}_3}} \left(\frac{\partial G}{\partial c} \right)^{-\frac{1}{\bar{\sigma}_1 + \bar{\sigma}_3}} - \left(\frac{\partial F}{\partial d} \right)^{\frac{1}{\bar{\sigma}_1 + \bar{\sigma}_3}} \left(\frac{\partial G}{\partial d} \right)^{-\frac{1}{\bar{\sigma}_1 + \bar{\sigma}_3}} \right], \\
G_3(\nu, c, d) &= -\bar{\sigma}_1 l_1 \left(\frac{\partial G_2}{\partial c} \frac{\partial G_2}{\partial d} \right)^{-1} J[F, G_2].
\end{aligned}$$

(IV) Calculation of $\#(G_2, G_3)$

In order to study the number of the roots of the system $G_2(\nu, c, d) = 0$, $G_3(\nu, c, d) = 0$, one can eliminate the variable c , and obtain a scalar equation with variables (ν, d) , which was given in [53], and we recall it as follows.

$$\begin{aligned}
g(\nu, d) &= \gamma(\nu) + c_1(\nu) \nu^{\bar{\sigma}_1 d} + c_2(\nu) \nu^{1-d} + c_3(\nu) \nu^d + O(\nu^{2(1-d)}, \nu^{2d}) \\
&\quad + \sum_{j=1}^{N(k)} c_{4j}(\nu) \nu^{\bar{\sigma}_3(1-d)j} + O(\nu^{\bar{\sigma}_3(1-d)(N(k)+1)}) \\
&\quad + H(\nu, \nu^d, \nu^{1-d}, \omega\left(\frac{\nu^d}{\rho_0}, -\alpha_1\right), \omega\left(\frac{m_{141}}{r_0} \nu^{1-d}, -\beta_1\right)),
\end{aligned} \tag{5.3.19}$$

where

$$\gamma(\nu) = 1 - \left(\hat{m}_1^{\bar{\sigma}_1}(\nu) k_1^{\bar{\sigma}_3}(\nu) \right)^{\frac{1}{\bar{\sigma}_1 + \bar{\sigma}_3}}, \quad c_1(0) = *k_2(0) = *\bar{\mu}_{30},$$

$$c_2(0) = *m_{142}(0)(k_1(0) - \hat{m}_1(0)) = *\varepsilon_2,$$

$$c_3(0) = *m_{143}(0)(k_1(0) - \hat{m}_1(0)) = *\bar{\mu}_{30},$$

$$c_{41}(0) = *\hat{m}_2(0),$$

and H is C^k , $H = O\left(\nu^{p_1 d} \omega\left(\frac{\nu^d}{\rho_0}, \alpha_1\right), \nu^{p_3(1-d)} \omega\left(\frac{m_{141}}{r_0} \nu^{1-d}, \beta_1\right)\right)$.

In order to obtain the cyclicity of Ehh1c , we will study the number of roots of the equation $g(\nu, d) = 0$ for $d \in \mathcal{I}_\nu$, $\nu > 0$ sufficiently small and $\forall(a, \bar{\mu}) \in A_0 \times \bar{V}_{10}$. We need the following two lemmas.

Lemma 5.3.1. [53] *If $a_0 = \frac{1}{3}(\sigma_1 = 1)$, then in the chart F.R. on $r = 0$, the first saddle quantity α_2 of P_1 satisfies $\alpha_2 = *\bar{\mu}_{30}$.*

Lemma 5.3.2. *The regular transition map $R : \Sigma_3 \longrightarrow \Sigma_4$ defined in (5.3.14) satisfies that $\frac{\partial^2 R_2}{\partial \tilde{y}_3^2}(0, 0) \neq 0$ in family (5.1.1).*

Proof. From Lemma 5.1.1, if $\delta_2 = \frac{3}{2}$, the nilpotent elliptic point is of codimension 4, and system (5.1.7) becomes

$$\begin{cases} \dot{v}_3 = z_3, \\ \dot{z}_3 = -v_3^3 + bz_3v_3 + O(v_3^5) + z_3^2 O(|(v_3, z_3)|^2), \end{cases} \quad (5.3.20)$$

where $b = \frac{5}{\sqrt{3}}$. By the near-identity transformation,

$$\begin{cases} v_3 = X_1, \\ z_3 = Y_1 + \frac{b - \sqrt{b^2 - 8}}{4} X_1^2, \end{cases} \quad (5.3.21)$$

and rescaling

$$X_1 = \frac{X}{\frac{1}{2}(b + \sqrt{b^2 - 8})}, \quad Y_1 = \frac{Y}{\frac{1}{2}(b + \sqrt{b^2 - 8})}, \quad (5.3.22)$$

we bring system (5.3.20) into a “standard form”

$$\begin{cases} \dot{X} = Y + a_0 X^2, \\ \dot{Y} = Y(X + \bar{\varepsilon} X^2 + X^3 h_1(X)) + X^4 h_2(X) + Y^2 \tilde{Q}(X, Y), \end{cases} \quad (5.3.23)$$

where $a_0 = \frac{1}{16}[b - \sqrt{b^2 - 8}]^2 = \frac{1}{3}$ and $\bar{\varepsilon} = 0$. $h_1(X)$, $h_2(X)$ and $\tilde{Q}(X, Y)$ are C^∞ .

To obtain the normal form near the singular point P_4 , we make the following blow-up

$$X = -r, \quad Y = r^2 \bar{y} \quad (5.3.24)$$

then we have

$$\begin{cases} \dot{r} = -(\frac{1}{3} + \bar{y})r, \\ \dot{\bar{y}} = -\frac{1}{3}\bar{y} + 2\bar{y}^2 - \bar{y}r^2 \bar{h}_1(r) + r\bar{h}_2(r), \end{cases} \quad (5.3.25)$$

where \bar{h}_1 and \bar{h}_2 are C^∞ functions.

We divide the above system (5.3.25) by $\frac{1}{3} + \bar{y}$. By the transformation

$$r = r_4, \quad \bar{y} = \frac{1}{6} + O(r_4) + (4 + O(r_4))\tilde{y}_4 + O(\tilde{y}_4^2), \quad (5.3.26)$$

we obtain the normal form near the singular point P_4

$$\begin{cases} \dot{r}_4 = -r_4, \\ \dot{\tilde{y}}_4 = \left[\frac{2}{3} + \sum_{i=1}^k \varsigma_i (r^2 \tilde{y}_4^3)^i \right] \tilde{y}_4, \end{cases}$$

where ς_i is the coefficient of the term $r^{2i} \tilde{y}_4^{3i+1}$.

If we make the blow-up

$$X = r, \quad Y = r^2 \tilde{y}, \quad (5.3.27)$$

similarly we will obtain the normal form near the singular point P_3

$$\begin{cases} \dot{r}_3 = r_3, \\ \dot{\tilde{y}}_3 = - \left[\frac{2}{3} + \sum_{i=1}^k \varsigma_i (r^2 \tilde{y}_3^3)^i \right] \tilde{y}_3. \end{cases}$$

Let $\bar{\Sigma}_3 = \Sigma_3 \cap \{\rho = 0\}$ and $\bar{\Sigma}_4 = \Sigma_4 \cap \{\rho = 0\}$, where $\{\rho = 0\}$ is the blow-up of the fiber $\bar{\mu} = 0$. Then by a sequence of changes of coordinates (5.1.2), (5.1.4), (5.1.6), (5.3.21), (5.3.22), (5.3.24), (5.3.25) and (5.3.27), $\bar{\Sigma}_3$ and $\bar{\Sigma}_4$ can be parameterized by \tilde{y}_3 and \tilde{y}_4 , respectively. Therefore, we have

$$\bar{\Sigma}_3 = \{(x, y) |$$

$$x = f_3(\tilde{y}_3) = -\frac{6}{r_0} [1 + O(r_0) - (6 + O(r_0))\tilde{y}_3 + (12 + O(r_0))\tilde{y}_3^2 + O(\tilde{y}_3^3)],$$

$$y = g_3(\tilde{y}_3) = \frac{9}{r_0^2} [1 + O(r_0) - (6 + O(r_0))\tilde{y}_3 + (12 + O(r_0))\tilde{y}_3^2 + O(\tilde{y}_3^3)] \},$$

$$\bar{\Sigma}_4 = \{(x, y) \mid$$

$$x = f_4(\tilde{y}_4) = \frac{6}{r_0} [1 + O(r_0) - (6 + O(r_0))\tilde{y}_4 + (12 + O(r_0))\tilde{y}_4^2 + O(\tilde{y}_4^3)],$$

$$y = g_4(\tilde{y}_4) = \frac{9}{r_0^2} [1 + O(r_0) - (6 + O(r_0))\tilde{y}_4 + (12 + O(r_0))\tilde{y}_4^2 + O(\tilde{y}_4^3)] \}.$$

Now we study the regular transition map $\Phi : \bar{\Sigma}_3 \longrightarrow \bar{\Sigma}_4$ along the invariant parabola

(5.1.8). By the formula in Theorem 2.2.1, we have

$$\begin{aligned} \Phi'(\tilde{y}_3) &= \frac{\Delta(\tilde{y}_3)}{\tilde{\Delta}(\Phi(\tilde{y}_3))} \exp \left(\int_0^T \left. \operatorname{div} X(\Gamma(t)) \right|_{(5.1.1), (5.1.8)} dt \right) \\ &= \frac{\Delta(\tilde{y}_3)}{\tilde{\Delta}(\Phi(\tilde{y}_3))} \exp \left(\int_{f_3(\tilde{y}_3)}^{f_4(\Phi(\tilde{y}_3))} \left. \frac{\operatorname{div} X(\Gamma(t))}{P(x, y)} \right|_{(5.1.1), (5.1.8)} dx \right), \end{aligned} \quad (5.3.28)$$

where T is time to travel from $\bar{\Sigma}_3$ to $\bar{\Sigma}_4$ along the invariant parabola,

$$\Delta(\tilde{y}_3) = \begin{vmatrix} \bar{P}(f_3(\tilde{y}_3), g_3(\tilde{y}_3)) & f_3'(\tilde{y}_3) \\ \bar{Q}(f_3(\tilde{y}_3), g_3(\tilde{y}_3)) & g_3'(\tilde{y}_3) \end{vmatrix},$$

and

$$\tilde{\Delta}(\Phi(\tilde{y}_3)) = \begin{vmatrix} \bar{P}(f_4(\Phi(\tilde{y}_3)), g_4(\Phi(\tilde{y}_3))) & f_4'(\Phi(\tilde{y}_3)) \\ \bar{Q}(f_4(\Phi(\tilde{y}_3)), g_4(\Phi(\tilde{y}_3))) & g_4'(\Phi(\tilde{y}_3)) \end{vmatrix}.$$

For simplicity, we let

$$\mathcal{F}(x) := \left. \frac{\operatorname{div} X(\gamma(t))}{\bar{P}(x, y)} \right|_{(5.1.1), (5.1.8)} = \frac{4\lambda + 2(\delta_2 + 2)x}{\delta_2 x^2 + 4\lambda x + 1 + \lambda^2}.$$

Since

$$\begin{aligned} \lim_{r_0 \rightarrow 0} \Phi'(0) &= \lim_{r_0 \rightarrow 0} \frac{\Delta(0)}{\tilde{\Delta}(0)} \exp \left(\int_{f_3(0)}^{f_4(0)} \mathcal{F}(x) dx \right) \\ &= \exp \left(\int_{-\infty}^{\infty} \mathcal{F}(x) dx \right) = \exp \left(-\frac{16\lambda\pi}{\delta_2 \sqrt{\Delta_0}} \right), \end{aligned}$$

then we have

$$\Phi'(0) = \exp\left(-\frac{16\lambda\pi}{\delta_2\sqrt{\Delta_0}}\right) + \phi(r_0),$$

where $\phi(r_0) = o(1)$ as $r_0 \rightarrow 0$.

From (5.3.28), we have

$$\begin{aligned}\Phi''(\tilde{y}_3) &= \frac{\Delta'(\tilde{y}_3)\tilde{\Delta}(\Phi(\tilde{y}_3)) - \Delta(\tilde{y}_3)\tilde{\Delta}'(\Phi(\tilde{y}_3))\Phi'(\tilde{y}_3)}{\tilde{\Delta}^2(\Phi(\tilde{y}_3))} \exp\left(\int_{f_3(\tilde{y}_3)}^{f_4(\Phi(\tilde{y}_3))} \mathcal{F}(x) dx\right) \\ &\quad + \frac{\Delta(\tilde{y}_3)}{\tilde{\Delta}(\Phi(\tilde{y}_3))} \exp\left(\int_{f_3(\tilde{y}_3)}^{f_4(\Phi(\tilde{y}_3))} \mathcal{F}(x) dx\right) \\ &\quad \times \left[\mathcal{F}(f_4(\Phi(\tilde{y}_3)))f_4'(\Phi(\tilde{y}_3))\Phi'(\tilde{y}_3) - \mathcal{F}(f_3(\tilde{y}_3))f_3'(\tilde{y}_3)\right].\end{aligned}$$

Therefore,

$$\begin{aligned}\Phi''(0) &= \frac{\Delta'(0)\tilde{\Delta}(0) - \Delta(0)\tilde{\Delta}'(0)\Phi'(0)}{\tilde{\Delta}^2(0)} \exp\left(\int_{f_3(0)}^{f_4(0)} \mathcal{F}(x) dx\right) \\ &\quad + \frac{\Delta(0)}{\tilde{\Delta}(0)} \exp\left(\int_{f_3(0)}^{f_4(0)} \mathcal{F}(x) dx\right) \left[\mathcal{F}(f_4(0))f_4'(0)\Phi'(0) - \mathcal{F}(f_3(0))f_3'(0)\right].\end{aligned}$$

Since

$$\begin{aligned}&\lim_{r_0 \rightarrow 0} \Phi''(0) \\ &= \lim_{r_0 \rightarrow 0} \left[\frac{\Delta'(0)}{\Delta(0)} - \frac{\tilde{\Delta}'(0)\Phi'(0)}{\tilde{\Delta}(0)}\right] \Phi'(0) + \left[\mathcal{F}(f_4(0))f_4'(0)\Phi'(0) - \mathcal{F}(f_3(0))f_3'(0)\right] \Phi'(0) \\ &= \lim_{r_0 \rightarrow 0} \left[\frac{\Delta'(0)}{\Delta(0)} + \frac{12(\delta_2 + 2)}{\delta_2}\right] \Phi'(0)(1 - \Phi'(0)) \\ &= 12 \exp\left(-\frac{16\lambda\pi}{\delta_2\sqrt{\Delta_0}}\right) \left[1 - \exp\left(-\frac{16\lambda\pi}{\delta_2\sqrt{\Delta_0}}\right)\right] \neq 0,\end{aligned}$$

so we have

$$\Phi''(0) = 12 \exp\left(-\frac{16\lambda\pi}{\delta_2\sqrt{\Delta_0}}\right) \left[1 - \exp\left(-\frac{16\lambda\pi}{\delta_2\sqrt{\Delta_0}}\right)\right] + \psi(r_0),$$

where $\psi(r_0) = o(1)$ as $r_0 \rightarrow 0$.

Since $\Delta_0 > 0$ and $\lambda \neq 0$, so for the transition map $R : \Sigma_3 \rightarrow \Sigma_4$, we have

$$\frac{\partial^2 R_2}{\partial \tilde{y}_3^2}(0, 0) = \Phi''(0) \neq 0.$$

Therefore, we finish the proof of the lemma. □

End of proof for Theorem 5.2.1

We treat the following two cases $\bar{\mu}_{30} \geq 0$ and $\bar{\mu}_{30} < 0$ separately.

(1). $\bar{\mu}_{30} \geq 0$.

For the graphic Ehh1c, we have

$$\gamma(0) = 1 - \left(\hat{m}_1^{\bar{\sigma}_1}(0)k_1^{\bar{\sigma}_3}(0)\right)^{\frac{1}{\bar{\sigma}_1 + \bar{\sigma}_3}}.$$

If $\bar{\mu}_{30} \geq 0$, then by Proposition 6.1 in [53], we have $k_1(0) \leq 1$. Since $\hat{m}_1(0) = \Phi'(0) < 1$, then we have $\gamma(0) \neq 0$. Hence, $Cycl(Ehh1c) \leq 2$.

(2). $\bar{\mu}_{30} < 0$.

Since $a_0 = \frac{1}{3}$, so $\sigma_1 = p_1 = 1$ and $\sigma_3 = \frac{2}{3}$. The the function $g(\nu, d)$ in (5.3.19) has the form

$$g(\nu, d) = \gamma(\nu) + \delta_{11}(\nu)\nu^d + \delta_{12}(\nu)\nu^d\omega\left(\frac{\nu^d}{\rho_0}, \alpha_1\right) + O\left(\nu\omega^2\left(\frac{\nu^d}{\rho_0}, -\alpha_1\right)\omega\left(\frac{\nu^d}{\rho_0}, \alpha_1\right)\right), \\ + c_{41}(\nu)\nu^{\bar{\sigma}_3(1-d)} + o(\nu^{\bar{\sigma}_3(1-d)}),$$

where $\delta_{11}(0)$ can vanish, $\delta_{12}(0) = *\alpha_2$ and $c_{41}(0) = *\hat{m}_2(0)$.

By Lemma 5.3.1 and Lemma 5.3.2, we have

$$\delta_{12}(0) = *\alpha_2 = *\bar{\mu}_{30} \neq 0, \\ c_{41}(0) = *\hat{m}_2(0) = *\frac{\partial^2 R_2}{\partial \bar{y}_3^2}(0, 0) \neq 0.$$

Now we study the root of $g(\nu, d)$ for $(\nu, d) \in (0, \varepsilon^2) \times I_\nu$ with $\varepsilon > 0$ sufficiently small. Firstly, we can kill the term $\gamma(\nu)$. Differentiate $g(\nu, d)$ with respect to d , and divide by $\ln \nu$, then we have

$$g_0(\nu, d) := \frac{1}{\ln \nu} \frac{\partial}{\partial d} g(\nu, d) \\ = *\delta_{11}(\nu)\nu^d + *\delta_{12}(\nu)\nu^d\omega\left(\frac{\nu^d}{\rho_0}, \alpha_1\right) + O\left(\nu\omega^2\left(\frac{\nu^d}{\rho_0}, -\alpha_1\right)\omega\left(\frac{\nu^d}{\rho_0}, \alpha_1\right)\right) \\ + *c_{41}(\nu)\nu^{\bar{\sigma}_3(1-d)} + o(\nu^{\bar{\sigma}_3(1-d)}).$$

Then we can kill the ν^d term as follows.

$$g_1(\nu, d) := \frac{\nu^d}{\ln \nu} \frac{\partial}{\partial d} \left(g_0(\nu, d)\nu^{-d} \right) \\ = *\delta_{12}(\nu)\nu^{\bar{\sigma}_1 d} + O\left(\nu\omega^2\left(\frac{\nu^d}{\rho_0}, -\alpha_1\right)\omega\left(\frac{\nu^d}{\rho_0}, \alpha_1\right)\right) + *c_{41}(\nu)\nu^{\bar{\sigma}_3(1-d)} + o(\nu^{\bar{\sigma}_3(1-d)}).$$

Denote

$$\bar{l}_1(\nu) := *\delta_{12}(\nu), \quad \bar{l}_2(\nu) := *c_{41}(\nu),$$

and we have $\bar{l}_1(0) \neq 0$ and $\bar{l}_2(0) \neq 0$.

1. If $\bar{l}_1(0)\bar{l}_2(0) > 0$, then $g_1(\nu, d) \neq 0$ for $(\nu, d) \in (0, \varepsilon^2) \times I_\nu$ with $\varepsilon > 0$ sufficiently small.
2. If $\bar{l}_1(0)\bar{l}_2(0) < 0$, then $\frac{\partial g_1}{\partial d}(\nu, d) \neq 0$ for $(\nu, d) \in (0, \varepsilon^2) \times I_\nu$ with $\varepsilon > 0$ sufficiently small.

By Rolle's Theorem, $\forall (a, \bar{\mu}) \in A_0 \times \bar{V}_{10}$, $g(\nu, d)$ has at most 3 zeros in $(\nu, d) \in (0, \varepsilon^2) \times I_\nu$. Therefore, by (5.3.18), system (5.3.9) has at most 5 zeros, i.e., $Cycl(Ehh1c) \leq 5$.

For the intermediate graphics Ehh1b, its finite cyclicity has been proved in [53] by showing that the transition map $T : \Pi_3 \longrightarrow \Pi_4$ passing through the blown-up sphere is nonlinear.

Therefore, we finish the proof of Theorem 5.2.1.

6 Finite cyclicity of (I_{11b}^1)

For the graphic (I_{11b}^1) , it is an HH-type graphic with a nilpotent elliptic point is at infinity. Compared to the graphic (I_{9b}^1) , there is an additional attracting saddle-node on the invariant parabola as shown in Fig. 6.1 .

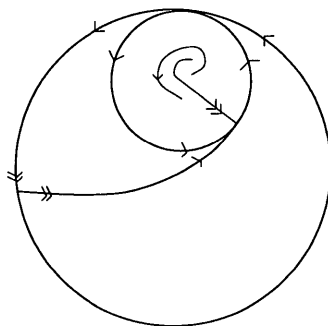


Figure 6.1: The graphic (I_{11b}^1) .

In this chapter, firstly we will give a main theorem stating that the graphic (I_{11b}^1) has finite cyclicity in section 6.1, and then we prove the main theorem by showing that all the upper boundary graphics, intermediate graphics and lower boundary graphics have finite cyclicity in section 6.2, 6.3 and 6.4, respectively. Finally, we has an open case for

the cyclicity of Ehh3e of (I_{11b}^1) and we leave it as future work.

6.1 Main Theorem

Theorem 6.1.1. *The graphic (I_{11b}^1) has finite cyclicity inside quadratic systems.*

Since the graphics (I_{11b}^1) has a nilpotent singular point at infinity, we can limit ourselves to the limit periodic sets which have an invariant line ($\bar{\mu}_1 = 0$). Moreover the connection along this line is fixed. Therefore, we only need to look to the limit periodic sets Ehh1–Ehh8.

To prove the finite cyclicity of the graphic (I_{11b}^1) , we have to prove that all the upper boundary graphics, the intermediate graphics and lower boundary graphics of Ehh1–Ehh8 have finite cyclicity.

We begin with the upper boundary graphics.

6.2 The upper boundary graphic

Proposition 6.2.1. *For the graphic (I_{11b}^1) , $Cycl(Ehhia) \leq 1, i = 1, 2, \dots, 12$.*

Proof. By Remark 4.2.2. □

6.3 The lower boundary graphic

For each family of graphic Ehhi ($i = 1, 2, \dots, 8$), we use $\bar{V}_i \subset \mathbb{S}^2$ to denote the set of $\bar{\mu} = (\bar{\mu}_1, \bar{\mu}_2, \bar{\mu}_3)$ in which the family Ehhi exists, and use \bar{V}_{i0} to denote a small neighborhood of $\bar{\mu}_0$, where $\bar{\mu}_0 \in \bar{V}_i$. We use always A_0 to denote a small neighborhood of a_0 , where $a_0 \in (0, \frac{1}{2})$.

6.3.1 Ehh1c, Ehh2e and Ehh3e

We study the displacement maps defined on the sections τ_1 and τ_2 with images on the sections Π_1 and Σ_4 as shown in Fig. 6.2.

Exactly as we did for the lower boundary graphic Ehh1c of (I_{9b}^1) , firstly we parameterize the sections Π_1 and Σ_4 . On the section τ_1 , the coordinates are (r_1, ρ_1) , and we have

$$r_1 = \nu^{1-c}, \quad \rho_1 = \nu^c,$$

with $(\nu, c) \in (0, \varepsilon^2) \times I_\nu$ where $I_\nu = (\frac{\ln \varepsilon}{\ln \nu}, \frac{\ln u \varepsilon}{\ln \nu}) \subset (0, 1)$.

Similarly, on the section τ_2 , we have

$$r_2 = \nu^{1-d}, \quad \rho_2 = \nu^d,$$

with $(\nu, d) \in (0, \varepsilon^2) \times I_\nu$ to parameterize the section τ_2 . Then we study the number of

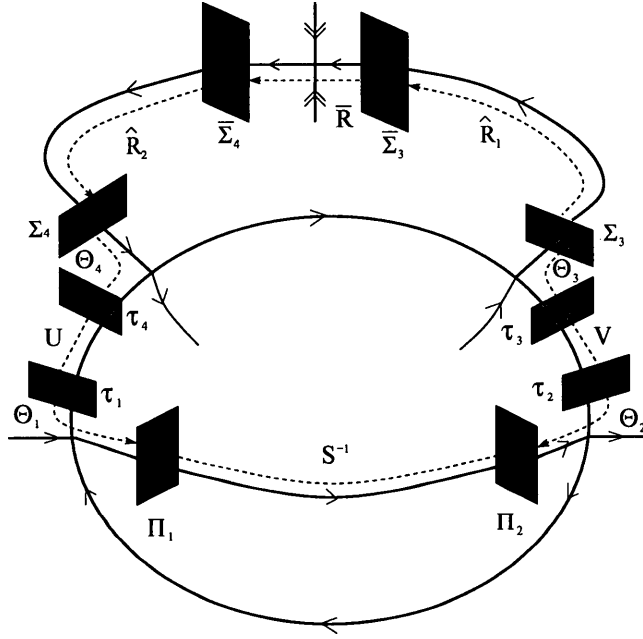


Figure 6.2: Transition maps for the graphics Ehh1c, Ehh2e and Ehh3e of (I_{11b}^1)

roots of the system

$$\begin{cases} T_1(\nu, c) = T_2(\nu, d), \\ T_3(\nu, c) = T_4(\nu, d), \end{cases} \quad (6.3.1)$$

for $(a, \bar{\mu}) \in A_0 \times \bar{V}_{i0}$ ($i = 1, 2, 3$) with $(c, d) \in I_\nu \times I_\nu$ and ν, ε sufficiently small.

The transition maps T_i ($i = 1, 2, 3, 4$) have the same definitions as those of Ehh1c for graphic (I_{9b}^1) . The transition maps Θ_i ($i = 1, 2, 3, 4$), U , V and S^{-1} are the same as those defined for (I_{9b}^1) , except the transition map $R : \Sigma_3 \rightarrow \Sigma_4$.

For (I_{9b}^1) , R is merely a regular transition map, while for (I_{11b}^1) here, R can be de-

composed as

$$\begin{aligned}
R: \Sigma_3 &\longrightarrow \Sigma_4 \\
(\nu, \tilde{y}_3) &\longrightarrow (\nu, R_2(\nu, \tilde{y}_3)) \\
R &= \widehat{R}_2 \circ \overline{R} \circ \widehat{R}_1,
\end{aligned} \tag{6.3.2}$$

where the transition maps \widehat{R}_1 , \overline{R} and \widehat{R}_2 are given by (4.2.4), (4.2.5) and (4.2.6). Therefore, we have

$$\begin{cases} R_1(\nu, \tilde{y}_3) = \nu, \\ R_2(\nu, \tilde{y}_3) = \hat{m}_0(\nu) + \hat{m}_1(\nu)\tilde{y}_3 + O(\tilde{y}_3^2), \end{cases} \tag{6.3.3}$$

where

$$\begin{aligned}
\hat{m}_0(\nu) &= n_0(\nu) + O(m), \\
\hat{m}_i(\nu) &= m(\nu)[l_i(\nu)n_1(\nu) + O(m)], \quad i = 1, 2, \dots
\end{aligned}$$

By equation (5.3.18), the number of solutions of system (6.3.1) is at most 2 plus the number of solutions of the scalar equation $g(\nu, d) = 0$ for $d \in \mathcal{I}_\nu$, $\nu > 0$ sufficiently small and $\forall (a, \bar{\mu}) \in A_0 \times \overline{V}_{i0}$ ($i = 1, 2, 3$), and $g(\nu, d) = 0$ is given as follows [53].

$$\begin{aligned}
g(\nu, d) &= \gamma(\nu) + c_1(\nu)\nu^{\bar{\sigma}_1 d} + c_2(\nu)\nu^{1-d} + c_3(\nu)\nu^d + O(\nu^{2(1-d)}, \nu^{2d}) \\
&\quad + m(\nu) \sum_{j=1}^N c_{4j}(\nu)\nu^{\bar{\sigma}_3(1-d)j} + O(m(\nu)\nu^{\bar{\sigma}_3(1-d)(N(k)+1)}) \\
&\quad + H(\nu, \nu^d, \nu^{1-d}, \omega(\frac{\nu^d}{\rho_0}, -\alpha_1), \omega(\frac{m_{141}}{r_0}\nu^{1-d}, -\beta_1)),
\end{aligned} \tag{6.3.4}$$

where

$$\gamma(\nu) = 1 - \left(\hat{m}_1^{\bar{\sigma}_1}(\nu) k_1^{\bar{\sigma}_3}(\nu) \right)^{\frac{1}{\bar{\sigma}_1 + \bar{\sigma}_3}}, \quad c_1(0) = *k_2(0) = *\bar{\mu}_{30},$$

$$c_2(0) = *m_{142}(0)(k_1(0) - \hat{m}_1(0)) = *\varepsilon_2,$$

$$c_3(0) = *m_{143}(0)(k_1(0) - \hat{m}_1(0)) = *\bar{\mu}_{30},$$

$$c_{41}(0) = *l_2(0)n_1(0),$$

and H is C^k , $H = O\left(\nu^{p_1 d} \omega\left(\frac{\nu^d}{\rho_0}, \alpha_1\right), \nu^{p_3(1-d)} \omega\left(\frac{m_{141}}{r_0} \nu^{1-d}, \beta_1\right)\right)$.

6.3.1.1 Ehh1c and Ehh2e

Since

$$\gamma(\nu) = 1 - \left(\hat{m}_1^{\bar{\sigma}_1}(\nu) k_1^{\bar{\sigma}_3}(\nu) \right)^{\frac{1}{\bar{\sigma}_1 + \bar{\sigma}_3}}, \quad (6.3.5)$$

for graphic Ehh1c, we have $k_1(\nu)$ is bounded and $\hat{m}_1(\nu) \rightarrow 0$ as $\nu \rightarrow 0$, so $\gamma(0) = 1$.

Hence, $\forall(a, \bar{\mu}) \in A_0 \times \bar{V}_{10}$, $g(\nu, d) \neq 0$ for $(\nu, d) \in (0, \varepsilon^2) \times I_\nu$. Therefore, system (6.3.1) has at most 2 small zeros, i.e., $Cycl(Ehh1c) \leq 2$.

For graphic Ehh2e, we have $k_1(\nu) \rightarrow 0$ and $\hat{m}_1(\nu) \rightarrow 0$ as $\nu \rightarrow 0$, so $\gamma(0) = 1$.

Hence, $\forall(a, \bar{\mu}) \in A_0 \times \bar{V}_{20}$, $g(\nu, d) \neq 0$ for $(\nu, d) \in (0, \varepsilon^2) \times I_\nu$. Therefore, system (6.3.1) has at most 2 small zeros, i.e., $Cycl(Ehh2e) \leq 2$.

6.3.1.2 Ehh3e

The family Ehh3 exists if and only if $\bar{\mu}_0 := (0, 0, -1)$. We treat the following cases depending on the value of a_0 .

- Case $a_0 \in (0, \frac{1}{2}) \setminus \mathbb{Q}$

Let $N = [\frac{1}{\bar{\sigma}_3(a_0)}]$. In this case, the function $g(\nu, d)$ can be simplified to

$$g(\nu, d) = \gamma(\nu) + c_1(\nu)\nu^{\bar{\sigma}_1 d} + O(\nu^{\bar{\sigma}_1 d}) + c_2(\nu)\nu^{1-d} + c_3(\nu)\nu^d + O(\nu^{2(1-d)}, \nu^{2d}) \\ + m(\nu) \sum_{j=1}^{[\frac{1}{\bar{\sigma}_3}]} c_{4j}(\nu)\nu^{\bar{\sigma}_3(1-d)j} + O(m(\nu)\nu^{\bar{\sigma}_3(1-d)([\frac{1}{\bar{\sigma}_3}]+1)}).$$

We define the following procedure

$$DD : \begin{cases} g_0(\nu, d) = \frac{1}{\ln \nu} \frac{\partial}{\partial d} g(\nu, d), \\ g_j(\nu, d) = \frac{\nu^{\bar{\sigma}_3(1-d)j}}{\ln \nu} \frac{\partial}{\partial d} (g_{j-1}(\nu, d)\nu^{-\bar{\sigma}_3(1-d)j}), \quad j = 1, \dots, [\frac{1}{\bar{\sigma}_3}]. \end{cases} \quad (6.3.6)$$

Then after $[\frac{1}{\bar{\sigma}_3}] + 1$ steps of successive derivation and division, we get

$$g_{[\frac{1}{\bar{\sigma}_3}]}(\nu, d) = *c_1(\nu)\nu^{\bar{\sigma}_1 d} + *c_2(\nu)\nu^{1-d} + *c_3(\nu)\nu^d + O(\nu^{\bar{\sigma}_1 d}, \nu^{2(1-d)}, \nu^{2d}),$$

where $c_1(0) = *\bar{\mu}_{30} \neq 0$, $c_2(0) = *\varepsilon_2 \neq 0$ and $c_3(0) = *\bar{\mu}_{30} \neq 0$.

Denote

$$\bar{l}_1(\nu) := *c_1(\nu), \quad \bar{l}_2(\nu) := *c_2(\nu), \quad \bar{l}_3(\nu) := *c_3(\nu),$$

and we have $\bar{l}_1(0)\bar{l}_2(0)\bar{l}_3(0) \neq 0$.

If $\bar{\sigma}_1 > 1$,

1. $\bar{l}_2(0)\bar{l}_3(0) > 0$, then $g_{[\frac{1}{\bar{\sigma}_3}]}(\nu, d) \neq 0$ for $(\nu, d) \in (0, \varepsilon^2) \times I_\nu$ with $\varepsilon > 0$ sufficiently small;
2. $\bar{l}_2(0)\bar{l}_3(0) < 0$, then $\frac{\partial}{\partial d}g_{[\frac{1}{\bar{\sigma}_3}]}(\nu, d) \neq 0$ for $(\nu, d) \in (0, \varepsilon^2) \times I_\nu$ with $\varepsilon > 0$ sufficiently small.

If $\bar{\sigma}_1 < 1$,

1. $\bar{l}_1(0)\bar{l}_2(0) > 0$, then $g_{[\frac{1}{\bar{\sigma}_3}]}(\nu, d) \neq 0$ for $(\nu, d) \in (0, \varepsilon^2) \times I_\nu$ with $\varepsilon > 0$ sufficiently small;
2. $\bar{l}_1(0)\bar{l}_2(0) < 0$, then $\frac{\partial}{\partial d}g_{[\frac{1}{\bar{\sigma}_3}]}(\nu, d) \neq 0$ for $(\nu, d) \in (0, \varepsilon^2) \times I_\nu$ with $\varepsilon > 0$ sufficiently small.

Hence, $g(\nu, d) = 0$ has at most $[\frac{1}{\bar{\sigma}_3}] + 2$ roots. Therefore, system (6.3.1) has at most $[\frac{1}{\bar{\sigma}_3}] + 4$ zeros, i.e., $Cycl(Ehh3e) \leq [\frac{1}{\bar{\sigma}_3}] + 4$.

- Case $a_0 \in (0, \frac{1}{2}) \cap \mathbb{Q} \setminus \{\frac{1}{n+2}, \frac{2n-1}{4n}\}$

In this case, we have $q_1 \geq 2$, $\sigma_1 < p_1$ and $p_3 \geq 2$. For $\nu > 0$ sufficiently small, we have $\bar{\sigma}_1 < p_1$ and $[\frac{1}{\bar{\sigma}_3}] < p_3$, then the function $g(\nu, d)$ can be simplified to

$$g(\nu, d) = \gamma(\nu) + c_1(\nu)\nu^{\bar{\sigma}_1 d} + O(\nu^{\bar{\sigma}_1 d}) + c_2(\nu)\nu^{1-d} + c_3(\nu)\nu^d + O(\nu^{2(1-d)}, \nu^{2d}) \\ + m(\nu) \sum_{j=1}^{q_3} c_{4j}(\nu)\nu^{\bar{\sigma}_3(1-d)j}.$$

Exactly as we did for the case $a_0 \in (0, \frac{1}{2}) \setminus \mathbb{Q}$, we obtain $Cycl(Ehh3e) \leq q_3 + 4$.

- Case $a_0 = \frac{1}{n+2}$, $n \in \mathbb{N}$, $n \neq 1, 2$

In this case, we have $\sigma_1(a_0) < p_1 = n > 1$ and $\sigma_3(a_0) = \frac{p_3}{q_3} = \frac{2n}{n+2} \in (1, 2)$, so $q_3 \geq 2$. Then the function $g(\nu, d)$ can be simplified to

$$g(\nu, d) = \gamma(\nu) + c_2(\nu)\nu^{1-d} + c_3(\nu)\nu^d + O(\nu^{2(1-d)}, \nu^{2d}).$$

Apply DD process for one step to kill the $\gamma(\nu)$ term, similar to the argument of the case $a_0 \in (0, \frac{1}{2}) \setminus \mathbb{Q}$, we obtain $\text{Cycl}(Ehh3e) \leq 4$.

- Case $a_0 = \frac{2n-1}{4n}$, $n \in \mathbb{N}$, $n \neq 1$

In this case, we have $\sigma_1(a_0) = \frac{2}{2n-1}$, $p_1 = 2$, $q_1 = 2n - 1$ and $\sigma_3(a_0) = \frac{1}{n}$, $p_3 = 1$, $q_3 = n$. Since $\sigma_1 < 1$, the function $g(\nu, d)$ can be simplified to

$$g(\nu, d) = \gamma(\nu) + c_1(\nu)\nu^{\bar{\sigma}_1 d} + O(\nu^{\bar{\sigma}_1 d}) + m(\nu) \sum_{j=1}^{n-1} c_{4j}(\nu)\nu^{\bar{\sigma}_3(1-d)j} + \delta_{31}(\nu)\nu^{1-d} \\ + \delta_{32}(\nu)\nu^{1-d}\omega\left(\frac{m_{141}}{r_0}\nu^{1-d}, \beta_1\right) + O\left(\nu\omega^2\left(\frac{m_{141}}{r_0}\nu^{1-d}, -\beta_1\right)\omega\left(\frac{m_{141}}{r_0}\nu^{1-d}, \beta_1\right)\right),$$

where $c_1(0) = *\bar{\mu}_{30} \neq 0$, $\delta_{31}(0)$ can vanish, and $\delta_{32}(0) = *\beta_2$. Here β_2 is the first saddle quantity of P_3 in the chart F.R. on $r = 0$, and $\beta_2 \neq 0$ by Lemma 6.14 in [53].

Apply DD process for n steps to kill the $\gamma(\nu)$ term and $\nu^{\bar{\sigma}_3(1-d)j}$ ($j = 1, 2, \dots, n-1$) terms, then we get

$$g_n(\nu, d) = *c_1(\nu)\nu^{\bar{\sigma}_1 d} + O(\nu^{\bar{\sigma}_1 d}) + *\delta_{31}(\nu)\nu^{1-d} + *\delta_{32}(\nu)\nu^{1-d}\omega\left(\frac{m_{141}}{r_0}\nu^{1-d}, \beta_1\right) \\ + O\left(\nu\omega^2\left(\frac{m_{141}}{r_0}\nu^{1-d}, -\beta_1\right)\omega\left(\frac{m_{141}}{r_0}\nu^{1-d}, \beta_1\right)\right).$$

Let $g_{n+1}(\nu, d) = \frac{\nu^{1-d}}{\ln \nu} \frac{\partial}{\partial d} \left(\nu^{-(1-d)} g_n(\nu, d) \right)$, then

$$g_{n+1}(\nu, d) = *c_1(\nu) \nu^{\bar{\sigma}_1 d} + O(\nu^{\bar{\sigma}_1 d}) + *\delta_{32}(\nu) \nu^{(1-d)\bar{\sigma}_3} \\ + O\left(\nu \omega^2 \left(\frac{m_{141}}{r_0} \nu^{1-d}, -\beta_1 \right) \omega \left(\frac{m_{141}}{r_0} \nu^{1-d}, \beta_1 \right) \right),$$

so $\forall (a, \bar{\mu}) \in A_0 \times V_{I_3}$, either $g_{n+1}(\nu, d) \neq 0$ or $\frac{\partial g_{n+1}}{\partial d}(\nu, d) \neq 0$ for $(\nu, d) \in (0, \varepsilon^2) \times I_\nu$

with $\varepsilon > 0$ sufficiently small, so we obtain $Cycl(Ehh3e) \leq n + 4$.

• Case $a_0 = \frac{1}{4}$

In this case $\sigma_1(\frac{1}{4}) = 2$, $p_1 = 2$, $q_1 = 1$ and $\sigma_3(\frac{1}{4}) = 1$, $p_3 = q_3 = 1$. the function $g(\nu, d)$ can be simplified to

$$g(\nu, d) = \gamma(\nu) + \delta_0(\nu) \nu^d + \delta_{11}(\nu) \nu^{2d} + \delta_{12}(\nu) \nu^{2d} \omega \left(\frac{\nu^d}{\rho_0} \nu^{1-d}, \alpha_1 \right) \\ + O\left(\nu^2 \omega^2 \left(\frac{\nu^d}{\rho_0} \nu^{1-d}, -\alpha_1 \right) \omega \left(\frac{\nu^d}{\rho_0} \nu^{1-d}, \alpha_1 \right) \right) + \delta_{31}(\nu) \nu^{1-d} \\ + \delta_{32}(\nu) \nu^{1-d} \omega \left(\frac{m_{141}}{r_0} \nu^{1-d}, \beta_1 \right) + O\left(\nu \omega^2 \left(\frac{m_{141}}{r_0} \nu^{1-d}, -\beta_1 \right) \omega \left(\frac{m_{141}}{r_0} \nu^{1-d}, \beta_1 \right) \right),$$

where $\delta_{11}(0)$ and $\delta_{31}(0)$ can vanish, $\delta_{12}(0) = *\bar{\mu}_{30} \neq 0$ and $\delta_{32}(0) = *\beta_2 \neq 0$.

Apply DD process for 2 steps to kill the $\gamma(\nu)$ term and ν^d term, then we get

$$g_1(\nu, d) = *\delta_{11}(\nu) \nu^{2d} + *\delta_{12}(\nu) \nu^{2d} \omega \left(\frac{\nu^d}{\rho_0} \nu^{1-d}, \alpha_1 \right) \\ + O\left(\nu^2 \omega^2 \left(\frac{\nu^d}{\rho_0} \nu^{1-d}, -\alpha_1 \right) \omega \left(\frac{\nu^d}{\rho_0} \nu^{1-d}, \alpha_1 \right) \right) + *\delta_{31}(\nu) \nu^{1-d} \\ + *\delta_{32}(\nu) \nu^{1-d} \omega \left(\frac{m_{141}}{r_0} \nu^{1-d}, \beta_1 \right) + O\left(\nu \omega^2 \left(\frac{m_{141}}{r_0} \nu^{1-d}, -\beta_1 \right) \omega \left(\frac{m_{141}}{r_0} \nu^{1-d}, \beta_1 \right) \right),$$

Let

$$g_2(\nu, d) = \frac{\nu^{2d}}{\ln \nu} \frac{\partial}{\partial d} \left(\nu^{-2d} g_1(\nu, d) \right), \\ g_3(\nu, d) = \frac{\nu^{1-d}}{\ln \nu} \frac{\partial}{\partial d} \left(\nu^{-(1-d)} g_2(\nu, d) \right),$$

then

$$g_3(\nu, d) = * \delta_{12}(\nu) \nu^{\bar{\sigma}_1 d} + O\left(\nu^2 \omega^2\left(\frac{\nu^d}{\rho_0} \nu^{1-d}, -\alpha_1\right) \omega\left(\frac{\nu^d}{\rho_0} \nu^{1-d}, \alpha_1\right)\right) \\ + * \delta_{32}(\nu) \nu^{(1-d)\bar{\sigma}_3} + O\left(\nu \omega^2\left(\frac{m_{141}}{r_0} \nu^{1-d}, -\beta_1\right) \omega\left(\frac{m_{141}}{r_0} \nu^{1-d}, \beta_1\right)\right).$$

Then $\forall (a, \bar{\mu}) \in A_0 \times V_{I_3}$, either $g_3(\nu, d) \neq 0$ or $\frac{\partial g_3}{\partial d}(\nu, d) \neq 0$ for $(\nu, d) \in (0, \varepsilon^2) \times I_\nu$

with $\varepsilon > 0$ sufficiently small, so we obtain $Cycl(Ehh3e) \leq 7$.

• Case $a_0 = \frac{1}{3}$

If $a_0 = \frac{1}{3}$, the nilpotent elliptic point at infinity is of codimension 4, and the graphic

(I_{11b}^1) occurs in the following system

$$\begin{cases} \dot{x} = \frac{\sqrt{15}}{5}x - y + x^2, \\ \dot{y} = x + \frac{\sqrt{15}}{5}y + \frac{3\sqrt{15}}{10}x^2 + \frac{3}{2}xy, \end{cases} \quad (6.3.7)$$

which determines the regular part of the graphic.

For the passage near the blown-up sphere, on $r = 0$ in the chart F.R., we have

$$\bar{X}_{\rho=1} : \begin{cases} \dot{\bar{x}} = \bar{y} + \frac{1}{3}\bar{x}^2, \\ \dot{\bar{y}} = (-1 + \bar{x})\bar{y}, \end{cases} \quad (6.3.8)$$

Furthermore, we have $\sigma_1 = 1$ and $\sigma_3 = \frac{2}{3}$, so function $g(\nu, d)$ defined in (6.3.4) has the form

$$g(\nu, d) = \gamma(\nu) + \delta_{11}(\nu) \nu^d + \delta_{12}(\nu) \nu^d \omega\left(\frac{\nu^d}{\rho_0}, \alpha_1\right) + O\left(\nu \omega^2\left(\frac{\nu^d}{\rho_0}, -\alpha_1\right) \omega\left(\frac{\nu^d}{\rho_0}, \alpha_1\right)\right), \\ + c_2(\nu) \nu^{1-d} + m(\nu) c_{4j}(\nu) \nu^{\bar{\sigma}_3(1-d)} + O\left(\nu^{2(1-d)}, m \nu^{2\bar{\sigma}_3(1-d)}\right),$$

where $\delta_{11}(0)$ can vanish, $\delta_{12}(0) = *\alpha_2 \neq 0$, $c_2(0) = *\varepsilon_2 = 0$, $c_{41}(0) = *l_2(0)n_1(0)$ and $m(\nu)$ is sufficiently small for $(\nu, \bar{\mu}, a)$ close to $(0, \bar{\mu}_0, a_0)$.

Therefore, we need an additional generic condition to prove the cyclicity of the graphic Ehh3e, which we may derive from the high order term of the transition maps. This is the most difficult case for the graphic (I_{11b}^1) , and we leave it for future work.

6.3.2 Ehh4c

For the lower boundary graphic Ehh4c, it is the same as the lower boundary graphic Sxhh1c of (I_{13}^1) , so Ehh4c has finite cyclicity.

6.3.3 Ehh5c

The Lower boundary of Family Ehh5 passes through a hyperbolic saddle point in the chart F. R. as shown in Fig. 6.3. Let $\lambda(\nu)$ be the hyperbolicity ratio at this saddle point. Take sections $\bar{\Sigma}_1 = \{\tilde{y} = 1\}$ and $\bar{\Sigma}_3 = \{\tilde{x} = 1\}$ in the normal form coordinates of the saddle point.

We are going to study the displacement map defined on the section τ_1 :

$$L : \tau_1 \longrightarrow \Sigma_4,$$

$$L = \hat{T} - \tilde{T}.$$

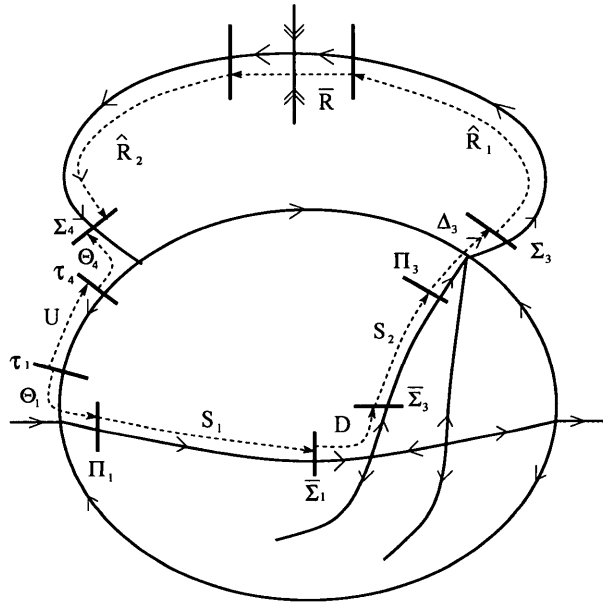


Figure 6.3: Transition maps for the graphic Ehh5c

The transition map \tilde{T} can be factorized as

$$\tilde{T} : \tau_1 \longrightarrow \Sigma_4,$$

$$\tilde{T} = \Theta_4 \circ U,$$

where

- $U : \tau_1 \longrightarrow \tau_4$ is a regular transition map, which is given by (5.3.16).
- $\Theta_4 : \tau_4 \longrightarrow \Sigma_4$ is the second type of Dulac map in the neighborhood of P_4 with $\bar{\sigma} = \bar{\sigma}_3$.

Therefore, for \tilde{T} , we have

$$\begin{cases} \tilde{T}_1(\nu, c) = \nu, \\ \tilde{T}_2(\nu, c) = -\frac{y_0}{r_0^{\bar{\sigma}_3}} m_{141}^{\bar{\sigma}_3}(\nu) \nu^{(1-c)\bar{\sigma}_3} [1 + O(\nu^c, \nu^{1-c}) + \theta_{41}(\nu, \nu^{1-c}, \omega(\frac{m_{141}}{r_0} \nu^{1-c}, -\beta_1))], \end{cases} \quad (6.3.9)$$

where θ_{41} satisfies the same properties as of θ_1 in (5.3.11).

For the transition map \hat{T} , we calculate it by the following decomposition

$$\begin{aligned} \hat{T} : \tau_1 &\longrightarrow \Sigma_4, \\ \hat{T} &= \hat{R}_2 \circ \bar{R} \circ \hat{R}_1 \circ \Delta_3 \circ S_2 \circ D \circ S_1 \circ \Theta_1, \end{aligned}$$

where

- $\Theta_1 : \tau_1 \longrightarrow \Pi_1$ is the second type of Dulac map in the neighborhood of P_1 with $\bar{\sigma} = \bar{\sigma}_1$.

- $S_1 : \Pi_1 \longrightarrow \bar{\Sigma}_1$ is a regular transition map. Since \bar{x} axis is fixed for $\bar{X}_{\rho=1}$, so S_1 can be written as

$$\begin{cases} S_{11}(\nu, \tilde{y}_1) = \nu, \\ S_{12}(\nu, \tilde{y}_1) = e_1(\nu) \tilde{y}_1 + O(\tilde{y}_1^2), \end{cases}$$

where $e_1(0) > 0$.

- $D : \bar{\Sigma}_1 \longrightarrow \bar{\Sigma}_3$ is the Dulac map near the saddle point, which has the expression (3.2.5).

- $S_2 : \bar{\Sigma}_3 \longrightarrow \Pi_3$ is a regular transition map, which can be written as

$$\begin{cases} S_{21}(\nu, \tilde{y}) = \nu, \\ S_{22}(\nu, \tilde{y}) = b_0(\nu) + b_1(\nu)\tilde{y} + O(\tilde{y}^2), \end{cases}$$

where $b_0(0) = 0$ and $b_1(0) > 0$.

- $\Delta_3 : \Pi_3 \longrightarrow \Sigma_3$ are the first type of Dulac maps in the neighborhood of P_3 with $\bar{\sigma} = \bar{\sigma}_3$.
- The transition maps \hat{R}_1, \bar{R} and \hat{R}_2 are given by (4.2.4), (4.2.5) and (4.2.6).

Hence, for \hat{T} , we have $\hat{T}_1(\nu, c) = \nu$. Let

$$\begin{aligned} \tilde{y}_1 &= \left(\frac{\nu^c}{\rho_0}\right)^{\bar{\sigma}_1} [y_0 + \theta_{11}(\nu, \nu^c, \omega(\frac{\nu^c}{\rho_0}, -\alpha_1))], \\ \tilde{y}_3 &= b_0(\nu) + b_1(\nu)e_1(\nu)^\lambda \tilde{y}_1^\lambda [1 + \phi_1(\nu, \tilde{x})], \\ \hat{y}_3 &= \left(\frac{\nu}{\nu_0}\right)^{\bar{\sigma}_3} [\tilde{y}_3 + \theta_{31}(\nu, \tilde{y}_3, \omega(\frac{\nu}{\nu_0}, -\beta_1))], \end{aligned}$$

where $\phi_1(\nu, \tilde{x}) \in I_0^\infty$, θ_{11} satisfies the same properties as of θ_1 in (5.3.11) and θ_{31} satisfies the properties (2.5.23). Then the second component of \hat{T} can be written as

$$\hat{T}_2(\nu, c) = n_0(\nu) + O(m) + m(\nu)[(l_1(\nu)n_1(\nu) + O(m(\nu)))\hat{y}_3 + O(\hat{y}_3^2)]. \quad (6.3.10)$$

By (6.3.9) and (6.3.10), the first derivative of $L_2(\nu, c)$ with respect to c is given as follows.

$$\begin{aligned} \frac{\partial L_2(\nu, c)}{\partial c} &= \frac{\partial \widehat{T}_2(\nu, c)}{\partial c} - \frac{\partial \widetilde{T}_2(\nu, c)}{\partial c} \\ &= m(\nu) \left[l_1(\nu) n_1(\nu) + O(m(\nu)) + O(\widehat{y}_3) \right] \left(\frac{\nu}{\nu_0} \right)^{\bar{\sigma}_3} \left[1 + \frac{\partial \theta_{31}}{\partial \widehat{y}_3}(\nu, \widetilde{y}_3, \omega(\frac{\nu}{\nu_0}, -\beta_1)) \right] \\ &\quad b_1(\nu) \left(\frac{e_1(\nu) y_0}{\rho_0^{\bar{\sigma}_1}} \right)^\lambda \nu^{\lambda \bar{\sigma}_1 c} \lambda \bar{\sigma}_1 \left[1 + \phi_2(\nu, \widetilde{x}) \right] \left[1 + \theta_{12}(\nu, \nu^c, \omega(\frac{\nu^c}{\rho_0}, -\alpha_1) + O(\nu^{\bar{\sigma}_1 c})) \right] \ln \nu \\ &\quad + \frac{y_0}{r_0^{\bar{\sigma}_3}} m_{141}^{\bar{\sigma}_3}(\nu) \nu^{(1-c)\bar{\sigma}_3} \bar{\sigma}_3 \left[1 + O(\nu^c, \nu^{1-c}) + \theta_{42}(\nu, \nu^{1-c}, \omega(\frac{m_{141}}{r_0} \nu^{1-c}, -\beta_1)) \right] \ln \nu, \end{aligned}$$

where $\phi_2(\nu, \widetilde{x}) \in I_0^\infty$, and θ_{12}, θ_{42} satisfy the same properties as of θ_1 in (5.3.11), also

$$\frac{\partial \theta_{31}}{\partial \widehat{y}_3} = O\left(\nu^{\bar{p}_3} \omega^{q_3}\left(\frac{\nu}{\nu_0}, -\beta_1\right) \ln \frac{\nu}{\nu_0}\right).$$

$\frac{\partial L_2(\nu, c)}{\partial c}$ has the same number of small roots as of

$$\begin{aligned} \bar{L}_2(\nu, c) &= \frac{\nu^{-(1-c)\bar{\sigma}_3}}{\ln \nu} \frac{\partial L_2(\nu, c)}{\partial c} \\ &= \frac{y_0}{r_0^{\bar{\sigma}_3}} m_{141}^{\bar{\sigma}_3}(\nu) \bar{\sigma}_3 + O(\nu^c, \nu^{1-c}) + \theta_{42}(\nu, \nu^{1-c}, \omega(\frac{m_{141}}{r_0} \nu^{1-c}, -\beta_1)) \\ &\quad + O\left(m(\nu) \nu^{(\bar{\sigma}_3 + \lambda \bar{\sigma}_1)c}\right). \end{aligned}$$

Since $\frac{y_0}{r_0^{\bar{\sigma}_3}} m_{141}^{\bar{\sigma}_3}(0) \bar{\sigma}_3 \neq 0$, so $\bar{L}_2(\nu, c) \neq 0$. Hence, $\forall (a, \bar{\mu}) \in A_0 \times \bar{V}_{50}$, $L_2(\nu, c)$ has at most one small root for $(\nu, c) \in (0, \varepsilon^2) \times I_\nu$ with $\varepsilon > 0$ sufficiently small, i.e., $Cycl(Ehh5c) \leq 1$.

6.3.4 Ehh6c

Compared to the lower boundary graphic Ehh5c, Ehh6c passes through a saddle-node point as shown in Fig 6.4. In the neighborhood of saddle-node point, take sections $\bar{\Sigma}_1 =$

$\{\tilde{y} = 1\}$ and $\bar{\Sigma}_3 = \{\tilde{x} = 1\}$ in the normal form coordinates. The other transition maps are the same as those of Ehh5c.

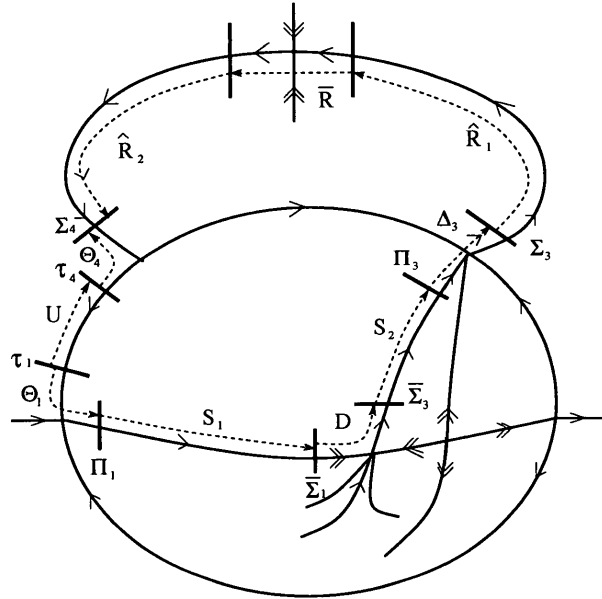


Figure 6.4: Transition maps for the graphic Ehh6c

$D : \bar{\Sigma}_1 \longrightarrow \bar{\Sigma}_3$ is the stable-centre transition map near the saddle-node point. Obviously, the first component $D_1(\nu, \tilde{x}) = \nu$. For the second component $D_2(\nu, \tilde{x}), \forall p, q \in \mathbb{N}$, we have

$$\frac{\partial^p D_2(\nu, \tilde{x})}{\partial \tilde{x}^p} = O(\tilde{x}^q).$$

For the displacement function L

$$L : \tau_1 \longrightarrow \Sigma_4,$$

$$L = \hat{T} - \tilde{T},$$

we have $L_1(\nu, c) = \nu$, and

$$\begin{aligned} \frac{\partial L_2(\nu, c)}{\partial c} &= \frac{\partial \widehat{T}_2(\nu, c)}{\partial c} - \frac{\partial \widetilde{T}_2(\nu, c)}{\partial c} \\ &= m(\nu) \left[l_1(\nu) n_1(\nu) + O(m(\nu)) + O(\hat{y}_3) \right] \left(\frac{\nu}{\nu_0} \right)^{\bar{\sigma}_3} \left[1 + \frac{\partial \theta_{31}}{\partial \tilde{y}_3}(\nu, \tilde{y}_3, \omega(\frac{\nu}{\nu_0}, -\beta_1)) \right] \\ &\quad (b_1(\nu) + O(\tilde{y})) O(\tilde{x}^{q-1}) \left(\frac{e_1(\nu) y_0}{\rho_0^{\bar{\sigma}_1}} \right) \nu^{\bar{\sigma}_1 c} \bar{\sigma}_1 \left[1 + \theta_{12}(\nu, \nu^c, \omega(\frac{\nu^c}{\rho_0}, -\alpha_1) + O(\nu^{\bar{\sigma}_1 c})) \right] \ln \nu \\ &\quad + \frac{y_0}{r_0^{\bar{\sigma}_3}} m_{141}^{\bar{\sigma}_3}(\nu) \nu^{(1-c)\bar{\sigma}_3} \bar{\sigma}_3 \left[1 + O(\nu^c, \nu^{1-c}) + \theta_{42}(\nu, \nu^{1-c}, \omega(\frac{m_{141} \nu^{1-c}}{r_0}, -\beta_1)) \right] \ln \nu. \end{aligned}$$

$\frac{\partial L_2(\nu, c)}{\partial c}$ has the same number of small roots as of

$$\begin{aligned} \bar{L}_2(\nu, c) &= \frac{\nu^{-(1-c)\bar{\sigma}_3}}{\ln \nu} \frac{\partial L_2(\nu, c)}{\partial c} \\ &= \frac{y_0}{r_0^{\bar{\sigma}_3}} m_{141}^{\bar{\sigma}_3}(\nu) \bar{\sigma}_3 + O(\nu^c, \nu^{1-c}) + \theta_{42}(\nu, \nu^{1-c}, \omega(\frac{m_{141} \nu^{1-c}}{r_0}, -\beta_1)) \\ &\quad + O\left(m(\nu) \nu^{(\bar{\sigma}_3 + \bar{\sigma}_1)c} \tilde{x}^{q-1}\right). \end{aligned}$$

Since $\frac{y_0}{r_0^{\bar{\sigma}_3}} m_{141}^{\bar{\sigma}_3}(0) \bar{\sigma}_3 \neq 0$, so $\bar{L}_2(\nu, c) \neq 0$. Hence, $\forall (a, \bar{\mu}) \in A_0 \times \bar{V}_{60}$, $L_2(\nu, c)$ has at most one small root for $(\nu, c) \in (0, \varepsilon^2) \times I_\nu$ with $\varepsilon > 0$ sufficiently small, i.e., $Cycl(Ehh6c) \leq 1$.

6.3.5 Ehh7c

The Lower boundary graphic of Ehh7 passes through a repelling saddle-node as shown in Fig 6.5. In the neighborhood of saddle-node, take sections $\bar{\Sigma}_2 = \{\tilde{x} = 1\}$ and $\bar{\Sigma}_4 = \{\tilde{y} = 1\}$ in the normal form coordinates.

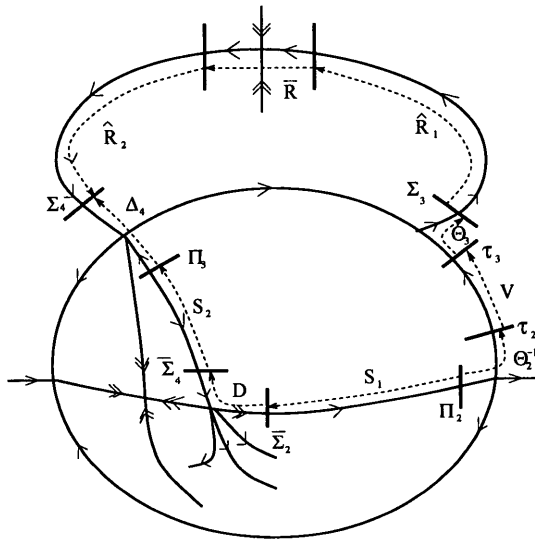


Figure 6.5: Transition maps for the graphic Ehh7c

We are going to study the displacement map defined on the section Π_2 :

$$L : \Pi_2 \longrightarrow \Sigma_4,$$

$$L = \hat{T} - \tilde{T}.$$

The transition map \tilde{T} can be factorized as

$$\tilde{T} : \Pi_2 \longrightarrow \Sigma_4,$$

$$\tilde{T} = \Delta_4 \circ S_2 \circ D \circ S_1,$$

where

- $S_1 : \Pi_2 \longrightarrow \bar{\Sigma}_2$ is a regular transition map. Since \bar{x} axis is fixed for $\bar{X}_{\rho=1}$, so S_1

can be written as

$$\begin{cases} S_{11}(\nu, \tilde{y}_2) = \nu, \\ S_{12}(\nu, \tilde{y}_2) = e_1(\nu)\tilde{y}_2 + O(\tilde{y}_2^2), \end{cases}$$

where $e_1(0) > 0$.

- $D : \bar{\Sigma}_2 \longrightarrow \bar{\Sigma}_4$ is the stable-centre transition map near the semi-hyperbolic point.

Obviously, the first component $D_1(\nu, \tilde{y}) = \nu$. The second component $D_2(\nu, \tilde{y})$ is a solution of the following differential equation

$$F(\tilde{y}, \nu, \bar{\mu}, a)d\tilde{x} - \tilde{x}d\tilde{y} = 0, \quad (6.3.11)$$

where $F(\tilde{y}, \nu, \bar{\mu}, a) = c_0(\nu, \bar{\mu}, a) + c_2(\nu, \bar{\mu}, a)\tilde{y}^2 + o(\tilde{y}^2)$ with $c_0(0, \bar{\mu}_0, a_0) = 0$ and $c_2(0, \bar{\mu}_0, a_0) \neq 0$.

- $S_2 : \bar{\Sigma}_4 \longrightarrow \Pi_4$ is a regular transition map, which can be written as

$$\begin{cases} S_{21}(\nu, \tilde{y}) = \nu, \\ S_{22}(\nu, \tilde{y}) = b_0(\nu) + b_1(\nu)\tilde{y} + O(\tilde{y}^2), \end{cases}$$

where $b_0(0) = 0$ and $b_1(0) > 0$.

- $\Delta_4 : \Pi_4 \longrightarrow \Sigma_4$ are the first type of Dulac maps in the neighborhood of P_4 with

$$\bar{\sigma} = \bar{\sigma}_3.$$

Let

$$h_\nu(\tilde{y}_2) := D_2 \circ S_{12}(\nu, \tilde{y}_2) = \exp\left(-\int_{S_{12}(\nu, \tilde{y}_2)}^1 \frac{d\tilde{y}}{F(\tilde{y}, \nu)}\right),$$

$$\tilde{y}_4 = S_{22}(\nu, h_\nu(\tilde{y}_2)).$$

Therefore, for \tilde{T} , we have

$$\begin{cases} \tilde{T}_1(\nu, \tilde{y}_2) = \nu, \\ \tilde{T}_2(\nu, \tilde{y}_2) = \left(\frac{\nu}{\nu_0}\right)^{\bar{\sigma}_3} \left[\tilde{y}_4 + \phi_4\left(\nu, \omega\left(\frac{\nu}{\nu_0}, -\beta_1\right), \tilde{y}_4\right) \right], \end{cases} \quad (6.3.12)$$

where ϕ_4 satisfies the properties (2.5.23).

The first derivative of $\tilde{T}_2(\nu, \tilde{y}_2)$ with respect to \tilde{y}_2 is given as follows.

$$\begin{aligned} \frac{\partial \tilde{T}_2(\nu, \tilde{y}_2)}{\partial \tilde{y}_2} &= \left(\frac{\nu}{\nu_0}\right)^{\bar{\sigma}_3} \left[1 + O\left(\nu^{\bar{\sigma}_3} \omega^q\left(\frac{\nu}{\nu_0}, -\beta_1\right) \ln\left(\frac{\nu}{\nu_0}\right)\right) \right] \\ &\quad \times \frac{\partial S_{22}(\nu, \tilde{y})}{\partial \tilde{y}} \frac{h_\nu(\tilde{y}_2)}{F(S_{12}(\nu, \tilde{y}_2), \nu)} \frac{S_{12}(\nu, \tilde{y}_2)}{\partial \tilde{y}_2}, \end{aligned}$$

and

$$\frac{\partial^2 \tilde{T}_2(\nu, \tilde{y}_2)}{\partial \tilde{y}_2^2} = \left(\frac{\nu}{\nu_0}\right)^{\bar{\sigma}_3} \frac{h_\nu(\tilde{y}_2)}{(F(S_{12}(\nu, \tilde{y}_2), \nu))^2} \tilde{H}(\nu, \tilde{y}_2),$$

where

$$\begin{aligned} \tilde{H}(\nu, \tilde{y}_2) &= \frac{\partial^2 S_{22}}{\partial \tilde{y}^2} h_\nu(\tilde{y}_2) \left(\frac{\partial S_{12}}{\partial \tilde{y}_2}\right)^2 + \frac{\partial S_{22}}{\partial \tilde{y}} \left(\frac{\partial S_{12}}{\partial \tilde{y}_2}\right)^2 - \frac{\partial S_{22}}{\partial \tilde{y}} \frac{\partial F(\tilde{y})}{\partial \tilde{y}} \left(\frac{\partial S_{12}}{\partial \tilde{y}_2}\right)^2 \\ &\quad - \frac{\partial S_{22}}{\partial \tilde{y}} F(S_{12}(\nu, \tilde{y}_2), \nu) \frac{\partial^2 S_{12}}{\partial \tilde{y}_2^2} + O\left(\nu^{\bar{\sigma}_3} \omega^{q-1}\left(\frac{\nu}{\nu_0}, -\beta_1\right) \ln\left(\frac{\nu}{\nu_0}\right)\right). \end{aligned}$$

Since $F(S_{12}(\nu, \tilde{y}_2), \nu) \neq 0$ and $h_\nu(\tilde{y}_2) > 0$, and

$$\lim_{(\tilde{y}_2, \nu, \bar{\mu}, a) \rightarrow (0, 0, \bar{\mu}_0, a_0)} \tilde{H}(\nu, \tilde{y}_2) = b_1(0)e_1(0)^2 > 0,$$

So for $\nu > 0$ small and $(\bar{\mu}, a)$ sufficiently close to $(\bar{\mu}_0, a_0)$, we have $\frac{\partial^2 \tilde{T}_2(\nu, \tilde{y}_2)}{\partial \tilde{y}_2^2} > 0$ in

the small neighborhood of $\tilde{y}_2 = 0$, i.e., $\tilde{T}_2(\nu, \tilde{y}_2)$ is convex.

For the transition map \widehat{T} , we calculate it by the following decomposition

$$\begin{aligned}\widehat{T} : \Pi_2 &\longrightarrow \Sigma_4 \\ \widehat{T} &= \widehat{R}_2 \circ \overline{R} \circ \widehat{R}_1 \circ \Theta_3 \circ V \circ \Theta_2^{-1},\end{aligned}$$

where

- $\Theta_2^{-1} : \Pi_2 \longrightarrow \tau_2$ is the inverse of the second type of Dulac map in the neighborhood of P_2 which can be written as

$$\begin{cases} \Theta_{21}^{-1}(\nu, \tilde{y}_2) = \nu, \\ \Theta_{22}^{-1}(\nu, \tilde{y}_2) = \tilde{y}_2^{-\frac{1}{\bar{\sigma}_1}} (N_1 + \theta_{21}(\nu, \tilde{y}_2)), \end{cases} \quad (6.3.13)$$

where $N_1 = \frac{\rho_0}{y_0^{\bar{\sigma}_1}}$ and $\theta_{21} \in I_0^\infty$.

- $V : \tau_2 \longrightarrow \tau_3$ is a regular transition map, which is given by (5.3.13).
- $\Theta_3 : \tau_3 \longrightarrow \Sigma_3$ is the second type of Dulac map in the neighborhood of P_3 with $\bar{\sigma} = \bar{\sigma}_3$.
- The transition maps \widehat{R}_1 , \overline{R} and \widehat{R}_2 are given by (4.2.4), (4.2.5) and (4.2.6).

Hence, we have $\widehat{T}_1(\nu, c) = \nu$ and the second component of \widehat{T} can be written as

$$\widehat{T}_2(\nu, \tilde{y}_2) = n_0(\nu) + O(m(\nu)) + m(\nu)[(l_1(\nu)n_1(\nu) + O(m(\nu)))\hat{y}_3 + O(\hat{y}_3^2)],$$

where

$$\hat{y}_3 = N_1^{-\bar{\sigma}_3} N_2 m_{141}^{\bar{\sigma}_3} \nu^{\bar{\sigma}_3} \tilde{y}_2^{-\frac{\bar{\sigma}_3}{\bar{\sigma}_1}} [1 + \theta_{22}(\nu, \tilde{y}_2)],$$

and $N_2 = -\frac{y_0}{r_0^{\bar{\sigma}_3}}$ and $\theta_{22} \in I_0^\infty$. Then the first derivative of $\widehat{T}_2(\nu, \tilde{y}_2)$ with respect to \tilde{y}_2 is given as follows.

$$\begin{aligned} \frac{\partial \widehat{T}_2(\nu, \tilde{y}_2)}{\partial \tilde{y}_2} &= m(\nu) \left[l_1(\nu) n_1(\nu) + O(m(\nu)) + O(\hat{y}_3) \right] \\ &\quad \times N_1^{-\bar{\sigma}_3} N_2 m_{141}^{\bar{\sigma}_3} \nu^{\bar{\sigma}_3} \left(-\frac{\bar{\sigma}_3}{\bar{\sigma}_1} \right) \tilde{y}_2^{-\frac{\bar{\sigma}_3}{\bar{\sigma}_1} - 1} [1 + \theta_{23}(\nu, \tilde{y}_2)], \end{aligned}$$

where $\theta_{23} \in I_0^\infty$. The second derivative of $\widehat{T}_2(\nu, \tilde{y}_2)$ with respect to \tilde{y}_2 is

$$\frac{\partial^2 \widehat{T}_2(\nu, \tilde{y}_2)}{\partial \tilde{y}_2^2} = m(\nu) N_1^{-\bar{\sigma}_3} N_2 m_{141}^{\bar{\sigma}_3} \nu^{\bar{\sigma}_3} \frac{\bar{\sigma}_3}{\bar{\sigma}_1} \tilde{y}_2^{-\frac{\bar{\sigma}_3}{\bar{\sigma}_1} - 2} \widehat{H}(\nu, \tilde{y}_2), \quad (6.3.14)$$

where

$$\begin{aligned} \widehat{H}(\nu, \tilde{y}_2) &= \left[l_1(\nu) n_2(\nu) + O(m(\nu)) + O(\hat{y}_3) \right] \frac{\bar{\sigma}_3}{\bar{\sigma}_1} \left(\nu \tilde{y}_2^{-\frac{1}{\bar{\sigma}_1}} \right)^{\bar{\sigma}_3} (1 + \theta_{24}(\nu, \tilde{y}_2)) \\ &\quad + \left[l_1(\nu) n_1(\nu) + O(m(\nu)) + O(\hat{y}_3) \right] \left(\frac{\bar{\sigma}_3}{\bar{\sigma}_1} + 1 \right) (1 + \theta_{25}(\nu, \tilde{y}_2)), \end{aligned}$$

and $\theta_{24}, \theta_{25} \in I_0^\infty$.

Note that on the section τ_2 , the coordinates are (r_2, ρ_2) with $r_2 \rho_2 = \nu$ for $\nu > 0$ small, so we only need to consider the domain $|r_2| < \varepsilon$ and $|\rho_2| < \varepsilon$ for $\varepsilon > 0$ small. In fact, from (6.3.13), we have $\rho_2 = \tilde{y}_2^{\frac{1}{\bar{\sigma}_1}} (N_1 + \theta_{21}(\nu, \tilde{y}_2))$, and $r_2 = \nu \tilde{y}_2^{-\frac{1}{\bar{\sigma}_1}} N_1^{-1} (1 + \widehat{\theta}_{21}(\nu, \tilde{y}_2))$ with $\widehat{\theta}_{21} \in I_0^\infty$. Therefore, we study the graphic on section τ_2 for sufficiently small $\varepsilon > 0$ such that $\nu \tilde{y}_2^{-\frac{1}{\bar{\sigma}_1}} \ll 1$. Hence, for $\nu > 0$ small and $(\bar{\mu}, a)$ sufficiently close to $(\bar{\mu}_0, a_0)$, we have $\widehat{H}(\nu, \tilde{y}_2) > 0$ in the small neighborhood of $\tilde{y}_2 = 0$

Since $N_2 < 0$, by (6.3.14), we have $\frac{\partial^2 \widehat{T}_2(\nu, \tilde{y}_2)}{\partial \tilde{y}_2^2} < 0$, i.e., $\widehat{T}_2(\nu, \tilde{y}_2)$ is concave. Note that $\widetilde{T}_2(\nu, \tilde{y}_2)$ is convex, so for $\forall (a, \bar{\mu}) \in A_0 \times \bar{V}_{70}$ and $\nu > 0$ sufficiently small, $L_2(\nu, \tilde{y}_2)$ has

at most two small roots in the small neighborhood of $\tilde{y}_2 = 0$, i.e., $Cycl(Ehh7c) \leq 2$.

6.3.6 Ehh8c

The Lower boundary graphic of Ehh8 passes through a hyperbolic saddle point in the chart F. R. as shown in Fig. 6.6. Let $\lambda(\nu)$ be the hyperbolicity ratio at this saddle point. Take sections $\bar{\Sigma}_2 = \{\tilde{x} = 1\}$ and $\bar{\Sigma}_4 = \{\tilde{y} = 1\}$ in the normal form coordinates of the saddle point.

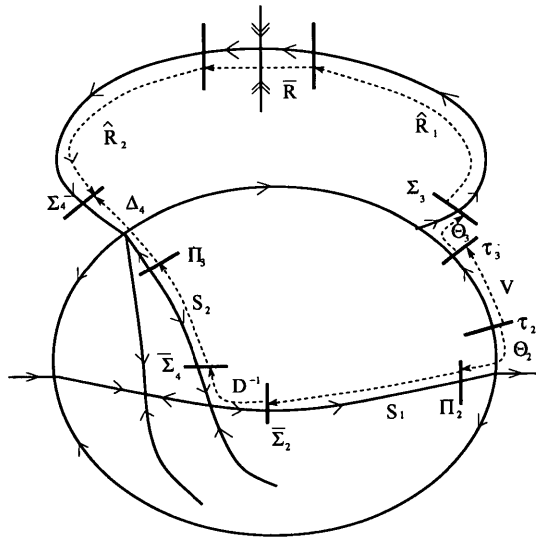


Figure 6.6: Transition maps for the graphic Ehh8c

We are going to study the displacement map defined on the section τ_2 :

$$L : \tau_2 \longrightarrow \Sigma_4,$$

$$L = \hat{T} - \tilde{T}.$$

The transition map \tilde{T} can be factorized as

$$\tilde{T} : \tau_1 \longrightarrow \Sigma_4,$$

$$\tilde{T} = \widehat{R}_2 \circ \overline{R} \circ \widehat{R}_1 \circ \Theta_3 \circ V,$$

where

- $V : \tau_2 \longrightarrow \tau_3$ is a regular transition map, which is given by (5.3.13).
- $\Theta_3 : \tau_3 \longrightarrow \Sigma_3$ is the second type of Dulac map in the neighborhood of P_3 with $\bar{\sigma} = \bar{\sigma}_3$.
- The transition maps \widehat{R}_1 , \overline{R} and \widehat{R}_2 are given by (4.2.4), (4.2.5) and (4.2.6).

Therefore, for \tilde{T} , we have

$$\begin{cases} \tilde{T}_1(\nu, c) = \nu, \\ \tilde{T}_2(\nu, c) = n_0(\nu) + O(m(\nu)) + m(\nu) \left[(l_1(\nu)n_1(\nu) + O(m))\hat{y}_3 + O(\hat{y}_3^2) \right], \end{cases} \quad (6.3.15)$$

where

$$\hat{y}_3 = -\frac{y_0}{r_0^{\bar{\sigma}_3}} m_{141}^{\bar{\sigma}_3}(\nu) \nu^{(1-c)\bar{\sigma}_3} \left[1 + O(\nu^c, \nu^{1-c}) + \theta_{31}(\nu, \nu^{1-c}, \omega\left(\frac{m_{141}}{r_0} \nu^{1-c}, -\beta_1\right)) \right],$$

and θ_{31} satisfies the same properties as of θ_1 in (5.3.11)

For the transition map \widehat{T} , we calculate it by the following decomposition

$$\widehat{T} : \tau_2 \longrightarrow \Sigma_4,$$

$$\widehat{T} = \Delta_4 \circ S_2 \circ D^{-1} \circ S_1 \circ \Theta_2,$$

where

- $\Theta_2 : \tau_2 \longrightarrow \Pi_2$ is the second type of Dulac map in the neighborhood of P_2 with

$$\bar{\sigma} = \bar{\sigma}_1.$$

- $S_1 : \Pi_1 \longrightarrow \bar{\Sigma}_2$ is a regular transition map, which can be written as

$$\begin{cases} S_{11}(\nu, \tilde{y}_1) = \nu, \\ S_{12}(\nu, \tilde{y}_1) = e_1(\nu)\tilde{y}_1 + O(\tilde{y}_1^2), \end{cases}$$

where $e_1(0) > 0$.

- $D^{-1} : \bar{\Sigma}_2 \longrightarrow \bar{\Sigma}_4$ is the Dulac map near the saddle point, which has the expression

$$(3.2.5).$$

- $S_2 : \bar{\Sigma}_4 \longrightarrow \Pi_4$ is a regular transition map, which can be written as

$$\begin{cases} S_{21}(\nu, \tilde{y}) = \nu, \\ S_{22}(\nu, \tilde{y}) = b_0(\nu) + b_1(\nu)\tilde{y} + O(\tilde{y}^2), \end{cases}$$

where $b_0(0) = 0$ and $b_1(0) > 0$.

- $\Delta_4 : \Pi_4 \longrightarrow \Sigma_4$ are the first type of Dulac maps in the neighborhood of P_4 with

$$\bar{\sigma} = \bar{\sigma}_3.$$

Hence, for \hat{T} , we have $\hat{T}_1(\nu, c) = \nu$. Let

$$\tilde{y} = \frac{e_1(\nu)y_0}{\rho_0^{\bar{\sigma}_1}} \nu^{c\bar{\sigma}_1} [1 + \theta_{21}(\nu, \nu^c, \omega(\frac{\nu^c}{\rho_0}, -\alpha_1) + O(\nu^{\bar{\sigma}_1 c}))],$$

$$\tilde{y}_4 = b_0(\nu) + b_1(\nu)\tilde{y}^{\frac{1}{\lambda}} [1 + \psi_1(\nu, \tilde{y})],$$

where $\psi_1(\nu, \tilde{y}) \in I_0^\infty$ and θ_{21} satisfies the same properties as of θ_1 in (5.3.11). Then the second component of \widehat{T} can be written as

$$\widehat{T}_2(\nu, c) = \left(\frac{\nu}{\nu_0}\right)^{\bar{\sigma}_3} [\tilde{y}_4 + \theta_{41}(\nu, \tilde{y}_4, \omega(\frac{\nu}{\nu_0}, -\beta_1))]. \quad (6.3.16)$$

By (6.3.16), the first derivative of $\widehat{T}_2(\nu, c)$ with respect to c is given as follows.

$$\begin{aligned} \frac{\partial \widehat{T}_2(\nu, c)}{\partial c} &= \left(\frac{\nu}{\nu_0}\right)^{\bar{\sigma}_3} \left[1 + \frac{\partial \theta_{41}}{\partial \tilde{y}_4}(\nu, \tilde{y}_4, \omega(\frac{\nu}{\nu_0}, -\beta_1))\right] b_1(\nu) \frac{\bar{\sigma}_1}{\lambda} \left(\frac{e_1(\nu)y_0}{\rho_0^{\bar{\sigma}_1}}\right)^{\frac{1}{\lambda}} \\ &\quad \nu^{\frac{\bar{\sigma}_1 c}{\lambda}} \left[1 + \psi_2(\nu, \tilde{y})\right] \left[1 + \theta_{22}(\nu, \nu^c, \omega(\frac{\nu^c}{\rho_0}, -\alpha_1) + O(\nu^{\bar{\sigma}_1 c}))\right] \ln \nu, \end{aligned}$$

where $\psi_2(\nu, \tilde{y}) \in I_0^\infty$, and θ_{22} satisfies the same properties as of θ_1 in (5.3.11) also

$$\frac{\partial \theta_{41}}{\partial \tilde{y}_4} = O\left(\nu^{\bar{\sigma}_3} \omega^{q_3}\left(\frac{\nu}{\nu_0}, -\beta_1\right) \ln \frac{\nu}{\nu_0}\right).$$

Then

$$\begin{aligned} \frac{\partial^2 \widehat{T}_2(\nu, c)}{\partial c^2} &= \left(\frac{\nu}{\nu_0}\right)^{\bar{\sigma}_3} \left[1 + O\left(\nu^{\bar{\sigma}_3} \omega^{q_3}\left(\frac{\nu}{\nu_0}, -\beta_1\right) \ln \frac{\nu}{\nu_0}\right)\right] b_1(\nu) \left(\frac{\bar{\sigma}_1}{\lambda}\right)^2 \left(\frac{e_1(\nu)y_0}{\rho_0^{\bar{\sigma}_1}}\right)^{\frac{1}{\lambda}} \\ &\quad \nu^{\frac{\bar{\sigma}_1 c}{\lambda}} \left[1 + \theta_{23}(\nu, \nu^c, \omega(\frac{\nu^c}{\rho_0}, -\alpha_1) + O(\nu^{\bar{\sigma}_1 c})) + \psi(\nu, \tilde{y})\right] (\ln \nu)^2, \end{aligned}$$

where $\psi(\nu, \tilde{y}) \in I_0^\infty$. So $\forall (\nu, c) \in (0, \varepsilon^2) \times I_\nu$ with ε sufficiently small, $\frac{\partial^2 \widehat{T}_2(\nu, c)}{\partial c^2} > 0$,

i.e., $\widehat{T}_2(\nu, c)$ is convex.

By (6.3.15), the first derivative of $\widetilde{T}_2(\nu, c)$ with respect to c is given as follows.

$$\begin{aligned} \frac{\partial \widetilde{T}_2(\nu, c)}{\partial c} &= m(\nu) \left[(l_1(\nu)n_1(\nu) + O(m)) + O(\hat{y}_3) \right] \frac{y_0}{r_0^{\bar{\sigma}_3}} m_{141}^{\bar{\sigma}_3}(\nu) \nu^{(1-c)\bar{\sigma}_3} \bar{\sigma}_3 \\ &\quad \left[1 + O(\nu^c, \nu^{1-c}) + \theta_{42}(\nu, \nu^{1-c}, \omega(\frac{m_{141}}{r_0} \nu^{1-c}, -\beta_1)) \right] \ln \nu, \end{aligned}$$

where θ_{42} satisfies the same properties as of θ_1 in (5.3.11).

$$\frac{\partial^2 \tilde{T}_2(\nu, c)}{\partial c^2} = -m(\nu) \left[(l_1(\nu)n_1(\nu) + O(m)) + O(\hat{y}_3) \right] \frac{y_0}{r_0^{\bar{\sigma}_3}} m_{141}^{\bar{\sigma}_3}(\nu) \nu^{(1-c)\bar{\sigma}_3} \bar{\sigma}_3^2 \\ \left[1 + O(\nu^c, \nu^{1-c}, \nu^{(1-c)\bar{\sigma}_3}) + \theta_{43}(\nu, \nu^{1-c}, \omega(\frac{m_{141}}{r_0} \nu^{1-c}, -\beta_1)) \right] (\ln \nu)^2.$$

So $\forall (\nu, c) \in (0, \varepsilon^2) \times I_\nu$ with ε sufficiently small, $\frac{\partial^2 \tilde{T}_2(\nu, c)}{\partial c^2} < 0$, i.e., $\tilde{T}_2(\nu, c)$ is concave.

Note that $\hat{T}_2(\nu, c)$ is convex and $\tilde{T}_2(\nu, c)$ is concave, so $\forall (a, \bar{\mu}) \in A_0 \times \bar{V}_{80}$, $L_2(\nu, c)$ has at most two small roots for $(\nu, c) \in (0, \varepsilon^2) \times I_\nu$ with ε sufficiently small, i.e., $Cycl(Ehh8c) \leq 2$.

6.4 The intermediate boundary graphic

Let Γ be any intermediate HH-graphic of elliptic type. Similar to the intermediate concave graphics of saddle type, take sections Π_3 and Π_4 defined (2.5.21) in the normal form coordinates in the neighborhood of P_3 and P_4 respectively. We will study the displacement map

$$L : \Pi_3 \longrightarrow \Pi_4 \\ L = R - T^{-1},$$

where $R : \Pi_3 \longrightarrow \Pi_4$ is the transition map along the regular orbit in the normal form coordinates, and $T : \Pi_4 \longrightarrow \Pi_3$ is the transition map passing through the blown-up singularity.

For the transition map R , from proposition 4.3.1, we know that for $\nu > 0$ sufficiently small, any i^{th} derivative of the second component of transition map $R(\nu, \tilde{y}_3)$ with respect to \tilde{y}_3 is close to zero.

To study the transition map T on the blown-up sphere, let $\pi_i = \{\rho_i = \rho_0\} (i = 3, 4)$ be the two line sections in the chart F. R. on $r = 0$ parameterized by $\tilde{y}_i (i = 3, 4)$, respectively. Then we are reduced to study the one dimensional transition map

$$T_2(0, \tilde{y}_4) : \pi_4 \longrightarrow \pi_3,$$

or its inverse

$$T_2^{-1}(0, \tilde{y}_3) : \pi_3 \longrightarrow \pi_4.$$

6.4.1 Family Ehh1

It has been proved in [53] that $T_2(0, \tilde{y}_4) : \pi_4 \longrightarrow \pi_3$ is either the identity or nonlinear for \tilde{y}_4 . Since $\bar{T}_2(0, \tilde{y}_4)$ is analytic and bijective, so $T_2^{-1}(0, \tilde{y}_3) : \pi_3 \longrightarrow \pi_4$ is either the identity or nonlinear for \tilde{y}_3 . Thus for both cases, the intermediate graphics of the family Ehh1 have finite cyclicity.

6.4.2 Families Ehh2 and Ehh3

For family Ehh i ($i = 2, 3$), we have a family of intermediate graphics Ehh i b, Ehh i c and Ehh i d as in Fig. 6.8 (a). For the graphic (I_{9b}^1) , it was proved in [53] that $Cycl(Ehhic) \leq$

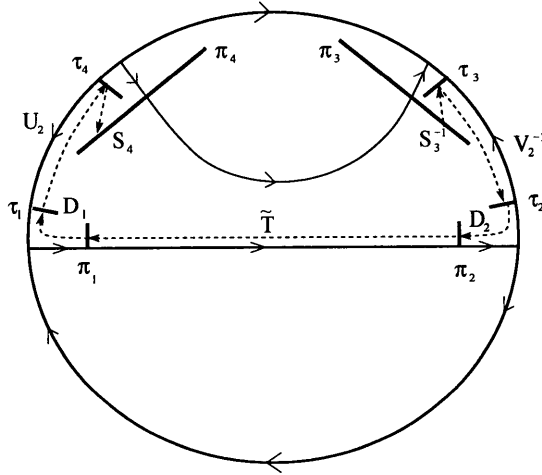


Figure 6.7: Transition maps for the intermediate graphics of Ehh1

1 and $Cycl(Ehhid) \leq 2 (i = 2, 3)$. For the graphic (I_{11b}^1) , the transition near the additional attracting saddle-node behaves like a transition near P_3 which does not influence the proof of the finite cyclicity of graphics Ehhic and Ehhid ($i = 2, 3$).

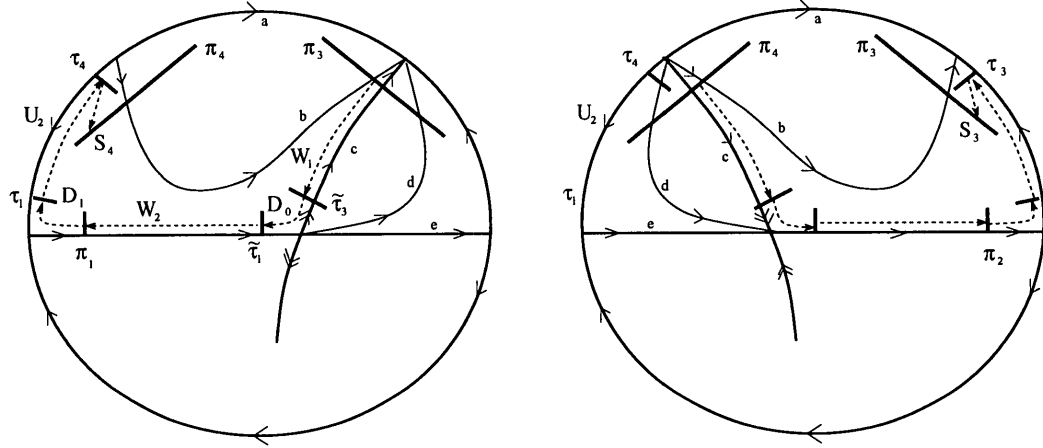
To study the cyclicity of the graphic Ehh2b, we study the transition map $T_2^{-1}(0, \tilde{y}_3)$ defined on π_3 in the neighborhood of the graphic Ehh2c.

Let $\tilde{\tau}_1 = \{\tilde{y} = y_0\}$ and $\tilde{\tau}_3 = \{\tilde{x} = x_0\}$ be two sections in the neighborhood of the saddle node. Then the corresponding transition map T_2^{-1} can be factorized as

$$T_2^{-1} : \quad \pi_3 \longrightarrow \pi_4$$

$$T_2^{-1} = S_4 \circ U_2 \circ D_1 \circ W_2 \circ D_0 \circ W_1,$$

where



(a) Family Ehh2

(b) Family Ehh3

Figure 6.8: Transition maps for the intermediate graphics of Ehh2 and Ehh3

- $W_1 : \pi_3 \longrightarrow \tau_3$, $W_2 : \tau_1 \longrightarrow \pi_1$, $U_2 : \tau_1 \longrightarrow \tau_4$ and $S_4 : \tau_4 \longrightarrow \pi_4$ are transition maps.
- $D_0 : \tilde{\tau}_3 \longrightarrow \tilde{\tau}_1$ is the stable-centre transition in the neighborhood of the saddle node in the normal form coordinates, and $\forall n_1, n_2 \in \mathbb{N}$

$$\frac{\partial^{n_1} D_0}{\partial \tilde{y}^{n_1}} = O(\tilde{y}^{n_2}). \quad (6.4.17)$$

- $D_1 : \pi_1 \longrightarrow \tau_1$ is a Dulac map near the saddle point.

Note that $\tilde{y}_1 = W_2 \circ D_0 \circ W_1(0, \tilde{y}_3)$ as the function of \tilde{y}_3 , which satisfies the flatness property (6.4.17), for T_2^{-1} , we have $\lim_{\tilde{y}_3 \rightarrow 0} T_2^{-1}(0, \tilde{y}_3) = -\infty$. Hence T_2^{-1} maps $(0, +\infty)$ to $(-\infty, +\infty)$. Since $T_2^{-1}(0, \tilde{y}_3)$ is analytic and bijective, it has to be nonlinear in \tilde{y}_3 ,

therefore it is nonlinear for $\tilde{y}_3 \in \mathbb{R}^+$, thus any intermediate graphic Ehh2b has finite cyclicity.

Since system $\overline{X}_{\rho=1}$ in (2.4.15) is invariant under the transformation

$$(-x, -t, -\bar{\mu}_1, -\bar{\mu}_3) \mapsto (x, t, \bar{\mu}_1, \bar{\mu}_3). \quad (6.4.18)$$

The family Ehh3 can be obtained from the family Ehh2 by transformation (6.4.18).

Hence, For the graphics Ehh3b, we have $T_2(0, \tilde{y}_4)$ maps $(0, +\infty)$ to $(-\infty, +\infty)$, and $T_2(0, \tilde{y}_4)$ is analytic, bijective and nonlinear, so $T_2^{-1}(0, \tilde{y}_3)$ exists and is nonlinear in \tilde{y}_3 .

Therefore, any intermediate graphic Ehh3b has finite cyclicity.

6.4.3 Family Ehh4

For the family Ehh4b, the lower boundary graphic passes through a hyperbolic saddle, it has the same structure as the family Sxhh1b of saddle type. Therefore, any intermediate graphic of Ehh4 has finite cyclicity.

6.4.4 Families Ehh5–Ehh8

We first consider family Ehh5. As shown in Fig. 6.9 (a), the lower boundary graphic Ehh5c passes through two saddle points. One is at infinity, the other lies on the invariant line $\bar{y} = 0$. We have a saddle connection.

In the normal form coordinates (\tilde{x}, \tilde{y}) near the finite saddle, take sections $\tilde{\tau}_1 = \{\tilde{x} = -x_0\}$ and $\tilde{\tau}_3 = \{\tilde{y} = y_0\}$. Let $D_0 : \tilde{\tau}_1 \longrightarrow \tilde{\tau}_3$ be the Dulac map, then the transition map

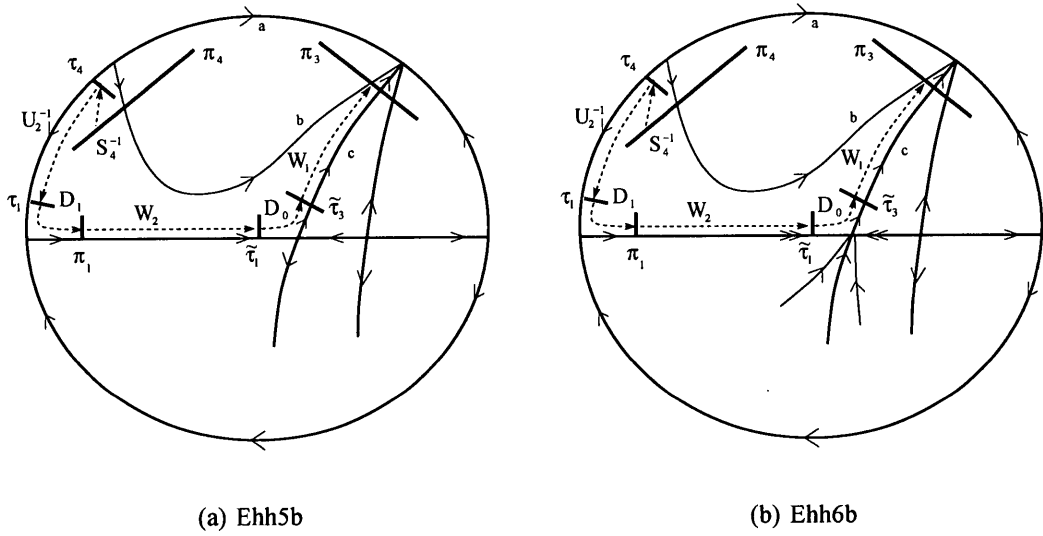


Figure 6.9: Transition maps for the intermediate graphics of Ehh5 and Ehh6

T_2 can be factorized as

$$T_2 = W_1 \circ D \circ W_2 \circ D_1 \circ U_2^{-1} \circ S_4^{-1}.$$

It was proved in [53] that $T_2(0, \tilde{y}_4)$, which maps $(-\infty, +\infty)$ to $(0, +\infty)$, is bijective, analytic and nonlinear. So $T_2^{-1}(0, \tilde{y}_3)$ exists and should be nonlinear in \tilde{y}_3 , therefore it is nonlinear for $\tilde{y}_3 \in \mathbb{R}^+$. Hence, any intermediate graphics Ehh5b have finite cyclicity.

For the family Ehh6b, it has a attracting saddle node on the lower boundary graphic. By the similar argument as Ehh5b, we have $T_2^{-1}(0, \tilde{y}_3)$ is nonlinear in \tilde{y}_3 . Hence, the intermediate graphics Ehh6b have finite cyclicity.

The family Ehh7 and Ehh8 can be obtained from the family Ehh5 and Ehh6 by the transformation (6.4.18) on the blown-up sphere $\{r = 0\}$, respectively. Therefore,

$T_2^{-1}(0, \tilde{y}_3)$ exists and is nonlinear in \tilde{y}_3 for the family Ehh7b and Ehh8b. Hence, any intermediate graphic of Ehh7b and Ehh8b have finite cyclicity.

Altogether, we finish the proof of Theorem 6.1.1.

Bibliography

- [1] A. Andronov, E. Leontovich, I. Gordon and A. Maier, *Theory of Bifurcations of Dynamical Systems on a Plane*, Israel Program for Scientific Translations, Jerusalem, 1971.
- [2] N. Bautin, *On the number of limit cycles which appear with the variation of coefficients from an equilibrium position of focus or center type*, Amer. Math. Soc. Trans. 100 (1954).
- [3] L. Chen and M. Wang, *The relative position, and the number of limit cycles of a quadratic differential system*, Acta Math. Sinica 22 (1979) 751-758.
- [4] Z. Denkowska and R. Roussarie, *A method of desingularization for analytic two-dimensional vector field families*, Bol. Soc. Brasil. Mat. (N.S.) 22 (1991), 93-126.
- [5] F. Dumortier, *Singularities of vector fields on the plane*, J. Differential Equations 23 (1977) 53-106.

- [6] F. Dumortier, *Singularities of Vector Fields*, Monografias de Matematica [Mathematical Monographs], 32. Instituto de Matematica Purae Aplicada, Rio de Janeiro, 1978.
- [7] F. Dumortier, *Techniques in the theory of local bifurcations: blow-up, normal forms, nilpotent bifurcations, singular perturbations*, Bifurcations and periodic orbits of vector fields (Montreal, 1992). 19-73, NATO Adv. Sci. Inst. Ser. C Math. Phys. Sci., 408, Edited by Dana Schlomiuk. Kluwer Acad. Publ., Dordrecht, 1993.
- [8] F. Dumortier and P. Fiddelaers, *Quadratic models for generic local 3-parameter bifurcations on the plane*, Trans. Amer. Math. Soc. 326 (1991) 101-126.
- [9] F. Dumortier, P. Fiddelaers and C. Li, *Generic unfolding of the nilpotent saddle of codimension four*, Global analysis of dynamical systems, 131-166, Inst. Phys., Bristol, 2001.
- [10] F. Dumortier, A. Guzmán and C. Rousseau, *Finite cyclicity of elementary graphics surrounding a focus or center in quadratic systems*, Qualitative Theory Dyn. System 3 (2002) 123-154.
- [11] F. Dumortier, Y. Ilyashenko and C. Rousseau, *Normal forms near a saddle-node and applications to finite cyclicity of graphics*, Ergodic Theory Dynam. Systems 22 (2002) 783-818.

- [12] F. Dumortier, M. El Morsalani and C. Rousseau, *Hilbert's 16th problem for quadratic systems and cyclicity of elementary graphics*, Nonlinearity 9 (1996) 1209-1261.
- [13] F. Dumortier and C. Rousseau, *Cubic Liénard equations with linear damping*, Nonlinearity 3 (1990) 1015-1039.
- [14] F. Dumortier, R. Roussarie and C. Rousseau, *Elementary graphics of cyclicity 1 and 2*, Nonlinearity 7 (1994) 1001-1043.
- [15] F. Dumortier, R. Roussarie and C. Rousseau, *Hilbert's 16th problem for quadratic vector fields*, J. Differential Equations 110 (1994) 86-133.
- [16] F. Dumortier, R. Roussarie and S. Sotomayor, *Generic 3-parameter families of vector fields in the plane, unfolding a singularity with nilpotent linear part. The cusp case*, Ergod. Theory Dynam. Sys. 7 (1987) 375-413.
- [17] F. Dumortier, R. Roussarie and S. Sotomayor, *Generic 3-parameter families of vector fields in the plane, unfoldings of saddle, focus and elliptic singularities with nilpotent linear parts*, Lecture Notes in Math., 1480, Springer-Verlag, Berlin, 1991.
- [18] F. Dumortier, R. Roussarie and S. Sotomayor, *Bifurcations of cuspidal loops*, Nonlinearity 10 (1997) 1369-1408.

- [19] F. Dumortier and C. Rousseau, *Study of the cyclicity of some degenerate graphics inside quadratic systems*, Commun. Pure Appl. Anal. 8 (2009) 1133-1157.
- [20] J. Ecalle, *Finitude des cycles limites et accéléro-sommation de l'application de retour*, 74-159, Lecture Notes in Math., 1455, Springer, Berlin, 1990.
- [21] M. El Morsalani, *Perturbations of graphics with semi-hyperbolic singularities*, Bull. Sci. Math. 120 (1996) 337-366.
- [22] J. Francoise, and C. C., Pugh, *Keeping track of limit cycles*, J. Differential Equations 65 (1986) 139-157.
- [23] J. Guckenheimer and P. Holmes, *Non-linear Oscillations, Dynamical Systems and Bifurcation of Vector fields*, Appl. Math. Sci. 42, Springer-Verlag, 1983.
- [24] A. Guzmán and C. Rousseau, *Genericity conditions for finite cyclicity of elementary graphics*, J. Differential Equations 155 (1999) 44-72.
- [25] D. Hilbert, *Mathematische Problem (lecture): The Second International Congress of Mathematicians, Paris 1900*. Nachr. Ges. Wiss. Gottingen Math.-Phys. Kl. (1900), 253-297; *Mathematical developments arising from Hilberts problems*. Proceedings of Symposium in Pure Mathematics F. Brower Ed., 28, pp.50-51. Amer. Math. Soc. Providence, RI, 1976.

- [26] Y. Il'yashenko, *Finiteness theorems for limit cycles*, Russian Math. Surveys 45 (1990) 129-203.
- [27] Y. Il'yashenko and S. Yakovenko, *Finite-smooth normal forms of local families of diffeomorphisms and vector fields*, Russian Math. Surveys 46 (1991) 1-43.
- [28] Y. Ilyashenko and S. Yakovenko, *Concerning the Hilbert sixteenth problem*, Concerning the Hilbert's 16th problem, 1-19, Amer. Math. Soc. Transl. Ser. 2, 165, Amer. Math. Soc., Providence, RI, 1995.
- [29] Y. Ilyashenko and S. Yakovenko, *Finite cyclicity of elementary polycycles in generic families*, Concerning the Hilbert's 16th problem. 21-95, Amer. Math. Soc. Transl. Ser. 2, 165, Amer. Math. Soc., Providence, RI, 1995.
- [30] Y. Ilyashenko, *Centennial history of Hilbert's 16th problem*, Bull. Amer. Math. Soc., 39 (2002) 301-354.
- [31] P. Joyal and C. Rousseau, *Saddle quantities and applications*, J. Differential Equations, 78 (1989) 374-389.
- [32] A.G. Khovanskii, *Cycles of dynamic systems on a plane and Rolle's theorem*, Sibirsk. Mat. Zh. 25 (1984) 198-203.

- [33] A. Kotova and V. Stanzo, *On few-parameter generic families of vector fields on the two-dimensional sphere. Concerning the Hilbert 16th problem*, 155-201, Amer. Math. Soc. Transl. Ser. 2, 165, Amer. Math. Soc., Providence, RI, 1995.
- [34] E. Leontovich-Andronova, *On the generation of limit cycle from separatrice*, Dokl. Acad. Nauka 78 (1951) 641-644.
- [35] J. Li, *Hilbert's 16th problem and bifurcations of planar polynomial vector fields*, Internat. J. Bifur. Chaos Appl. Sci. Engrg. 13 (2003) 47-106.
- [36] M. Morsalani and A. Mourtada, *Degenerate and non-trivial hyperbolic 2-polycycles: two independant Ecalle-Roussarie compensators and Khovanskii theory*, Nonlinearity 7 (1994) 1593-1604.
- [37] A. Mourtada, *Cyclicité finie des polycycles hyperboliques de champs de vecteurs du plan: mise sous forme normale*, Bifurcations of planar vector fields (Luminy, 1989), 272-314, Lecture Notes in Math., 1455, Springer, Berlin, 1990.
- [38] A. Mourtada, *Degenerate and non-trivial hyperbolic polycycles with two vertices*, J. Differential Equations 113 (1994) 68-83.
- [39] R. Roussarie, *A note on finite cyclicity property and Hilbert's 16th problem*, Dynamical systems, Valparaiso 1986, 161-168, Lecture Notes in Math., 1331, Springer, Berlin, 1988.

- [40] R. Roussarie, *On the number of limit cycles which appear by perturbation of separatrix loop of planar vector fields*, Bol. Soc. Brasil. Mat. 17 (1986) 67-101.
- [41] R. Roussarie, *Cyclicité finie des lacets et des points cuspidaux*, Nonlinearity 2 (1989) 73-117.
- [42] R. Roussarie, *Desingularization of unfoldings of cuspidal loops*, Geometry and analysis in nonlinear dynamics (Groningen, 1989), 41-55, Pitman Res. Notes Math. Ser., 222, Longman Sci. Tech., Harlow, 1992.
- [43] R. Roussarie, *Bifurcations of Planar Vector Fields and Hilbert's Sixteenth Problem*, Progress in Mathematics, 164. Birkhäuser Verlag, Basel, 1998.
- [44] R. Roussarie and C. Rousseau, *Finite cyclicity of nilpotent graphics of pp-type surrounding a center*, Bull. Belg. Math. Soc. Simon Stevin 15 (2008), no. 5, Dynamics in perturbations, 889-920.
- [45] C. Rousseau, *Normal forms, bifurcations and finiteness properties of vector fields*. Normal forms, bifurcations and finiteness problems in differential equations, 431-470, NATO Sci. Ser. II Math. Phys. Chem., 137, Kluwer Acad. Publ., Dordrecht, 2004.

- [46] C. Rousseau and H. Zhu. *PP-graphics with a nilpotent elliptic singularity in quadratic system and Hilbert's 16th problem*, J. Differential Equations 196 (2004) 169-208.
- [47] S. Shi, *A concrete example of the existence of four limit cycles for plane quadratic system*, Scientia Sinica 23 (1980) 154- 158.
- [48] S. Sternberg, *On the structure of local homeomorphisms of euclidean n -space. II*, Amer. J. Math. 80 (1958) 623-631.
- [49] F. Takens, *Unfoldings of certain singularities of vector fields: generalized Hopf bifurcations*, J. Differential Equations 14 (1973) 476-493.
- [50] Y. Ye, S. Cai, L. Chen, K. Huang, D. Luo, Z. Ma, E. Wang, M. Wang and X. Yang, *Theory of Limit Cycles*, Translated from the Chinese by Chi Y. Lo. Second edition. Translations of Mathematical Monographs, 66. American Mathematical Society, Providence, R.I., 1986. xi+435 pp.
- [51] Z. Zhang, T. Ding, W. Huang and Z. Dong, *Qualitative Theory of Differential Equations*, Translated from the Chinese by Anthony Wing Kwok Leung. Translations of Mathematical Monographs, 101. American Mathematical Society, Providence, RI, 1992. xiv+461 pp.

- [52] H. Zhu, *Finite cyclicity of graphics with a nilpotent singularity of saddle or elliptic type*, PhD thesis, Université de Montréal, 1999.
- [53] H. Zhu and C. Rousseau, *Finite cyclicity of graphics with a nilpotent singularity of saddle or elliptic type*, J. Differential Equations 178 (2002) 325-436.